Morphological, anatomical, and physiological investigation into the adaptive responses of *Paulownia tomentosa* to different abiotic stimuli.

Dissertation with the aim of achieving a degree of Doctor of Natural Sciences

at the Faculty of Mathematics, Informatics, and Natural Sciences

Department of Wood Biology

at Universität Hamburg

Submitted by

Layssa da Silva Costa

Hamburg, May 2024

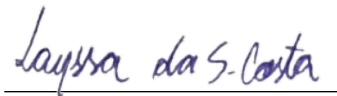**Eidesstattliche Versicherung | Declaration on Oath**

Hiermit erkläre ich an Eides statt, dass ich die vorliegende Dissertationsschrift selbst verfasst und keine anderen als die angegebenen Quellen und Hilfsmittel benutzt habe.

I hereby declare upon oath that I have written the present dissertation independently and have not used further resources and aids than those stated.

Ich versichere, dass dieses gebundene Exemplar der Dissertation und das in elektronischer Form eingereichte Dissertationsexemplar (über den Docata-Upload) und das bei der Fakultät (zuständiges Studienbüro Biologie) zur Archivierung eingereichte gedruckte gebundene Exemplar der Dissertationsschrift identisch sind.

I, the undersigned, declare that this bound copy of the dissertation and the dissertation submitted in electronic form (via the Docata upload) and the printed bound copy of the dissertation submitted to the faculty (Doctoral Office Biology) for archiving are identical.

Hamburg, May 2024

Layssa da S. Costa

Layssa da Silva Costa

Acknowledgments

My PhD journey was an experience marked by unexpected challenges and periods of uncertainty due to the pandemic. However, I am profoundly grateful for the support and encouragement of my network of colleagues, friends, and family, which were fundamental for me to write this project. First, I sincerely thank my supervisor, Prof. Dr. Jörg Fromm, for believing in my potential and giving me the opportunity, insightful guidance, and numerous constructive discussions that helped enrich this project and made completing this thesis possible. I also sincerely appreciate the help of Mrs. Katharina Erdt, the technician of our research group, for the technical support, ensuring our laboratory's safety, and valuable conversations during our encounters. In addition, I express my gratitude to the members of the Thünen Institute, especially the gardeners, who provided support during the greenhouse experiments, as well as Dr. Immo Heinz, Mr. Sergej Kaschuro, Dr. Emilin Joma da Silva, and Dr. Anna Bogun for their company during the breaks, making the workspace a place of joy and mutual support. I am grateful to Prof. Dr. Adriana de Fátima Gomes Gouvea, whose early teaching helped shape the foundational knowledge required for my academic journey.

Finally, I would like to express my gratitude to my dear friends Ana Caroline Miron Pereira and Anna Carolina Martins Moraes, for making this journey much more fun with our studying sessions, sharing experiences, and conversations; my family members, who encouraged my life choices and gave me remote support during this journey; my partner Saul Lazzarini and my dear friends Layla Sboron and Mario Leal de la Rosa, who actively supported me during the process. I thank my friends Janna Varady, Jirka Manuel Petersen, Nour Alhuda Altaie, and Negar Ghadernezhad, who have been with me since I moved to Germany, helping me to navigate and integrate into the German culture.

Abstract

Concerns about climate change have sparked interest in using fast-growing trees for sustainable forestry and atmospheric CO_2 reduction. *Paulownia* spp. is particularly promising due to its rapid growth and adaptability to adverse climatic and edaphic conditions, making it popular for commercial plantations and reforestation. Within this context, it is crucial to gain insights into the adaptability responses of Paulownia trees to the globally projected climatic conditions. This study primarily aims to evaluate the morphological, physiological, and anatomical responses of young *Paulownia tomentosa* to elevated CO_2 levels and cyclic drought stress. Secondly, to characterize the bioelectric activity of these trees in response to damaging stimuli and post-drought re-irrigation. The research comprises three experimental setups: (1) Seed-grown Paulownia were exposed to a CO_2 concentration of 950 ppm throughout one growing season to assess gas exchange, stem anatomical modifications, elemental composition of guard cells and mesophyll chloroplasts, and growth responses. (2) Three-year-old trees underwent recurrent drought cycles to examine gas exchange, photosynthetic efficiency, leaf pigment composition, hydraulic architecture, and growth adaptations during one growing season. (3) Bioelectric responses were characterized in three-year-old Paulownia trees subjected to burn damage stimuli and soil rehydration after drought, using intercellular and extracellular (EEG) methods. The results from the CO_2 experiment show that Paulownia seedlings cultivated at elevated CO_2 had significantly higher net CO_2 uptake. At the same time, stomatal conductance and transpiration remained unchanged, enhancing water use efficiency compared to plants grown at ambient CO_2. The wider stem vessels suggested enhanced water transport under elevated CO_2. Increased photosynthetic activity and wood anatomy alterations led to higher growth performance, with a significantly higher height and shoot biomass increment and an increasing trend toward the root biomass and stem diameter. Drought generally reduced net CO_2 uptake, stomatal conductance, and transpiration but increased chlorophyll and anthocyanin content, thus maintaining and protecting the photosynthetic activity during early stress stages. Post-drought water use efficiency remained higher due to semi-conservative water use strategies. Drought-stressed plants developed narrower vessels but increased vessel frequency, suggesting a trend toward hydraulic safety. However, recurrent drought cycles negatively impacted growth parameters, such as the total biomass increment, stem diameter, height, and number of leaves. Concerning bioelectric activity, damaging stimuli induced depolarization and hyperpolarization responses in the plasma membrane of healthy leaf cells.

Additionally, the activity was characterized by oscillations in the electrical potential of the leaf petioles in distal leaves, concurrent with stomatal closure and reduced photosynthesis, indicative of systemic signaling. During dark periods, electrical signals coincided with transient stomatal opening and enhanced respiratory activity. Upon re-irrigation, leaf cells displayed hyperpolarizing responses accompanied by slight variations in gas exchange parameters, which may suggest a focus on hydraulic repair over photosynthesis. Approximate entropy analysis of the EEG signals revealed that *P. tomentosa*, under stress (drought and injury), shifts to more complex and unpredictable bioelectric dynamics. Conversely, complexity decreases following re-irrigation, indicating a more synchronized bioelectric response. In conclusion, the findings suggest that *P. tomentosa* may benefit from elevated CO_2 levels when water is sufficiently available. By adjusting their metabolic and morphological traits, young trees can withstand frequent and severe drought. Future research should thoroughly investigate how these environmental drivers interact and other factors like temperature to evaluate the species' adaptability under different climate scenarios. Additionally, this study introduces initial insights into the bioelectric responses of *P. tomentosa* to damaging stimulus and post-drought re-irrigation, providing valuable data that could advance early stress detection technologies in its cultivation.

Zusammenfassung

Bedenken bezüglich des Klimawandels haben das Interesse an der Verwendung schnell wachsender Bäume für nachhaltige Forstwirtschaft und CO_2-Reduktion geweckt. *Paulownia* spp. ist besonders vielversprechend aufgrund seines schnellen Wachstums und seiner Anpassungsfähigkeit an ungünstige klimatische und edaphische Bedingungen, was es beliebt für kommerzielle Plantagen und Aufforstungen macht. In diesem Kontext ist es entscheidend, Einblicke in die Anpassungsfähigkeit der Paulownia-Bäume an die global prognostizierten Klimabedingungen zu gewinnen. Diese Studie zielt in erster Linie darauf ab, die morphologischen, physiologischen und anatomischen Reaktionen junger *Paulownia tomentosa* auf erhöhte CO_2-Konzentrationen und zyklischen Trockenstress zu bewerten. Zweitens, die bioelektrische Aktivität dieser Bäume als Reaktion auf schädigende Reize und nachfolgende Bewässerung nach Trockenheit zu charakterisieren. Die Forschung umfasst drei Versuchsanordnungen: (1) Samengezogene Paulownien wurden einer CO_2-Konzentration von 950 ppm während einer Wachstumssaison ausgesetzt, um den Gasaustausch, anatomische Modifikationen des Stammes, die elementare Zusammensetzung von Schließzellen und Mesophyll-Chloroplasten sowie Wachstumsreaktionen zu beurteilen. (2) Dreijährige Bäume durchliefen wiederkehrende Trockenheitszyklen, um Gasaustausch, photosynthetische Effizienz, Blattpigmentzusammensetzung, hydraulische Architektur und Wachstumsanpassungen während einer Wachstumsperiode zu untersuchen. (3) Die bioelektrischen Reaktionen von dreijährigen Paulownia-Bäumen, die Verbrennungsschäden und der Rehydrierung des Bodens nach Trockenheit ausgesetzt waren, wurden mit interzellulären und extrazellulären (EEG) Methoden charakterisiert. Die Ergebnisse des CO_2-Experiments zeigen, dass bei *Paulownia*-Sämlingen, die bei erhöhtem CO_2 angebaut wurden, die Netto-CO_2-Aufnahme signifikant höher war. Gleichzeitig blieben stomatäre Leitfähigkeit und Transpiration unverändert, was die Wassernutzungseffizienz im Vergleich zu Pflanzen, die bei Umgebungs-CO_2 angebaut wurden, erhöhte. Die breiteren Stammgefäße deuteten auf einen verbesserten Wassertransport unter erhöhtem CO_2 hin. Erhöhte photosynthetische Aktivität und Veränderungen in der Holzanatomie führten zu einer höheren Wachstumsleistung, mit einem signifikant höheren Höhen- und Sprossbiomassezuwachs und einem zunehmenden Trend zur Wurzelbiomasse und Stammstärke. Trockenheit reduzierte im Allgemeinen die Netto-CO_2-Aufnahme, die stomatäre Leitfähigkeit und die Transpiration, erhöhte jedoch den Chlorophyll- und Anthocyangehalt und bewahrte so die

Photosyntheseaktivität in den frühen Stressphasen. Die Wassernutzungseffizienz blieb nach der Trockenheit aufgrund semi-konservativer Wasserstrategien höher. Durch Trockenheit gestresste Pflanzen entwickelten engere Gefäße, aber die Gefäßfrequenz nahm zu, was auf einen Trend zur hydraulischen Sicherheit hindeutet. Jedoch hatten wiederkehrende Trockenheitszyklen negative Auswirkungen auf Wachstumsparameter wie den gesamten Biomassezuwachs, Stammdurchmesser, Höhe und Blattzahl. Hinsichtlich der bioelektrischen Aktivität lösten schädigende Reize Depolarisations- und Hyperpolarisationsreaktionen in der Plasmamembran gesunder Blattzellen aus. Zusätzlich war die Aktivität durch Oszillationen des elektrischen Potentials der Blattstiele in distalen Blättern gekennzeichnet, zeitgleich mit Stomataschluss und reduzierter Photosynthese, was auf systemische Signalgebung hinweist. Während der Dunkelheit fielen die elektrischen Signale mit einer vorübergehenden Öffnung der Stomata und einer erhöhten Atmungsaktivität zusammen. Nach der Wiederbewässerung zeigten die Blattzellen hyperpolarisierende Reaktionen, begleitet von leichten Variationen in den Gasaustauschparametern, was auf eine Konzentration auf hydraulische Reparaturen über der Photosynthese hindeuten könnte. Die approximative Entropieanalyse der EEG-Signale ergab, dass *P. tomentosa* unter Stress (Trockenheit und Verletzung) zu einer komplexeren und unvorhersehbareren bioelektrischen Dynamik übergeht. Im Gegensatz dazu nimmt die Komplexität nach der Wiederbewässerung ab und deutet auf eine synchronisierte bioelektrische Reaktion hin. Zusammenfassend legen die Ergebnisse nahe, dass *P. tomentosa* von erhöhten CO_2-Niveaus profitieren könnte, wenn ausreichend Wasser verfügbar ist. Indem sie ihre metabolischen und morphologischen Eigenschaften anpassen, können junge Bäume häufige und schwere Trockenheit überstehen. Zukünftige Forschungen sollten gründlich untersuchen, wie diese Umweltfaktoren interagieren und andere Faktoren wie Temperatur berücksichtigen, um die Anpassungsfähigkeit der Art unter verschiedenen Klimaszenarien zu bewerten. Darüber hinaus bietet diese Studie erste Einblicke in die bioelektrischen Reaktionen von *P. tomentosa* auf schädliche Reize und die Wiederbewässerung nach einer Trockenheit, was wertvolle Daten liefert, die Technologien zur frühzeitigen Erkennung von Stress bei der Kultivierung von *P. tomentosa* verbessern könnten.

Table of contents

List of Figures

List of Tables

List of abbreviations

A	Net CO_2 uptake
aCO_2	ambient carbon dioxide
Anth	Anthocyanin
AP	Action potential
APa	Axial parenchyma
ApEn	Approximate entropy
Ca	Calcium
Chl	Chlorophyll
c_i	Intercellular CO_2 concentration
ci/ca	The ratio of intercellular CO_2 related to ambient CO_2 concentration
Cl	Chloride
dr	Drought-stressed plants
E	Transpiration
eCO_2	elevated carbon dioxide
EDX	Energy Dispersive X-ray microanalysis
EEG	Electroencephalogram
ES	Electrical signal
ETR	Electron transport rates
F	Fiber
FE-SEM	Field Emission Scanning Electron Microscopy
FFT	Fast Fourier Transform
Flv	Flavonol
Fv/Fm	The maximum quantum yield of the photosystem II
g_s	Stomatal conductance
IRGA	Infrared gas analyzer
K	Potassium
Ls	Stomata limitation value
Mg	Magnesium
NBI	Nitrogen Balance Index
NPQ	Non-photochemical quenching
P	Phosphorus
PM	Plasma membrane
ppm	Part per million
PSI	Photosystem I
PSII	Photosystem II
RP	Ray parenchyma
V	Vessel
VD	Vessel diameter
VF	Vessel frequency
VLA	Vessel lumen area
VP	Variation potential
S	Sulfur
SEM	Scanning electron microscopy
Sl	Stomata length
SD	Stomata density
SP	System potential
WUE	Water use efficiency

ww	Well-watered plants
Y(PSII)	The quantum yield of the photosystem II
Y(NO)	The quantum yield of the non-regulated energy dissipation
Y(NPQ)	The quantum yield of the non-photochemical quenching

1. GENERAL INTRODUCTION

Over recent decades, discussions regarding the human-induced impact on global warming have gained substantial momentum and attention. The core of the current concerns is linked to the rapid increase in atmospheric carbon dioxide (CO_2), which has propelled global surface temperatures to rise by over 1.1°C above pre-industrial times (Hampshire-Waugh, 2021). The climate models described in the most recent Intergovernmental Panel on Climate Change (IPCC) report project a temperature rise of 1.5°C to 4.4°C in the coming decades based on different emission scenarios (IPCC, 2023). The same report warned that surpassing the 1.5°C threshold increases the risk of more severe climate change impacts, increasing the intensity of agricultural and ecological droughts and associated wildfires (IPCC, 2023; United Nations Framework Convention on Climate Change, (n.d)).

Considering this issue, implementing adaptation and mitigation strategies becomes imperative to limit the temperature rise by 1.5°C. However, fulfilling the growing demand for wood products in this context represents a formidable challenge (Jakubowski, 2022). A recent study indicates that afforestation efforts with commercial purposes are feasible for climate change mitigation while simultaneously providing wood products (Forster et al., 2021). The study emphasizes that forest growth rate determines cumulative CO_2 mitigation. Therefore, there is a growing market interest in fast-growing tree species owing to their efficiency in biomass production, helping to achieve mitigation targets (Forster et al., 2021; Jakubowski, 2022).

Paulownia, a genus native to China and Southeast Asia, has become popular for integration into forest plantation technologies due to its adaptability to diverse soils and climates and its multiple ecological and economic advantages (Moreno et al., 2017). Several studies carried out on Paulownia species, and their hybrids have demonstrated their promising potential for carbon sequestration (Magar et al., 2018), phytoremediation of heavy metal-contaminated soils (Drzewiecka et al., 2021), use for biofuel (Domínguez et al., 2017; López et al., 2012), mixed pulp for paper production (Ates et al., 2008), lightweight wood applications (Barbu et al., 2022), and medicinal properties of high value extracts (Adach et al., 2020). Hence, Paulownia emerged as a versatile genus, presenting viable solutions to address global challenges across multiple domains.

The genus has been extensively integrated into intercropping systems in North China (Jensen, 2016) and in diverse plantation systems across a wide range of climatic regions worldwide, including Spain, Italy, Austria, Turkey, Israel, India, Japan, the United States, Canada, Mexico, and Brazil (Rodriguez-Seoane et al., 2020; Zuazo et al., 2013).

The growing economic importance and vast use of *Paulownia* sp. in reforestation efforts raises the need to understand its resilience and adaptability to the environmental changes foreseen for the next decades. This understanding could yield practical insights to enhance forestry practices and ecological conservation strategies.

The structure of this work is presented in (Figure 1-1).
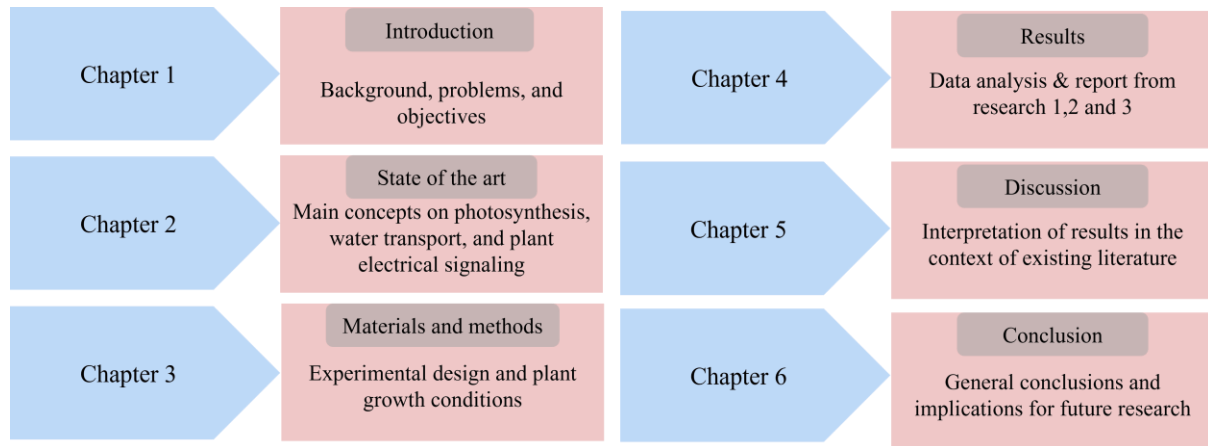
Figure 1-1 Thesis structure.

1.2. Objectives

Paulownia tomentosa is among the most cultivated species within the *Paulownia* genus (Ghazzawy et al., 2024). However, its physiological responses to the rising levels of CO_2 and the increased frequency of stress conditions such as drought remain understudied. Additionally, investigations into the electrophysiological responses of trees to different stress conditions are limited. Particularly, the bioelectric activity of *Paulownia tomentosa* subjected to stresses, such as localized damage, has not yet been evaluated. In this context, this study aims to provide information on the physiological acclimation and adaptative mechanisms of *Paulownia tomentosa* in response to elevated CO_2 (eCO_2) and drought stress. This study also aims to characterize electrical signaling in the species and its role in regulating essential physiological responses during localized damage and drought recovery.

1.3. Problems

1.3.1. Increasing atmospheric CO_2 concentration

Carbon dioxide is the key component of the so-called greenhouse gases (GHG). According to recent data from the NOAA Global Monitoring Laboratory (2024), atmospheric CO_2 levels recorded at the Mauna Loa observatory reached 423 ppm in August 2024, representing a 50% elevation from pre-industrial levels. By the end of the century, atmospheric CO_2 is projected to range between 430 to above 1000 ppm, depending on the specific RPC (Representative Concentration Pathway) scenario (IPCC, 2014).

Carbon dioxide is a critical substrate for photosynthesis and plays a key role in regulating essential physiological processes in plants, including stomatal conductance and transpiration. The interplay between stomatal parameters and water transport influences overall photosynthetic efficiency (Qaderi et al., 2019), highlighting the significance of vascular system development. This raises fundamental questions on the effects of elevated CO_2 on *Paulownia tomentosa*, such as how an increased atmospheric CO_2 concentration influences photosynthetic activity, stomatal behavior, and water use efficiency. Does an increase in CO_2 concentration affect the hydraulic architecture of *Paulownia tomentosa*? What are the effects of elevated CO_2 on the overall biomass yield of *Paulownia tomentosa*? And how do these relate to its photosynthetic performance and hydraulic structure?

To address these questions, we exposed seedlings of *Paulownia tomentosa* to an elevated atmospheric CO_2 concentration of 950 ppm for one growth season to assess alterations in gas exchange parameters, water use efficiency, hydraulic architecture, and biomass production. We propose that (1) elevated CO_2 stimulates photosynthesis and decreases stomatal conductance, enhancing water use efficiency in *Paulownia tomentosa*. (2) *Paulownia tomentosa* develops a more efficient hydraulic system under elevated CO_2, enhancing photosynthesis and final biomass production.

1.3.2. Increasing drought frequency and intensity

Ongoing warming is expected to intensify the global water cycle, potentially exacerbating drought severity in numerous regions across the globe (IPCC, 2021). For example, droughts that occurred once per decade in the 1850–1900 period are likely 1.7 times more frequent (IPCC, 2021). Each additional 1°C of warming could increase the risk of drought by 5-10% in drought-prone areas, such as the Southern US, the Mediterranean, and Africa (Hampshire-

Waugh, 2021). Therefore, terrestrial ecosystems and crops are already experiencing drought impacts due to warmer temperatures, which are expected to increase steadily.

Drought is the major abiotic factor affecting gross primary production and causing crop yield losses via its direct impacts on photosynthesis and indirectly via other associated stresses, such as wildfires and increasing plant's susceptibility to pests (Alemu., 2020; Schmitt et al., 2022; Xu et al., 2019). Species from the genus Paulownia have been introduced across numerous countries, increasing the probability of their exposure to drought conditions. *Paulownia tomentosa* is recognized as a resistant species to diverse environments. However, what physiological strategies contribute to its resilience in a changing climate? To investigate this issue, we exposed three-year-old trees to recurrent drought cycles. We tested gas exchange parameters, stomata variables, chlorophyll fluorescence, and leaf pigment composition in drought-acclimated leaves. The impacts of the drought cycles on the characteristics of the water transport conduits and biomass production were finally investigated.

Herein we propose that (1) cyclic episodes of drought significantly impair photosynthesis in *Paulownia tomentosa*, primarily by reducing stomatal conductance and photochemical efficiency, ultimately leading to diminished biomass production; (2) Photoprotective mechanisms, such as non-photochemical quenching and anthocyanins are activated under drought stress; (3) *Paulownia tomentosa* adjusts its hydraulic architecture by decreasing vessel size.

1.3.3. Plant electrical signaling and photosynthetic regulation

Despite lacking a central nervous system, plants continuously perceive environmental stimuli and adapt their physiological functions accordingly. They sense changing conditions at the cellular level via transmembrane-sensitive proteins, translating the physical signals into electrical and chemical signals to trigger physiological responses (Lamers et al., 2020). These signals can course through their structure, coordinating responses essential for survival and reproduction (Mudrilov et al., 2021; Osakabe et al., 2013). Electrical signals are a primary mechanism for rapid communication between cells and organs following stimulus perception (Fromm, 2006). These electrical currents originate from transient changes in the plasma membrane potential, driven by the activity of ion channels and H^+-pumps (de Oliveira et al., 2020; Fromm & Lautner., 2006; Szechyńska-Hebda & Karpiński., 2017).

Plant electrophysiology assays aim to decipher these signals' roles in many physiological and biochemical functions (Tran et al., 2019). Remarkable progress across different plant species

has been made in recent years, with studies demonstrating that electrical signals are intrinsically associated with photosynthetic regulation (Lautner et al., 2005; Surova et al., 2016; Vuralhan-Eckert et al., 2018), respiration (Lautner et al., 2013; Surova et al., 2016), changes in phloem translocation (Fromm & Bauer, 1994), alterations in gene expression (Mousavi et al., 2013), and biosynthesis of phytohormones (Dziubińska et al., 2003; Hlaváčková et al., 2006). However, research on plant electrophysiology has predominantly focused *on Mimosa pudica, Dionaea muscipula*, and agricultural plants, highlighting the need for a broader scope of studies to understand better the electrical behaviors across a more diverse range of plant species.

Concerns over the growing population and climate change have increased the need to implement new technologies to enhance agricultural and forestry practices. Recent research into plant electrical activity has been, therefore, also directed towards profiling bioelectric patterns to gain insights into plants' physiological states (Simmi et al., 2020; Tran et al., 2019; Saraiva et al., 2017), analogous to the use of technologies such as electrocardiograms (ECG) and electroencephalograms (EEG) in animals to monitor the bioelectric activity of the heart and brain (Fromm & Lautner., 2006; Tran et al., 2019).

In the context of monitoring plant bioelectric activity, several questions remain unanswered in this recently explored field. For example, can plant fitness be assessed in real time, providing new insights into plant physiology? To begin addressing this question, it is essential to characterize the basic bioelectric features of plants. This is particularly pertinent within the genus Paulownia, where research in this field remains largely undeveloped, highlighting a substantial gap in our knowledge. Understanding these bioelectric features may make it feasible to assess plant fitness promptly, enabling early detection of stress and contributing to the maintenance of plant health.

Therefore, this study aims to characterize the local and systemic electrical signaling of 3-year-old *Paulownia tomentosa* trees in response to burn damage and re-irrigation stimuli. Additionally, the study aims to investigate their role in the systemic physiological adjustments, including photosynthetic and respiratory activity and stomata movement in response to mechanical damage (local burn) and re-irrigation after drought stress exposure.

We hypothesize that (1) local damage generates bioelectrical responses in distal regions and (2) causes metabolic adjustments in healthy leaves. (3) Re-irrigation generates bioelectrical responses, (4) triggering stomata opening and uptake of CO_2 for photosynthesis. (5) The complexity of the extracellular signals varies significantly in response to the stimuli.

2. STATE OF THE ART

2.1. Overview of the plant responses to elevated atmospheric CO_2 concentrations

Plants play a key role in stabilizing the carbon budget and maintaining the carbon sink in terrestrial ecosystems (Xu et al., 2015), holding approximately 45% of the carbon within their above- and belowground biomass, as well as in the soils through litter fall and rhizodeposition (Waring et al., 2020). Each tonne of wood is estimated to sequester 1.5 tonnes of CO_2 from the atmosphere, accounting for emissions generated during processing (Hampshire-Waugh, 2021). Numerous studies highlight that the rising levels of atmospheric CO_2 may enhance carbon absorption through what is referred to as the "CO_2 fertilization effect" (Bastos & Fleischer., 2021; Choat et al., 2018), given that CO_2 is the primary substrate of photosynthesis, and, thus, a fundamental driver of biomass production (Gamage et al., 2018). Indeed, a recent analysis of over a hundred studies on plant growth responses to elevated CO_2 concentrations has shown a significant enhancement, with aboveground biomass increasing by 13% and belowground biomass by 12% (Han et al., 2023).

Enhanced photosynthesis is generally the foundation of the beneficial effects of elevated CO_2, especially in species carrying the C_3 metabolism. This occurs because (1) the enzyme ribulose 1,5-bisphosphate carboxylase/oxygenase (Rubisco) is not saturated with CO_2 at current atmospheric concentrations, and (2) an increase in the internal CO_2 concentration relative to O_2 around Rubisco can decrease its oxygenase activity, thereby reducing photorespiration and increasing the efficiency of carbon assimilation (Thompson et al., 2017; Zheng et al., 2019).

An additional generally recognized mechanism is the regulatory effect of increased CO_2 concentrations on stomatal dynamics, leading to a reduction in stomatal conductance (g_s). For instance, a comprehensive meta-analysis, which utilized the data from prolonged CO_2 exposure experiments involving 15 different European forest tree species, demonstrated that elevated CO_2 reduced g_s by 21% (Medlyn et al., 2001). More recently, a meta-analysis synthesizing data from 616 published studies on terrestrial ecosystems also reported a decrease in g_s in response to CO_2 enrichment, indicating that this response is consistent across a broad range of plant species (Liang et al., 2023).

According to the optimal stomatal theory, the stomata functions to optimize the balance between maximizing photosynthesis and minimizing water loss through transpiration, thereby achieving an ideal water use efficiency (Gardner et al., 2022). In parallel, optimal photosynthesis requires an adequate supply of water and minerals that are majorly conveyed through the transpiration stream, with the flow resistance defined by the hydraulic properties

of the xylem (Manzoni et al., 2013). The convergence of these factors fundamentally determines leaf functionality and, hence, plant biomass production and growth (Levesque et al., 2017; Manzoni et al., 2013).

Current research efforts have targeted photosynthetic CO_2 assimilation responses to climate change. Although rising atmospheric CO_2 generally leads to improved photosynthesis, results on g_s may vary depending on the specific environmental factors (temperature and air humidity) and species-specific stomata sensitivity. For instance, a Free-Air CO_2 Enrichment (FACE) experiment conducted on a plantation forest of *Pinus taeda* L. and *Liquidambar styraciflua* revealed no significant alterations in g_s in response to elevated CO_2 (Ellsworth et al., 2011). Differently, in a pot experiment, short-term exposure to eCO_2 increased g_s in *Arabidopsis thaliana* (Zinta et al., 2014).

Furthermore, there remains a lack of information about the effects of eCO_2 on the development of the vascular tissue of woody species. It is particularly important because stomatal conductance and water transport are interrelated, resulting in changes in overall photosynthetic processes (Qaderi et al., 2019). Within the genus Paulownia, the impact of eCO_2 on the xylem vessels has yet to be investigated. Research into physiological aspects like photosynthesis, stomatal behavior, and xylem structure under eCO_2 is essential for comprehending the adaptation of species and water regulation to changing atmospheric CO_2 conditions.

2.2. Overview of the plant responses to drought stress

Since plants are sessile, they are continuously exposed to various environmental stressors, among which drought is the most significant threat. This is particularly substantial because water is the predominant component of actively metabolizing organisms, and essential biochemical reactions require water (Kathpalia & Bhatla., 2018). Drought is meteorologically defined as a period characterized by insufficient rainfall that reduces soil moisture and increases evapotranspiration (Menga, 2023), resulting in sustained water loss through transpiration (Bandurska, 2022). At the cellular level, reducing water content significantly impairs physiological activities, reproduction, and overall productivity (Bandurska, 2022). Drought was responsible for the hydraulic collapse and dieback of conifers (Arend et al., 2021) and trees from tropical rainforests (Rowland et al., 2015), representing the main route to widespread plant mortality in short timescales (Cardoso et al., 2020; Choat et al., 2018). In the agricultural context, drought is estimated to account for over 50% of global yield losses (Skirycz & Inzé, 2010).

To counteract stress and survive adverse conditions, plants have evolved adaptive responses summarized in drought escape, avoidance, and tolerance (Kooyers, 2015; Skirycz & Inzé, 2010). Drought escape refers to the strategy where plants accelerate their development and reproduction to complete their life cycle before drought conditions intensify (Kooyers, 2015). Conversely, drought avoidance involves plants enhancing their water use efficiency (WUE), thereby reducing transpiration and limiting vegetative growth to prevent dehydration during temporary periods of drought stress (Kooyers, 2015). Stress tolerance encompasses mechanisms that enable plants to cope with prolonged stress conditions. These include the synthesis of metabolites that mitigate the damage from osmotic stress, thereby maintaining plant functions and facilitating damage repair once the stress is alleviated (Bandurska, 2022). Drought avoidance and tolerance are stress resistance mechanisms that are particularly beneficial during growing seasons marked by episodic droughts.

Plants exposed to drought experience increasing stress intensity across the stages: (1) At the initial, mild level, physiological traits are minimally affected; (2) at a moderate level, the root system cannot sufficiently replenish water lost through transpiration, prompting the onset of stomatal regulation; (3) at a severe level, water availability drops to a point where productive functions are unsustainable, forcing the plant into survival mode (Vadez et al., 2024).

The responses to drought vary based on the duration and severity of the exposure. In the short term, drought impacts include a gradual cessation of photosynthesis, reduced canopy cooling via transpiration, and increased photodamage risk (Choat et al., 2018). Over longer periods, effects include increasing depletion of non-structural carbohydrate reserves (Choat et al., 2018). Additionally, there is an activation of coping mechanisms such as ROS scavengers and accumulation of osmotically active metabolites, which reduce the energy and nutrients available for growth but enhance plant resilience, which is crucial for withstanding prolonged periods of drought and recovering once water becomes available again (Bandurska, 2022). Persistent drought can lead to mortality due to carbon starvation or embolism spread through the vascular network (systemic embolism), resulting in hydraulic failure (Choat et al., 2018).

Resistance to drought, therefore, involves optimizing water use while sustaining photosynthetic activity (Bandurska, 2022; Hu et al., 2023), restricting the risk of hydraulic failure, and successfully recovering from critical states (Choat et al., 2018), which is particularly challenging in adult trees. Maintaining the integrity of the water transport may arise from short-term acclimation and indicates adaptive plasticity that leads to structural remodeling, which

varies among species. This may include adjustments of leaf area, leaf shedding, cuticular conductance, stomatal anatomy, root-to-shoot ratio, and xylem anatomical traits (Choat et al., 2018). Recovery encompasses restoring hydraulic functionality by refilling embolized vessels and reactivating the meristematic activity to produce new vascular tissue (Choat et al., 2018). Acclimation and recovery are considered key aspects of resilience, comprising the capacity of plants to endure and sustain their physiological functions among disturbances (Gessler et al., 2020).

Understanding tree responses to drought stress is essential for gaining insights into adaptive strategies and enhancing the accuracy of predictions regarding how trees will respond to drought, thereby improving our understanding of their resilience under future climatic conditions.

2.3. Aspects of water transport in higher plants

Plant growth and survival depend on their ability to regulate the synthesis of carbohydrates and prevent dehydration (McElrone et al., 2013; Qaderi & Dixon, 2019). Through stomata opening, CO_2 diffuses from the atmosphere, transverse structures present in the mesophyll tissue, and ultimately reaches the carboxylation sites of Rubisco in the stroma. Simultaneously, a vapor concentration gradient between the humid air spaces inside the leaf and the relatively arid external atmosphere drives the diffusion of water vapor from the leaf into the surrounding air (Kathpalia & Bhatla, 2018). Although less than 5% of absorbed water is utilized for cellular metabolism and growth, the vast majority is expelled as vapor during stomatal opening for CO_2 uptake, a process referred to as transpiration (Venturas et al., 2017; Walker et al., 2016). The transpiration of terrestrial plants plays a crucial role in the global water cycle, contributing to about 30% of annual precipitation (Beerling & Franks, 2010). At the leaf level, up to 400 molecules of water are lost for each CO_2 molecule absorbed (McElrone et al., 2013), presenting a dilemma, as regulating water loss by reducing stomatal aperture can constrain photosynthesis by impeding CO_2 diffusion from air to chloroplast stroma. Thus, plants modulate their water use through their metabolism and hydraulic traits. In trees, where water transport occurs over long distances, transpiration is the predominant driving force for the vast volume of ascent of sap at little energetic cost (Choat et al., 2018), with stomatal and xylem characteristics being key elements determining the hydraulic conductance, the maximum transpiration rates (Fichot et al., 2009), and finally, the acclimation to the environment and survival.

2.3.1. The structure of the secondary xylem: Aspects of the long-distance water transport and flow strategies

The secondary xylem, a highly specialized vascular tissue, develops from the centripetal activity of the vascular cambium, which responds to environmental factors (Qaderi et al., 2019). It comprises a short- and long-distance transport network and provides essential mechanical support to the plant structure (Eckert et al., 2019). In angiosperms, the cambial derivatives differentiate into ray and axial parenchyma cells, fibers, vessel elements, and occasionally tracheid, resulting in a multicellular network (Janssen et al., 2020). Vessels are formed via programmed cell death, establishing a long-distance pathway for transporting water, minerals, and organic molecules (Qaderi et al., 2019). Fibers primarily provide structural support, while the parenchyma tissue plays a role in the short-distance translocation of water and nutrients and the storage of non-structural carbohydrates (Janssen et al., 2020). Ray parenchyma cells have also been demonstrated to play a role in refilling embolized vessels in *Vitis vinifera* (Brodersen et al., 2010).

Due to the tension-driven movement of the water column within the xylem, trees must sustain water potential above a critical threshold to prevent cavitation and subsequent air blockage of the conduits and crown dehydration. Studies have demonstrated that the anatomical structure of the xylem is intricately linked to its hydraulic functions. For instance, a recent meta-analysis assessing the xylem traits and hydraulic properties of neotropical trees showed that an increased fraction of axial parenchyma and fiber lumen is associated with higher water transport efficiency and lower resistance to embolism (Janssen et al., 2020). In contrast, trees with xylem consisting of thick-walled fibers exhibit greater embolism resistance, highlighting significant trade-offs between hydraulic efficiency and safety (Janssen et al., 2020).

Vessel diameter, length, and properties of inter-vessel pits also impact the trade-offs between hydraulic safety and efficiency (Janssen et al., 2020; Hacke et al., 2000). According to the Hagen-Poiseuille equation, hydraulic conductivity increases with the 4th power of the vessel diameter (Rodriguez-Zaccaro & Groover, 2019); therefore xylem sap transport enhances with increasing vessel size (Sorce & Anfodillo, 2013). Conversely, vessels with narrower diameters limit water transport but have been associated with embolism resistance. For example, *Quercus robur* trees that survived drought stress exhibited smaller vessels in their growth rings compared to those that died, suggesting that larger vessel sizes may contribute to the trees' vulnerability (Levanic et al., 2011). In *Syzygium aromaticum*, the membrane area of inter-

vessel pits decreased with vessel size under drought, improving tree resistance to embolism (Liu et al., 2023). Therefore, while a reduced pit membrane area may increase water flow resistance, an increased total membrane area could presumably raise the likelihood of forming 'leaky' pits with larger membranes, thus increasing the risk of air-seeding and its spread (Christiman et al., 2009). This refers to the 'rare pit' theory.

The 'air-seeding' hypothesis states that xylem cavitation occurs when the tension in the water column exceeds a critical threshold, leading to the aspiration of a gas bubble across a pit membrane (Venturas et al., 2017). Eventually, increasing tension leads to an expanding air bubble, resulting in embolism and interruption of the continuous transpiration stream. Embolized vessels negatively affect tree hydraulic conductivity (Nikinmaa et al., 2014) and can lead to hydraulic failure during extended drought and high transpiration demand.

Thus, vessel characteristics reflect a compromise between maximizing water transport efficiency and minimizing the risk of hydraulic failure (Rodriguez-Zaccaro & Groover, 2019). These traits may be dynamically adjusted in response to environmental oscillations during the tree life span.

2.3.2. Aspects of the stomata regulation

Stomata, microscopic pores on the leaf surface, are central players in gas exchange between plants and the atmosphere, as well as for leaf functionality, regulating photosynthesis and leaf temperature by releasing water vapor (Wang et al., 2022). They function as valves decelerating the progression of the xylem toward extreme tensions, essential for preserving the functionality of the hydraulic system. Stomata pores are surrounded by two guard cells and subsidiary cells, comprising the stomata complex. Guard cells are responsive to various environmental stimuli, including light, soil moisture levels, the concentration of CO_2 within the leaf intercellular spaces, and toxins (Lima et al., 2018; Singh et al., 2017). These stimuli induce changes in the osmotic pressure within guard cells, thus regulating the opening and closing of the stomata pore through the fluxes of osmotically active ions across specific ion channels and transporters (Lima et al., 2018; MacRobbie, 2006). Phototropins in guard cells are activated through autophosphorylation upon the perception of blue light. Activated phototropin phosphorylates the BLUE LIGHT SIGNALING1 (BLUS1) (Kollist et al., 2014), generating signaling that leads to the phosphorylation of a penultimate threonine residue (pT) of the plasma membrane (PM) H^+- ATPase, the subsequent binding of a 14-3-3 protein and activation of the pump

(Kollist et al., 2014; Toda et al., 2022). Consequently, pumping H^+ ions out of the cytoplasm leads to apoplast acidification, hyperpolarizing the PM and activating the inward-rectifying K^+ channels (Taiz & Zeiger, 2010). Increased cytosolic K^+ concentrations are counterbalanced by the uptake of counter-ions such as Cl^-, NO_3^-, and malate^{2-}. Accumulation of these ions reduces the water potential within the guard cell necessary for water influx and the subsequent increase in turgor pressure required for stomatal opening (Agurla et al., 2018; Kollist et al., 2014; Roux & Leonhardt, 2018). In contrast, stomatal closure is caused by reduced activity of the H^+-ATPase (Osakabe et al., 2013), coupled with abscisic acid (ABA)-induced activation of protein kinases such as OPEN STOMATA1 (OST1), Calcium-dependent protein kinase (CPK), and GUARD CELL HYDROGEN PEROXIDASE1 (GHR1), activating the PM anion channels (Kollist et al., 2014). Efflux of anions leads to a PM depolarization event that activates the outward-rectifying K^+ channels, reducing the osmotic turgor pressure within the guard cells and closing the stomata (Bahtla, 2018; Daszkowska-Golec & Szarejko, 2013; Roux & Leonhardt, 2018).

Stomata exhibit responsiveness to environmental disturbances that impact plant water potential, with the degree of sensitivity being an important aspect of plant resilience to abiotic stress. For instance, during soil drought, root mechanosensitive proteins detect turgor loss (Huber & Bauerle, 2016; Silva et al., 2020), triggering signals that stimulate ABA biosynthesis in plastids across local and systemic regions. ABA is transported to guard cells, initiating the depolarization event that leads to stomata closure (Osakabe et al., 2013), enhancing plant resistance to the stress factor (Kalra & Bhatla, 2018). Plants may close stomata in response to elevated CO_2 through the conversion of CO_2 into bicarbonate (HCO_3^-) by the catalytic activity of the beta Carbonic Anhydrases βCA1 and βCA4, promoting the inhibition of the HIGH LEAF TEMPERATURE1 (HT1) and activation of the OST1 (Kollist et al., 2014; Ma & Bai, 2021).

2.4. Photosynthesis

During photosynthesis, plants harvest solar radiation and atmospheric CO_2 to synthesize high-energy organic molecules essential for their metabolic functions and growth (Blankenship, 2021). This process is recognized as the foremost mechanism of primary production in the biosphere, providing the building blocks for the sustenance of living organisms. Approximately 50 billion tonnes of carbon are fixed by terrestrial photosynthesis (Running, 1986), also emphasizing its valuable contribution to the global carbon cycle.

Photosynthesis is broadly defined as the process through which green plants convert inorganic raw materials (CO_2 and H_2O) into organic compounds and release oxygen (O_2) to the atmosphere under the action of light (A. Lal, 2018; Blankenship, 2021). This process is carried out in the chloroplast and encompasses two intercorrelated reactions widely recognized as photochemical and biochemical phases. The processes are emphasized in the global equation:

$$6CO_2 + 12H_2O + \text{light energy} \longrightarrow C_6H_{12}O_6 + 6O_2 + 6H_2O$$
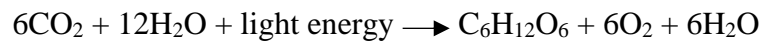
Photochemical reactions take place in the extensive membrane system found within the chloroplast, known as the thylakoid membrane, and the biochemical reaction is carried out in the medium contained in the interior of the chloroplast, known as stroma (A. Lal, 2018; Blankenship, 2021).

2.4.1. First phase of photosynthesis: Photochemistry

The photochemical phase is the primary step of the photosynthetic process. It is carried out by four multi-subunit protein complexes embedded in the thylakoid, including the photosystem II (PSII), photosystem I (PSI), the cytochrome b_6f, and F-type ATPase (CF1 CF0-ATP synthase) (Figure **2-1**) (Nevo at al., 2012). Electrons generated through the catalytic oxidation of water by PSII are transferred to PSI via the plastoquinone/plastoquinol (PQ) pool, cytochrome b_6f, and plastocyanin (PC). From PSI, electrons are transported to ferredoxin and ultimately to nicotinamide adenine dinucleotide phosphate ($NADP^+$) to generate the reductant NADPH (Nevo et al., 2012; Rochaix, 2011). During electron transport, an electrochemical gradient is generated across the thylakoid membrane due to both water photolysis and oxidation of plastoquinol (PQH_2) by the cytochrome b_6f, which leads to the accumulation of H^+ ions in the thylakoid lumen. This proton-motive force drives the synthesis of adenosine triphosphate (ATP) via the ATP synthase (Nevo et al., 2012). Thus, photochemistry converts light energy into utilizable chemical energy forms, such as NADPH and ATP. These molecules are subsequently used to power CO_2 assimilation during the biochemical phase in the stroma (A. Lal, 2018).

The photochemical phase is generally divided into light absorption, electron transfer in reaction centers, and energy stabilization (Blankenship, 2021). Photons are primarily absorbed by the pigment-protein antenna complexes (or light harvest complexes) LHCII and LHCI associated with PSII and PSI, respectively (A. Lal, 2018). These complexes comprise chlorophylls,

carotenes, and xanthophylls (accessory pigments) that absorb photons across the visible light spectrum. The carotenoids absorb photons in the blue-green light range (400-450 nm), while the chlorophylls absorb light in the blue and red ranges (400nm and 700 nm). Excited chlorophyll molecules in Light-Harvesting Complexes II (LHCII) and I (LHCI) transfer excitation energy via resonance to their respective reaction centers (RCs: P680 and P700), raising the RCs from the ground to an excited state, thereby initiating the primary photochemical reactions (A. Lal, 2018; Stirbet et al., 2019). The coordinated light reactions establish a non-cyclic electron transport chain, with electrons donated to $NADP^+$ replenished by electrons from water oxidation (A. Lal, 2018). Electrons may be redirected from Photosystem I (PSI) back to the PQ pool, promoting proton translocation into the thylakoid lumen, and enhancing the proton gradient across the thylakoid membrane (Roach et al., 2014). This mechanism is defined as cyclic electron flow and typically occurs to balance the production of ATP and NADPH under normal growth conditions (A. Lal, 2018). Cyclic electron flow contributes to the acidification of the thylakoid lumen, which is necessary to activate photoprotective mechanisms under high light intensity and low carbon assimilation, conditions that reduce the availability of $NADP^+$ and ADP (A. Lal, 2018; Takahashi et al., 2008).

Figure 2-1 The spatial arrangement of the major protein complexes in the thylakoid membrane. The figure was taken from Blankenship (2021, p.8). [Re-used with permission from Wiley Books, license number: 5740380732200].
Chlorophyll and accessory molecules associated with the light harvest complexes from PSII (LHCII) and PSI (LHCI) absorb photons and funnel excitation energy to their respective reaction center chlorophylls (P680 and P700). P680 is oxidized by pheophytin (chlorophyll molecule lacking Mg^{2+}), which then sequentially transfers the electron to plastoquinone A (QA) and to plastoquinone B (QB). QB requires two electrons from QA to be fully reduced to PQ^{2-}, which occurs in two steps. PQ^{2-} picks up two H^+ ions from chloroplast stroma to form PQH_2. PQH_2 is oxidized by Cyt *b6f*, releasing two H^+ ions in the thylakoid lumen, transferring one electron to P700 via

14

plastocyanin (PC) and another back to Qi (plastoquinone binding site in Cyt *b6f*) to subsequent form new PQH_2. The electron lost by P680 is replaced through water oxidation by the oxygen-evolving complex (Mn_4CaO_5), where Yz (Tyr 161) is the responsible electron transporter. In PSI, the electron received by Cyt *b6f* is transferred to A0 (Chl a-like molecule), then to phylloquinone, to the iron-sulfur cluster proteins FX, FA, and FB, and ferredoxin (Fd), where it is finally transferred to $NADP^+$ through the catalytic activity of the ferredoxin-NADP reductase (FRN). The proton motive force generated during the electron transport chain drives ATP synthesis via the ATP synthase's rotational catalysis.

Light absorbed by chlorophylls can (1) drive photochemistry, (2) dissipate into heat, and (3) be re-emitted as fluorescence (Maxwell & Johnson, 2000). These three light pathways occur in competition, dynamically changing with light intensity and leaf health status. Chlorophyll fluorescence, resulting from excited chlorophyll decaying to its ground state and emitting longer-wavelength photons, generally accounts for 3-6% of plant light dissipation (A. Lal, 2018). Photochemistry reactions must occur faster (usually in picoseconds) for efficient photosynthesis (A. Lal, 2018). Given the inverse relationship between the efficiency of one of these three processes and the yield of the other two, chlorophyll fluorescence methods are useful for assessing photochemical efficiency.

A decrease in chlorophyll fluorescence due to the photochemical process refers to photochemical quenching, whereas non-photochemical quenching (NPQ) describes a reduction unrelated to photochemistry (Malnoe, 2018). Stress conditions can disrupt light-dependent processes, leading to PSII overexcitation and NPQ activation. NPQ mechanisms protect the D1 protein (a component of the PSII complex) from excessive degradation due to increased ROS production, helping to prevent photoinhibition (A. Lal, 2018).

Zeaxanthin, synthesized from violaxanthin via the xanthophyll cycle, is an important non-photochemical quenching mechanism. It is triggered upon acidification of the thylakoid lumen, which, in turn, activates the violaxanthin de-epoxidase, converting violaxanthin into antheraxanthin and, ultimately, to zeaxanthin (Takahashi et al., 2008). Zeaxanthin accepts excess energy from excited chlorophylls when reaction centers are closed (primary electron acceptors are already reduced), dissipating this energy as heat and preventing the formation of singlet oxygen (A. Lal, 2018). Photoprotective molecules also include pigments such as flavonoids (e.g., anthocyanins and flavonols), which protect plants by absorbing excess light and scavenging reactive oxygen species (Daryanavard et al., 2023; Xu & Rothstein., 2018).

2.4.2. Second phase of photosynthesis: Carbon assimilation

The biochemical phase of photosynthesis encompasses the fixation of CO_2 through distinct photosynthetic pathways, such as C_3, C_4, and Crassulacean Acid Metabolism (CAM) (Ghazzawy et al., 2024). Species utilizing C_3 metabolism, including those of the *Paulownia* genus, account for 85% of global plant diversity (Ghazzawy et al., 2024). Recent findings regarding physiology, biochemistry, and transcriptional levels of *Paulownia fortunei* have prompted the hypothesis that its rapid growth could be attributed to a combined C_3 and CAM metabolic integration, given the opening of the stomata during the night and increased activity of the enzyme phosphoenolpyruvate carboxylase (PEPC) (Cao et al., 2021). Nonetheless, additional research is required to substantiate this characterization (Young & Lundgren., 2022).

In C_3 photosynthesis, CO_2 fixation initiates via the Calvin-Benson-Bassham (CBB) cycle, yielding a three-carbon molecule as the initial fixed carbon compound. Conversely, CAM plants undertake nocturnal CO_2 fixation into bicarbonate (HCO_3^-) via the enzyme carbonic anhydrase. HCO_3^- is used as a substrate for the carboxylation of phosphoenolpyruvate to form oxaloacetate (OAA), catalyzed by the enzyme PEPC (A. Lal, 2018). OAA is subsequently reduced by the enzyme malic acid dehydrogenase to form malate, which is stored in the vacuole as malic acid (A. Lal, 2018). During daylight, malate is metabolized into pyruvate and CO_2; the latter is trapped within the leaf owing to stomatal closure and, thus, assimilated into the CBB cycle (Ghazzawy et al., 2024).

The CBB cycle involves 13-enzyme-catalyzed reactions occurring in the chloroplast stroma, with the enzyme Rubisco (ribulose 1,5-bisphosphate carboxylase/oxygenase) being central to the process (A. Lal, 2018; von Caemmerer, 2020). The culmination of the CBB cycle leads to the synthesis of triose phosphates, which are further utilized for the synthesis of complex organic compounds, including sugars, polysaccharides, and various metabolites and hormones necessary for plant development, growth, and health (A. Lal, 2018; von Caemmerer, 2020).

In the initial stage of the CBB cycle, CO_2 is condensed with its acceptor molecule Ribulose - 1,5- bisphosphate (RuBP) by Rubisco catalytic function, yielding an unstable six-carbon intermediate that immediately splits into two molecules of 3-phosphoglycerate (3-PGA). After this, the reduction phase initiates as phosphoglycerate kinase catalyzes the phosphorylation of 3-GPA to 1,3-bisphosphoglycerate (BPG), utilizing ATP generated from photochemistry. The conversion of BPG to glyceraldehyde 3-phosphate (G3P) is then catalyzed by NADPH-specific glyceraldehyde 3-phosphate dehydrogenase (A. Lal, 2018; Macdonald, 1987). Among six triose phosphate molecules produced, five are cycled back, undergoing a sequence of

condensation, isomerization, and rearrangement processes to regenerate three RuBP molecules using ATP, thereby continuing the CO_2 assimilation process (Macdonald, 1987). The remaining triose phosphate molecule can be either converted into transitory starch or transported to the cytosol in exchange for Pi for sucrose biosynthesis, which can be either used in cellular metabolism or translocated to sink tissues (A. Lal, 2018; Verbančič et al., 2018).

In addition to catalyzing the carboxylation of RuBP, Rubisco has an active site for oxygenation, resulting in the formation of a carbon intermediate that subsequently splits to produce one molecule of 3-GPA and another of the inhibitory 2-phosphoglycolate (2-GP) (A. Lal, 2018). The detoxification of 2-phosphoglycolate occurs via the photorespiratory pathway, involving enzymatic reactions in the chloroplast, peroxisome, and mitochondria to convert it into 3-PGA (Aroca et al., 2023; Fu et al., 2022). Rubisco catalyzes reactions with either CO_2 or O_2 depending upon their relative concentration in the microenvironment of the leaf. Generally, under normal conditions, oxygenation occurs at a rate of 25% (A. Lal, 2018). From the commercial point of view, photorespiration is considered a wasteful process because it consumes ATP during the conversion of glycerate to 3-PGA, and releases previously fixed CO_2 during the conversion of glycine to serine, reducing the overall efficiency of photosynthesis (A. Lal, 2018). On the other hand, it can benefit the plant under stress conditions by consuming excess electrons, contributing to energy dissipation and photoinhibition prevention (A. Lal, 2018; Busch et al., 2017). Additionally, photorespiration is a primary route for glycine and serine biosynthesis, which can be exported and incorporated into leaf proteins and metabolites, supporting downstream metabolic pathways beyond the C_3 cycle (Fu et al., 2022).

2.4.3. Assessing plant gas exchange

Following the identification of Rubisco's dual functionality, its biochemical characteristics have been foundational in developing mechanistic mathematical models for photosynthetic CO_2 assimilation, connecting the kinetic of Rubisco with leaf gas exchange processes (von Caemmerer, 2020). Theoretical models for understanding how plants assimilate carbon, particularly the Farquar, von Caemmerer and Berry are applied across scales to predict CO_2 assimilation on individual leaves to global ecosystems (Busch et al., 2017). Leaf net carbon assimilation can be measured using an infrared gas analyzer (IRGA), representing the balance between CO_2 fixed through photosynthesis and lost via photorespiration and mitochondrial respiration (Douthe et al., 2018). The technique additionally allows for indirect measurement of stomatal movement, inferred from water vapor exiting the leaf. Its precision and portability

make it a powerful tool in plant biology to assess leaf gas exchange dynamics (Douthe et al., 2018).

Currently, most gas exchange systems employ an 'open' configuration, utilizing infrared wavelengths to detect differences in CO_2 and water vapor concentrations between reference and sample airflows. This provides insights into the biochemical processes dynamically occurring in the leaf (Busch et al., 2024). Knowing the gas flow rate into the system and the leaf surface area enclosed in the sample chamber, it is possible to assess the net CO_2 uptake (*A*) and transpiration rates (*E*) (LI-COR, 2012).

2.5. Aspects of electrical signaling in plants

Plants constantly interact with their surroundings (de Oliveira et al., 2020). This condition led to the evolution of short and long-distance mechanisms that rapidly transmit information and trigger specific physiological adjustments in distal organs of the plant body (Mudrilov et al., 2021). These signals are displayed in different forms, including hydraulic waves (transmission of changes in turgor pressure), chemical signals (e.g., phytohormones and reactive oxygen species), and electrical signals (fluctuations in the electrochemical properties of the membranes) (Mudrilov et al., 2021; Volkov, 2012).

Electrical signals are characterized by rapid changes in the cell's plasma membrane potential. They transmit information more rapidly across extended ranges than chemical signals, making them an essential component of plant systemic signaling (Fromm & Lautner, 2006). Upon generation, these signals are propagated from the site of stimulus perception through the plant's vascular system (xylem and phloem) (Volkov, 2012; Szechyńska-Hebda & Karpiński., 2017).

2.5.1. Types of electrical signals in plants

The membrane potential is the electrochemical difference between the cytoplasmic and apoplastic media. In plants, the plasma membrane (PM) H^+-ATPase generates a proton motive force by pumping H^+ ions out of the cytosol, leading to the acidification of the apoplast and a membrane potential of about -150 mV (Bhatla, 2018; Sze & Palmgren, 1999), which is crucial for cellular functionality (Serre et al., 2021). Transient alterations in the PM potential are driven by shifts in the activity of H^+-ATPases and ion channels, modulating the flux of ions, predominantly K^+, Ca^{2+}, and Cl^- (de Toledo et al., 2019; Sukhova & Sukhov, 2021). In plant

electrophysiology, different types of electrical signals have been described, including the local electric potential (LEP), the rapid action potential (AP), the slow wave variation potential (VP), and, more recently, the system potential (SP) (Fromm & Lautner., 2006; Sukhova & Sukhov, 2021). The term "electrome" has also been proposed in plants to describe the sum of the complex network of ionic currents generated by various compartments of the system, including mitochondria and chloroplasts, which produce overlapping low-amplitude electrical signals across time and space (Parise et al., 2022; Saraiva et al., 2017).

Local electrical potentials in plants are characterized as subthreshold electrical responses caused by a brief H+-pump inactivation (Parise et al., 2022). They exhibit limited propagation, typically extending only a few millimeters (Sukhova & Sukhov, 2021).

APs are characterized by the "all-or-none" principle, whereby initiation occurs only upon the membrane potential surpassing a specific threshold. APs propagate with consistent amplitude and speed, with common rates ranging from 0.5 to 20 cm s^{-1} (Gallé et al., 2015; Vuralhan-Eckert et al., 2018). They are triggered by non-damaging stimuli, exhibit self-propagation, and are characterized by a refractory period during which the generation of subsequent APs is temporarily inhibited (Mudrilov et al., 2021; Tran et al., 2019). Propagation of APs occurs via symplastic connections of adjacent cells within the phloem (Fromm, 2006). The underlying mechanism of action potentials involves a transient depolarization, initiated by the activation of voltage-dependent Ca^{2+} channels, leading to an influx of Ca^{2+} ions into the cytoplasm, which in turn activates anion channels and transiently inactivates the H^+-ATPase (Mudrilov et al., 2021; Sukhova et al., 2023). This depolarization event initiates the activation of outward-rectifying K^+ channels and concurrent closure of Ca^{2+} channels, resulting in the inactivation of anion channels and reactivation of H^+-ATPase (Sukhova et al., 2023). These events collectively culminate in the repolarization phase (Sukhova et al., 2023).

VPs represent a unique class of electrical signals specific to plant systems (Sukhova & Sukhov., 2021). They are typically induced by localized tissue damage and do not conform to the "all-or-none" principle; their amplitude and duration vary with the stimulus intensity and undergo attenuation relative to the distance from the point of stimulus perception (Sukhova & Sukhov., 2021; Fromm & Lautner, 2006). VP is distinguished by an initial depolarization and a prolonged repolarization phase associated with a long-term increase in the cytoplasmic Ca^{2+}, which leads to a transient inactivation of the H^+- pump (Sukhova et al., 2023). During this depolarization wave, AP-like spikes are occasionally observed and constitute an additional feature of the VP (Sukhova et al., 2023; Sukhova & Sukhov, 2021). Although the basic

characteristics of VPs have been described, their propagation mechanism is still a subject of debate. VP is regarded as a local electrical reaction triggered by the spread of non-electrical signals (Sukhova et al., 2021; Sukhova et al., 2023). It is proposed that a wounding substance produced at the site of damage propagates through the xylem via hydraulic dispersion and turbulent diffusion, activating ligand-dependent Ca^{2+} channels on the path (Fromm & Lautner., 2006; Pavlovic, 2012; Sukhova et al., 2021; Sukhova & Sukhov., 2021). A second hypothesis refers to hydraulic waves initiated by a local pressure increase in the damage zone, which may affect mechanosensitive Ca^{2+} channels, further initiating the depolarization wave (Fromm & Lautner., 2006; Sukhova et al., 2021).

The system potentials (SPs) are the least studied plant ESs (Mudrilov et al., 2021). It is generally characterized as a hyperpolarization wave in response to several stressors, with varying shape and duration depending on the stress severity and distance from the site of damage. Because some of these features are also observed in VPs, it is believed that both ESs may be closely associated (Sukhova et al., 2023). The generation of SPs is believed to be linked to the activation of the H^+-ATPase in the plasma membrane, in which the nature is still unknown. It has been suggested that a small amplitude hydraulic signal may cause a slight to moderate elevation of cytoplasmic Ca^{2+} levels through activation of mechanosensitive Ca^{2+} channels (Sukhova et al., 2023). The hyperpolarization process may also involve inactivating inward-rectifying K^+ channels, reducing K^+ influx into the cell (Lautner et al., 2005; Sukhova et al., 2023).

2.5.2. Assessing the plant electrical signals

Research on plant electrophysiology mostly elucidates the basic properties of electrical signals in individual cells, like amplitude, velocity, and propagation (Tran et al., 2019). The intracellular approach enables a detailed investigation of specific cells' membrane potential and electrical signals. On the other hand, the duration of this technique is constrained due to the potential leakage of glass electrode electrolytes, which can alter the original bioelectric activity of the analyzed cell (Fromm & Lautner., 2006; Macedo et al., 2021). Extracellular methods quantify the changes in the external electrical fields of large groups of cells using surface or inserting electrodes (Fromm & Lautner., 2006; Li et al., 2021). These techniques offer the advantage of improving the temporal resolution of bioelectrical recordings, permitting the integration of other systems to simultaneously measure additional physiological activity for extended periods (Fromm & Lautner., 2006).

2.6.   Overview of the genus Paulownia

Paulownia belongs to the monogenetic family Paulowniaceae, previously assigned to Bignoneaceae and Scrophulariaceae (Scheneiderová & Šmejkal, 2014). The genus comprises at least nine species of flowering trees, including *P. albphloea*, *P. australis*, *P. elongata*, *P. fargesii*, *P. fortunei*, *P. kawakamii* and *P. tomentosa* (Zhu *et al.,* 1986), which naturally distributed in China and Southeast Asia (Rodriguez-Seoane et al., 2020).

Historical records dating back to 1049 B.C. describe the virtues of Paulownia timber and cultivation, which could make it the oldest plantation tree in the world (Jensen, 2016). Ancient texts commenting on the cultivation of Paulownia farming indicate the long-standing recognition of Paulownia's value in China (Jensen, 2016). In recent decades, an expanding scientific literature has delineated the potential and benefits of Paulownia for ornamental and commercial uses (Lugli et al., 2023). Despite its restricted natural distribution, the genus comprises highly adaptable pioneer species capable of thriving across various climates and soils (Jensen, 2016). Paulownia species stand out as highly adaptable trees for various applications, considering the broad spectrum of products and services they offer (Jensen, 2016). Paulownia can develop in temperatures from − 20°C to + 40°C, at altitudes up to 2000 meters, and in saline or nutrient-poor soils (El-Showk & El-Showk, 2003; Yadav et al., 2013). A mature Paulownia tree typically attains a height of 20 to 30 meters, exhibits a trunk diameter of 1 to 2 meters, possesses a root system extending up to 8 meters in depth, and develops a broad canopy (Ghazzawy et al., 2024). Seven-year-old paulownia trees typically reach heights of 8 to 12 meters with a canopy radius of 3 to 5 meters (Zhu et al., 1986). At ten years, they develop a trunk diameter of 30 to 40 cm at breast height and yield 0.3 to 0.5 m^3 of timber (Zhu et al., 1986). Under optimal conditions, Paulownia can grow 3 meters annually, producing valuable timber in 15 years, and can be harvested for lumber in 5 to 6 years. Five to seven-year-old Paulownia crops can yield 150 to 330 tons/ha of biomass, depending on planting density (Ates et al., 2008; Icka et al., 2016).

Paulownia wood is distinguished by its low density (0.35 g/cm³), ease of workability, good insulation properties, ring-porous structure, light coloration, straight grain, and satin luster, contributing to its aesthetically pleasing appearance (Ates et al., 2008; Icka et al., 2016). Its high tannin content further renders it resistant to rot, worms, and termites (Icka et al., 2016). Consequently, Paulownia timber is utilized in diverse applications such as interior construction, musical instrument fabrication, and furniture production (El-Showk & El-Showk, 2003).

A prior study by López et al. (2012) highlighted the Paulownia trihybrid (*P. elongata* x *P. fortunei* x *P. tomentosa*) for its favorable heating value and chemical composition for energy production, like its lower ash and higher cellulose content relative to other energy crops. These characteristics render it a solid biofuel source, establishing its significance as a promising energy crop (López et al., 2012). The trihybrid also presented a fiber length comparable to other hardwoods and a cellulose content of 440 g/Kg, with suitable physical and acceptable characteristics for paper production (López et al., 2012). Ates et al. (2008) reported that pulp derived from *Paulownia elongata* is suitable for paper production upon integration with longer fibers.

The biochemical profile of Paulownia leaves and flowers is rich in fats, sugars, and proteins, with a nitrogen content comparable to leguminous plants, making them suitable for livestock nutrition (Icka et al., 2016). Used as fodder or green fertilizer, the leaves provide 2.8% to 3% nitrogen and 0.4% potassium per 100 kg of biomass (Icka et al., 2016; Yadav et al., 2013). Additionally, bioactive compounds in the plant's leaves, wood xylem, bark, fruits, and flowers highlight their potential for medicinal applications (He et al., 2016).

Beyond its commercial utility, species of *Paulownia* have shown considerable effectiveness in mitigating environmental issues. It is called the "tree of the future" because of its rapid growth (Ghazzawy et al., 2024). Their integration into agroforestry systems offers a strategic approach to land optimization and climate change mitigation (Magar et al., 2018). Utilizing Paulownia can enhance microclimate conditions and soil quality and provide windbreak benefits to adjacent crops (El-Showk & El-Showk, 2003; Zhu et al., 1986). While intercropping with Paulownia may variably influence crop yields, the reduction in productivity is compensated by the gains in timber, fuel, fodder, and additional benefits (Yin, 1997).

A recent study by Mamirova et al. (2022) has shown that *Paulownia tomentosa* can thrive in soils contaminated with organochlorine pesticides and trace toxic elements. The hybrid *P. tomentosa* x *P. fortunei* has been identified as an effective accumulator of Cu, Zn, and Cd, whereas *P. elongata* x *P. fortunei* has been recognized for its accumulation of Zn, highlighting the potential of the genus Paulownia for soil phytoremediation efforts (Tzvetkova et al., 2015).

Moreover, Paulownia trees have been identified for their remarkable ability to sequester large amounts of CO_2, rendering them an attractive option for reforestation and carbon mitigation initiatives (Ghazzawy et al., 2024). They can effectively contribute to CO_2 fixation, with a single tree estimated to absorb 22 kg of CO_2 and emit 6 kg of O_2 each year (Icka et al., 2016).

Furthermore, Paulownia exhibits a deep and well-developed root system, enhancing plant resilience under unfavorable climatic conditions (Magar et al., 2018).

Considering these factors, it is imperative to comprehend the adaptative mechanisms of *Paulownia* species to future environmental fluctuations, highlighting the importance of this understanding for their sustainable management and conservation. Previous research has investigated growth characteristics, revealing that the hybrid *Paulownia elongata* x *elongata*-T4 performs better than *Paulownia tomentosa* x *fortunei*-TF under soil salinity conditions (Ivanova et al., 2018). Llano-Sotelo et al. (2009) documented that the gas exchange response of *Paulownia imperialis* surpasses that of *Paulownia fortunei* and *Paulownia elongata*, facilitating enhanced growth performance in drought conditions.

3. MATERIAL AND METHODS

3.1. Experiment 1: Effects of elevated CO_2 on the physiology and morphology of *Paulownia tomentosa*

3.1.1. Site of study and growth condition

The investigation occurred at the Institute for Wood Science's greenhouse in Hamburg, Germany (coordinates: 53°30' N and 10°12' E), situated at an elevation of 27 m above sea level, spanning from June to September 2020. The experiment involved plant growth in two chambers: one exposed to ambient CO_2 levels (approximately 410 ppm) and the other to elevated CO_2 levels (950 ppm). Climate parameters were monitored using the CC 600 climate model by RAM co. The chambers were maintained at an average temperature of approximately 24°C ± 1.6°C (Mean ± SD) and an average relative humidity of about 63% ± 6.5% (Mean ± SD) (Figure 3-1).
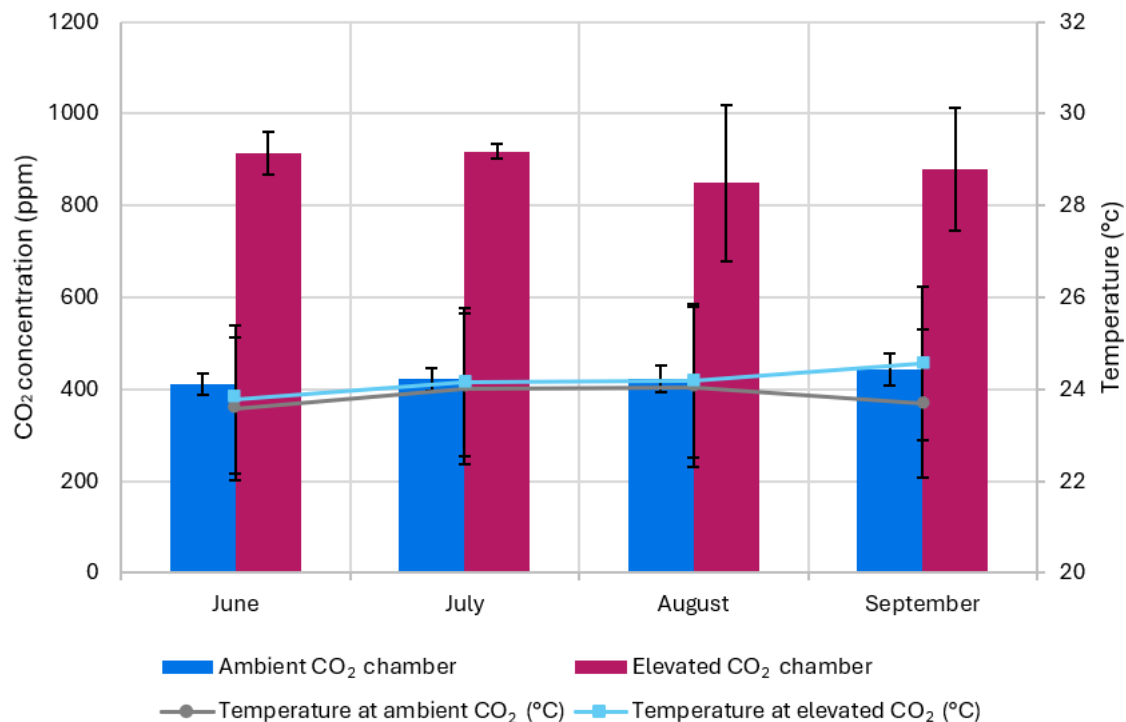
Figure 3-1 Climate variations in the experimental chambers. Temperature and CO_2 concentration (Mean ± SD) are shown. *Paulownia tomentosa* seeds were planted in June and plants were exposed to ambient (410 ppm) and elevated CO_2 concentration (950 ppm). Measurements were recorded from August following leaf development.

3.1.2. Plant material and experimental design

Paulownia seeds were individually cultivated in 2.5-liter pots. The growth substrate consisted of a medium-structured soil with a pH of 5.6, specifically Type Planting Soil (Plantaflor). This soil mixture is composed of 70% strongly decomposed frozen black peat, along with slightly to medium decomposed white peat, sand, nutrients (220 mg N/l, 220 mg P_2O_5/l, 300 mg K_2O/l, 110 mg Mg/l, 240 mg S/l, and 1.8 mg KCl/l), and, additionally, the soil was supplemented with NPK fertilizer (12-12-17) at a concentration of 1.8 kg/m^3.

Ten Paulownia seedlings were segregated into groups of five individuals each, with one group subjected to an aCO_2 chamber (approximately 410 ppm), and the other to an elevated CO_2 chamber (approximately 950 ppm). The substrate water was measured using a Theta HH2 (Delta-T devices) moisture meter, and soil moisture content was 49.63% ± 18.69% (Mean ± SD). The schematic representation of the experiment is presented in Figure 3-2.
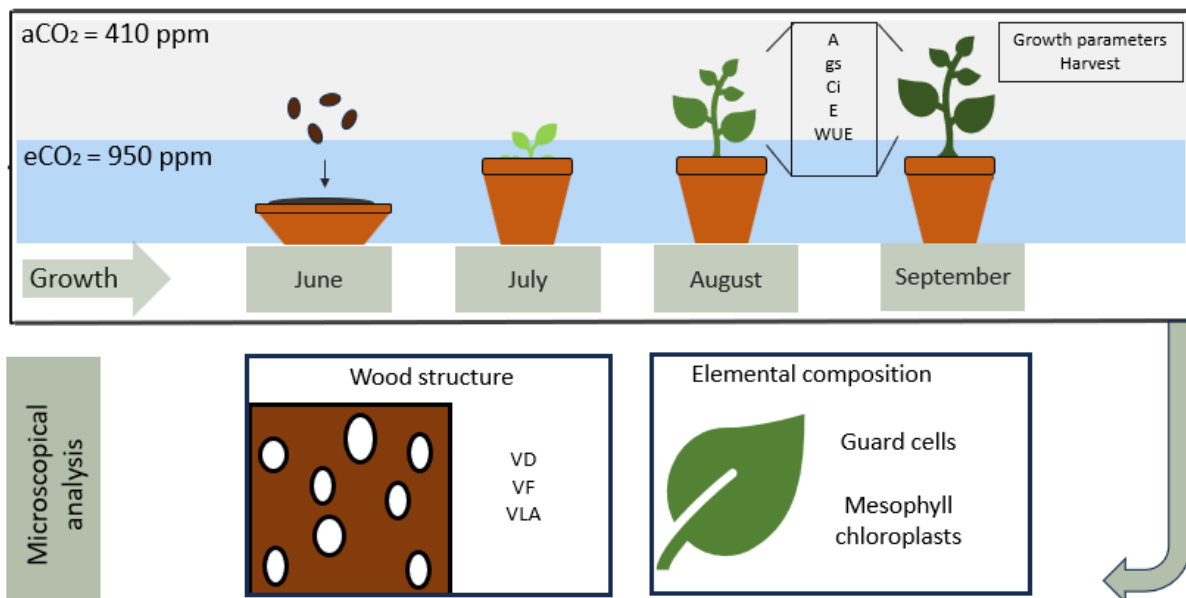
Figure 3-2. Schematic representation of the CO₂ experiment. Plants were grown from seeds in two separate CO_2 chambers, one containing an ambient CO_2 concentration (410 ppm) and another containing an elevated CO_2 concentration (950 ppm). Leaf gas exchange parameters were recorded once a week from August upon the development of the leaves. Plants were harvested at the end of the growth season (late September) to obtain measurements of growth variables and vessel characteristics.

3.1.3. Gas exchange measurements

The gas exchange parameters analyzed in this study included the rates of CO_2 uptake (A), stomatal conductance (g_s), intercellular CO_2 concentration (c_i), transpiration (E), and water use efficiency (WUE). The measurements were taken once a week using a photosynthesis system

(porometer) (Li 6400 XT, Li-Cor, Biosciences, Lincoln, NE, USA) with light-emitting diode (LED) light sources (6400-02 or −02B), between 8:30 and 15:30, from early August to late September (Figure 3-3). The measurements were configured to a CO_2 concentration of 400 ppm and 950 ppm, relative humidity of 70%, light intensity of 1000 µmol photons m^{-2} s^{-1}, and airflow of 500 µmol s^{-1}. Four plants were selected, and at least 3-4 mature leaves were measured per plant. Every leaf was acclimated for 5 minutes before data point collection, and 6-10 data points were taken per leaf. IRGA's matching was performed for every treatment. The water use efficiency parameter was calculated as the ratio of net CO_2 uptake rate and water vapor loss through transpiration.

Figure 3-3 Experimental *P. tomentosa* plants and gas exchange measurements. Plants were cultivated from seeds within two chambers, each maintained at a different CO_2 concentration (ambient CO_2 = 410 ppm; elevated CO_2 = 950 ppm). Gas exchange measurements were conducted weekly upon leaf development.

3.1.4. Morphological analysis

Young Paulownia trees were harvested at the end of the growth season. Dry roots and shoots were weighted separately to obtain the biomass measurements, and total biomass was

calculated as the sum of the dry weight of all plant organs. Paulownia stem diameter was measured at a height of 2 cm above the soil surface using a digital caliper. Height was collected at the end of the growth period using a 2 m tape.

3.1.5. Wood structure analysis

Paulownia stems were collected from two centimeters above the soil's surface and immediately preserved in a solution of 70% ethanol. To investigate the wood structure, 40 µm thick cross-sections were prepared using a sliding microtome (Sartorius MI, 31 A 30). To improve the contrast, the cuts were first treated with a 0.5% (w/v) astra-blue solution, followed by a subsequent application of a 1% (w/v) safranin solution. To remove excess stain, the wood samples underwent multiple washes with immersions in 95% ethanol between each staining phase and lastly in distilled water (Figure 3-4).

Temporary slides were prepared using 50% glycerine as a medium for subsequent evaluation of stem vessel characteristics. Vessel features investigated include vessel diameter (VD), vessel frequency (VF), and vessel lumen area (VLA). The mentioned parameters were analyzed using a light microscope (Axioskop 40, Zeiss, Göttingen, Germany) equipped with a 2.5× objective lens and a digital camera (AxioCam MRC). The entire cross-sections were screened and recorded using digital photographs (resolution: 1388 × 1040), which were merged using Adobe Photoshop CS6 software (Figure 3-4). For quantitative analysis, regions corresponding to the secondary xylem were selected (Figure 3-4), and at least 60 vessels were measured using Zen Pro version 2012 software. The vessel lumen area was calculated using the elliptical formula:

$$VLA = radius\ a\ *\ radius\ b\ *\ \pi$$

Where VLA is the vessel lumen area; radius a is the radius of the first measured diameter; radius b is the radius of the second measured diameter. The vessel lumen area was measured in square millimeters (mm^2).

The vessel diameter was calculated using the average formula:

$$VD = \Sigma d \div n$$

Where VD is the vessel diameter, Σd is the sum of the diameters, and n is the number of measured diameters. The vessel diameter unit was measured in micrometers (µm).

The vessel frequency was calculated using the following formula:

$$VF = n \div analysed\ area$$

Where VF is the vessel frequency, n is the number of measured vessels, and the analyzed area is the selected area in which the vessels were measured. The VF was calculated as the number of vessels per unit area (vessels mm^{-2}).
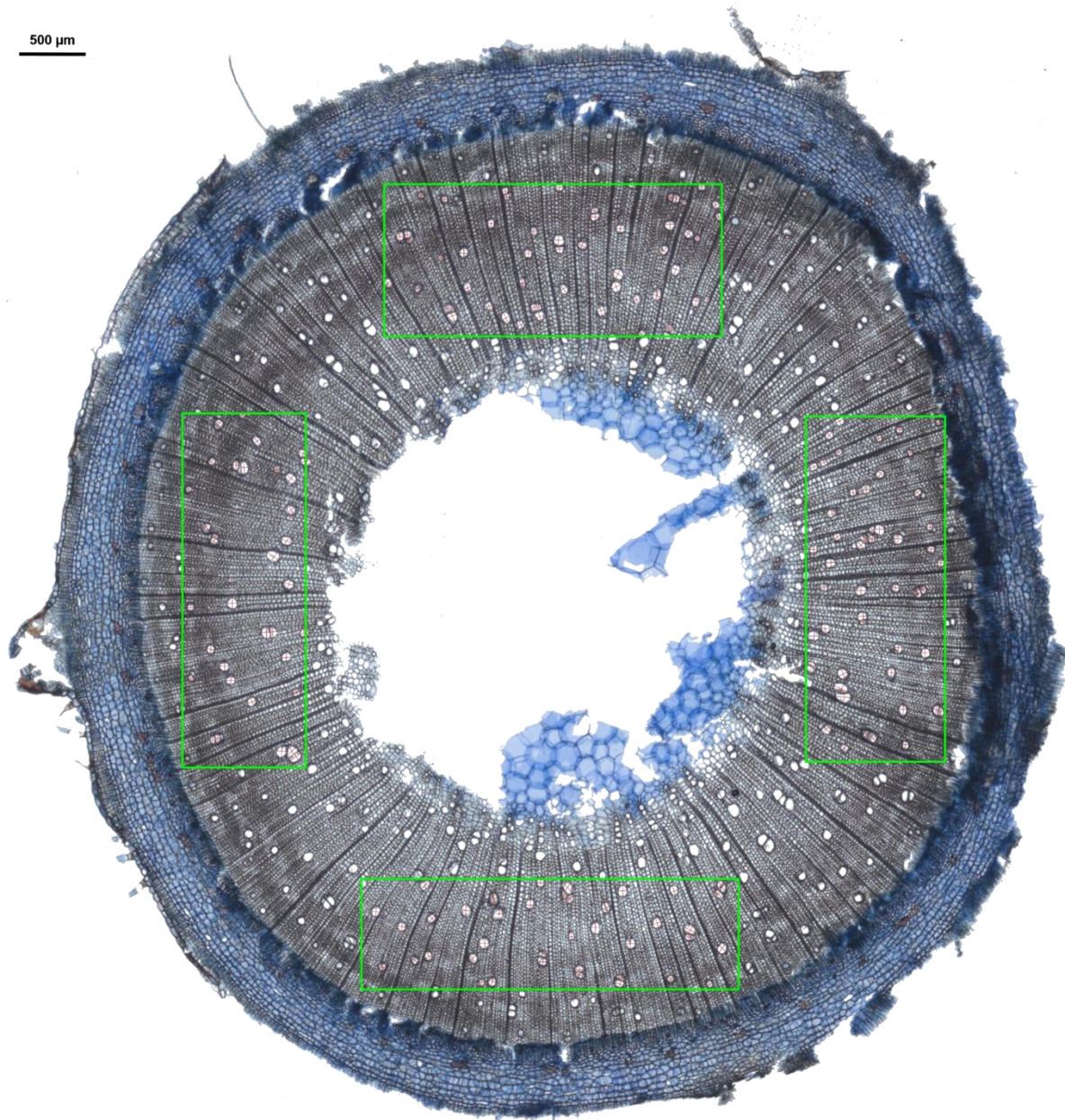
Figure 3-4 Microscopical cross-section view of the *P. tomentosa* stems for quantitative wood analysis. The woodcut was stained using a 0.5% Astra-blue and 1% safranin solution. The green rectangles in the figure represent the specific areas where vessel measurements were taken. The semi-major and semi-minor axes of the vessels are depicted in red, and the lengths are given. The photographs were recorded with a magnification of 2.5x under the lens of the Zeiss Axioskop 40, and the section thickness is 40 µm. Microscopical images were overlapped using the Adobe Photoshop CS6.

3.1.6. Energy dispersive X-ray microanalysis

At the end of the growth season, plant leaves were collected and immediately frozen in liquid nitrogen. This was followed by lyophilization at a condenser temperature of -110 °C and a drying time of 48 h using a Heto PowerDry LL1500 freeze dryer. The freeze-dried leaves were then carefully broken into small pieces and cross-sectionally placed on carbon conductive tape

on the top of metal stubs, which were subsequently carbon-coated using a high-pressure vacuum Bio-RAD CA508 SEM coating system. For sample visualization using FE-SEM, 1 cm wood blocks were prepared from the plant stem and coated using gold. SEM (Scanning Electron Microscopy) figures were created using the digital imaging processing system 2.6, and the guard cells and the chloroplasts of the mesophyll cells were selected for the elemental analysis using Energy Dispersive X-ray microanalysis (EDX). The measurements were carried out on an analytical scanning electron microscope (Hitachi Model S520, Hitachi Denshi, Ltd., Tokyo, Japan) with an acceleration voltage of 10 kV and a working distance of 15 mm. The microscope had a magnification range of 20 to 200,000×. The X-ray spectra and elemental composition were recorded using the WINEDS V4.0 microanalysis system.

3.1.7. Statistical analysis

A linear mixed-effects model (LMM) was developed to investigate the effects of elevated CO_2 on gas exchange parameters. This model treated time (week), treatment, and their interaction as fixed effects, while individual plants were treated as random effects. To validate the model results, the model residuals were tested for normality using the 'mcp.fnc' function. Variations between the days were verified using the Tukey HSD post-hoc test.

The Student's t-test was utilized to evaluate the variability between groups in the Energy-dispersive X-ray Microanalysis (EDX) results under the assumption of normal data distribution. Conversely, the Mann-Whitney U test was applied for datasets deviating from normal distribution, including height, stem diameter, biomass, and vessel characteristics.

To evaluate the associations between gas exchange parameters, biomass, and vessel characteristics, a Spearman's rank correlation analysis was performed.

Statistical significance was established at a threshold of $p < 0.05$. All statistical analyses were executed using R software, version 4.2.1.

3.2. Experiment 2: Effect of cyclic drought stress on the morphology and physiology of *Paulownia tomentosa*

3.2.1. Experiment design

Experiments were conducted at the University of Hamburg, coordinates 53°5'N latitude and 10°2'E longitude, from July to September. Three-year-old Paulownia trees (*Paulownia tomentosa*) were cultivated in a laboratory environment exposed to ambient natural light, temperature fluctuations, and air humidity. The plants grew on a growth substrate consisting of medium-structured soil with a pH-value of 5.6, specifically using Type Planting Soil (Plantaflor). This soil mixture is composed of 70% strongly decomposed frozen black peat, along with slightly to medium decomposed white peat, sand, nutrients (220 mg N/l, 220 mg P_2O_5/l, 300 mg K_2O/l, 110 mg Mg/l, 240 mg S/l, and 1.8 mg KCl/l). The soil was supplemented with 1.8 Kg/m^3 of NPK fertilizer (12-12-17).

Ten plants of comparable size were randomly segregated into two groups of 5 plants, each undergoing a distinct water treatment. The well-watered 'ww' group received daily irrigation, while the dry 'dr' group experienced recurrent drought cycles. Soil moisture levels were monitored using a Theta HH2 moisture meter from Delta-T devices. In the 'ww', plants were daily irrigated to ta soil moisture of 64.9% $\pm$ 6.33% (Mean $\pm$ SD) throughout the experiments (Figure 3-5). Drought stress was induced in the 'dr' group by abstaining from irrigation until visible wilting symptoms manifested. After a drought cycle, the 'dr' group was promptly irrigated to field saturation, and a new drought cycle was initiated. The soil moisture gradually declined compared to the controls as the drought persisted: by 2.4% on the first day, 28.5% on the 3rd day, 46.3% on the 5th day, 66.5% on the 7th day, 79.7% on the 9th day, and 83.8% by the end of the observation period. On average, each drought cycle spanned 11 days, starting with soil moisture at approximately 60.2% $\pm$ 6.56% (Mean $\pm$ SD) on the first day of irrigation and decreasing to 10.3% $\pm$ 2.6 (Mean $\pm$ SD) by the end of the cycle. Overall, plants in the 'dr' group underwent an approximate reduction in soil moisture of 45.27% $\pm$ 19.3% (Mean $\pm$ SD).

In the present study, the following leaf physiological parameters, gas exchange, leaf pigment composition, and chlorophyll fluorescence, were measured on 3 fully expanded canopy leaves developed under repeated cycles of drought stress. The plants were subjected to 4 cycles before measurements, and at this stage, leaf acclimation to drought conditions was expected. In this study, the presented data are from an additional exposure to 3 drought cycles (~11 days each), constituting cycles 5, 6, and 7. In total, the plants were exposed to 7 cycles of drought. Gas exchange measurements were performed every 2 days on cycles 5 and 6 (Figure 3-6). However,

two sampling points from cycle 6 were not obtained (days 3 and 11). A linear mixed-effect model was employed to address this issue. This model is particularly suited for handling missing data and zeros in repeated measures sampling experiments like the one conducted in this study. Measurements on the morphological variables (height, stem diameter, leaf number, and leaf area) and anatomical characteristics (vessel diameter, vessel lumen area, and frequency) were carried out at the end of the growth season to verify the overall impact of the drought stress on Paulownia plants.
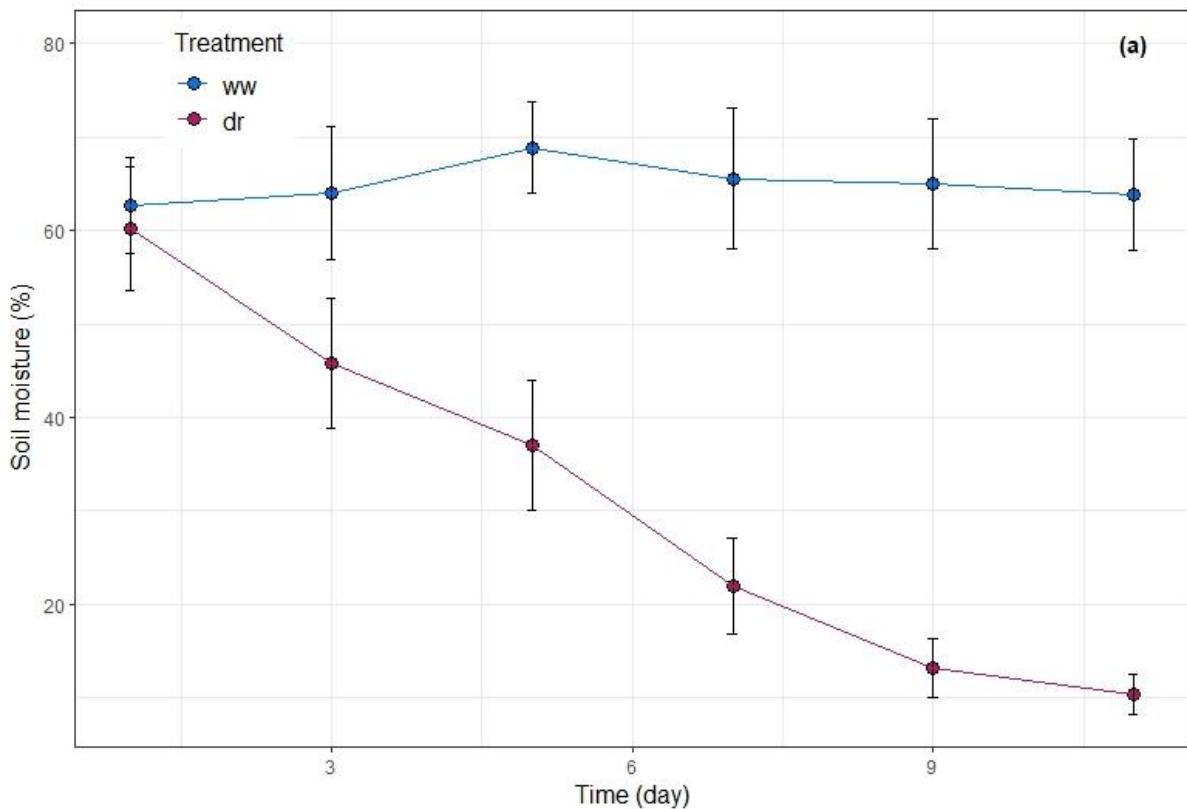
Figure 3-5. Soil moisture conditions during the drought experiment. Mean soil water levels throughout the days of the drought experiment are presented for both treatment groups: 'ww' (well-watered) and 'dr' (drought). Values are means ± standard deviation (SD), recorded bi-daily throughout the experiment.
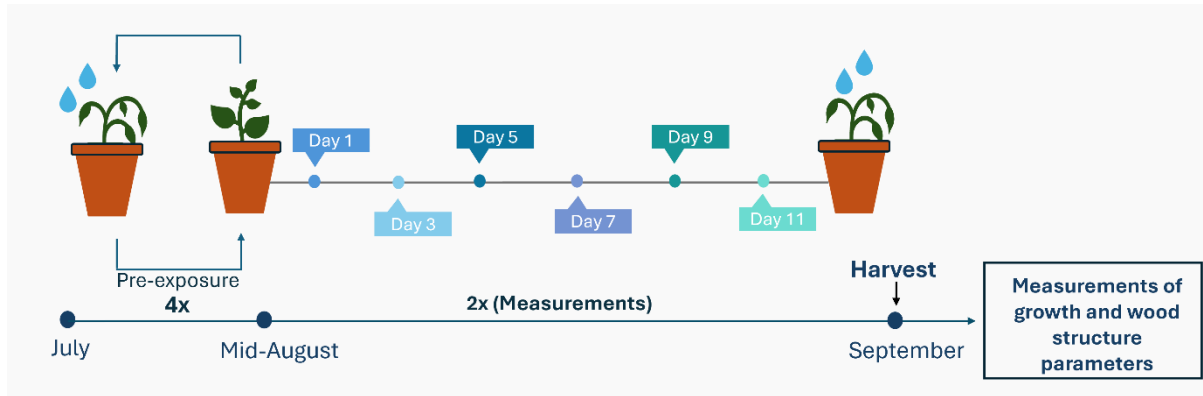
Figure 3-6. Schematic representation of the drought cycles and tested variables. The pre-exposure period started in July and extended for four drought cycles. Within each cycle, the plant-growing substrate was dried from field saturation to the point where plants manifested wilting symptoms. Gas exchange, chlorophyll fluorescence, and leaf pigment parameters were measured from mid-August, and the cumulative impact of the recurrent drought cycles on plant hydraulic characteristics and morphology was assessed at the end of the growth season.

3.2.2. Leaf gas exchange

Gas exchange parameters, such as net CO_2 uptake (A, µmol CO_2 m^{-2} s^{-1}), stomatal conductance (g_s, mmol H_2O m^{-2} s^{-1}), intercellular CO_2 concentration (c_i, µmol CO_2 mol^{-1}) and transpiration (E, mmol H_2O m^{-2} s^{-1}) were measured every 2 days on plants pre-exposed to drought (Figure 3-7). Measurements were taken using a photosynthesis system (porometer) (Li 6400 XT, Li-Cor, Biosciences, Lincoln, NE, USA) with light-emitting diode (LED) light sources (6400-02 or −02B), between 11:30 and 15:30. The measurements were configured to a CO_2 concentration of 415 ppm, light intensity of 1000 µmol photons m^{-2} s^{-1}, airflow of 500 µmol s^{-1}, and relative humidity of 43%. Leaves were acclimated for 5 minutes, and at least 10 data points were recorded per leaf. The water use efficiency (WUE) was based on the rates of net CO_2 uptake and transpiration:

$$WUE = A/E$$

Where A is the net CO_2 uptake rate and E is the transpiration rate.

The stomata limitation value (Ls) was calculated based on the ca-to-ci ratio:

$$Ls = 1 - ci/ca$$

Where c_i is the leaf intercellular CO_2 concentration and c_a is the ambient CO_2 concentration.
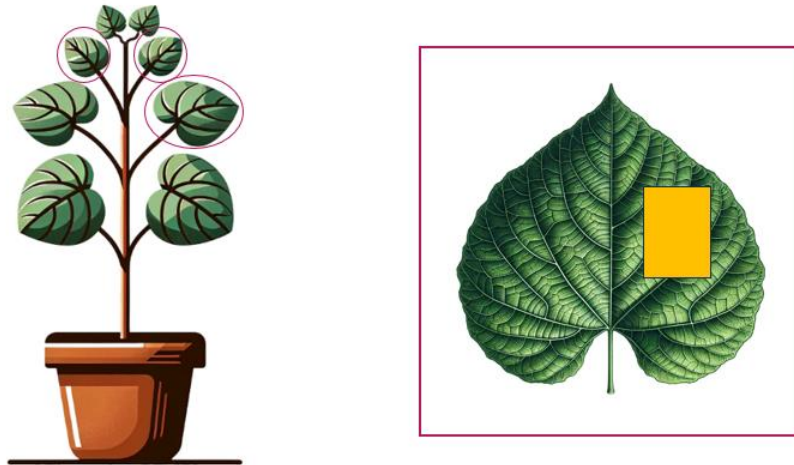
Figure 3-7. Stylized illustration of the leaf gas exchange measurements. Red cycles indicate the measured leaves and yellow squares indicate the approximate leaf area in which gas exchange parameters were taken. Every leaf was acclimated to the leaf chamber for 5 minutes before recording the data points.

3.2.3. Microscopical measurements of stomata characteristics

The stomatal characteristics were assessed using the leaf imprint technique. This involved applying a layer of clear nail varnish to the mid-region of the abaxial surface of a freshly plucked, fully expanded leaf from the second pair of canopy layers. After the varnish dried, a piece of transparent film was pressed moderately onto the varnished area and then carefully peeled off, capturing the leaf's imprint. These imprints were then mounted on standard microscope slides for analysis (Figure 3-8).

Stomata density and aperture measurements were conducted on 15-20 digital photographs captured from randomly selected fields on each slide. These photographs were taken using a light microscope (Axioskop 40, Zeiss, Göttingen, Germany) equipped with a 20× objective lens and an AxioCam MRC digital camera. The measurement of stomatal size was determined by recording the distance in micrometers between the points where the guard cells meet at either end of the stoma. Stomata density was calculated as the number of stomata per square millimeter of leaf area ($n\ mm^{-2}$), using the formula:

$$SD = n \div analysed\ area$$
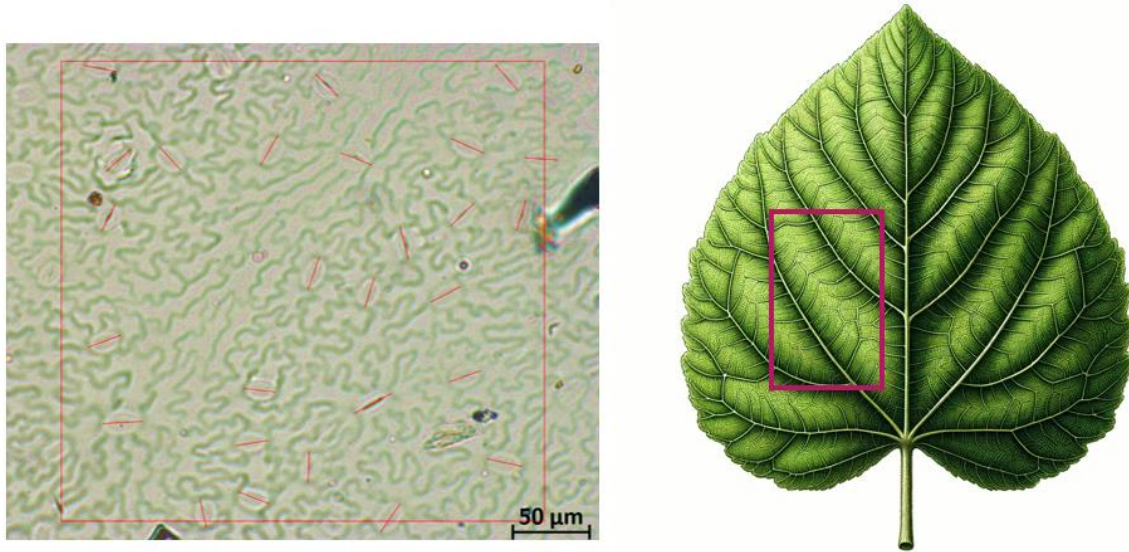
Figure 3-8. Illustration of the leaf imprint technique for measuring stomata characteristics. Microscopic image of the selected area for stomatal length and density measurements (left) and an illustration showing the measured area on the abaxial leaf surface, indicating where the microscopic regions were selected (right).

3.2.4. Chlorophyll fluorescence parameters

Chlorophyll fluorescence parameters were determined using a Y(II) modulated fluorometer (Opti-Sciences, Hudson, NH 03051, USA) (Figure 3-9). Plant material was dark adapted for 30 minutes, and measurements on minimum fluorescence (Fo) were obtained by applying a modulated light intensity in the range below 0.4 µmols, automatically adjusted using the fluorometer "AutoSet". Maximum fluorescence (Fm) was achieved by applying a saturation pulse of 6000 µmols for 0.8 seconds, and the variable fluorescence (Fv) was automatically calculated as the difference between Fm and Fo:

$$Fv = Fm - Fo$$

From which the maximum quantum yield (Fv/Fm) was calculated:

$$Fv/Fm = (Fm - Fo)/Fm$$

For light-adapted state measurements, plants were exposed to actinic light intensity of 474.73 ± 186.51 µmol m^{-2} s^{-1} (Mean $\pm$ SD) for 15 minutes to allow for a steady state of photosynthesis and subsequently obtain the steady-state level of fluorescence in the light (F') through applying a modulated light intensity in the range bellow 0.4 µmols. To obtain the maximum fluorescence level in the light (Fm'), a white-led saturation flash set to 6000 µmols for 0.8 seconds was applied. F' and Fm' values were subsequently used for the determination of the quantum photochemical yield of the photosystem II (Y(PSII), and electron transport rate (ETR) using the following equations:

$$Y(PSII) = (Fm' - Fs)/Fm'$$

$$ETR = Y(PSII) \times PAR \times \alpha \times \beta$$

Where α represents the leaf absorbance, which is calculated automatically, and β is the ratio that accounts for the distribution of energy between PSII and PSI reaction centers in the leaf. A typical β value is 0.5.

The calculation of non-photochemical quenching parameters was determined using the following equations:

$$Y(NO) = F'/Fm$$

Where Y(NO) is the non-photo protective value of the non-photochemical quenching.

$$Y(NPQ) = (F'/Fm') - Y(NO)$$

Where Y(NPQ) is the quantum yield of the non-photochemical quenching value.

$$NPQ = (Fm - Fm')/Fm'$$

Where NPQ is the non-photochemical quenching.

Measurements were taken twice during the observation period when soil water levels lowered to about 20% (7th day post irrigation, before wilting symptoms emerged). Data points were recorded in three different regions of the leaves of the three measured leaves (Figure 3-9). The ambient temperature during the measurements was 26.1°C ± 1.36°C (Mean ± SD), and the relative humidity was 51.9% ± 2.86% (Mean ± SD).

3.2.5. Determination of pigment content through reflectance measurements

The quantification of pigments such as chlorophyll, flavonols, and anthocyanins was carried out using an MPM-100 multi-pigment meter (Hudson, NH 03051, USA) (Figure 3-9). This device incorporates five light sources, three dedicated to fluorescence excitation, and the remaining two are utilized for assessing transmittance values. The chlorophyll content was calculated based on the ratio of transmitted light at near-infrared (850 nm) and far-red (720 nm) wavelengths using the following formula:

$$Chl = (T850nm/T720nm) - 1$$

Anthocyanin content was determined by calculating the logarithm of the ratio of fluorescence intensities measured at 660 nm (red) and 525 nm (green) wavelengths:

$$Anth = log \, (F660nm/F525)$$

Flavonol content was determined by calculating the logarithm of the ratio of fluorescence intensities measured at 660 nm (red) and 325 nm (UVA):

$$Flv = log \, (F660/F375)$$

Finally, the Nitrogen Balance Index (NBI) was calculated as the ratio of chlorophyll to flavonol content:

$$NBI = [(T850/T720) - 1] / log(F660/F375)$$

Measurements were conducted at seven distinct intervals in the progress of the two drought cycles. These assessments were performed on three leaves from the top canopy layer, with three data points recorded per leaf.
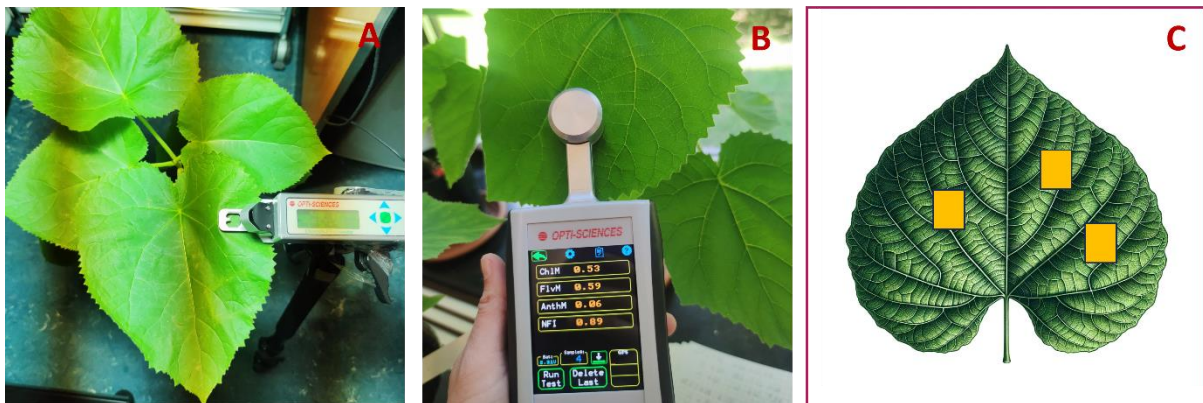
Figure 3-9. Assessment of chlorophyll fluorescence and pigment concentrations in Paulownia leaves. (A) Chlorophyll fluorescence in the light-adapted state. (B) Leaf pigment composition measurements, including chlorophyll, flavonols, and anthocyanins. (C) Illustration of the leaf sections (denoted by yellow squares) where pigment concentrations and chlorophyll fluorescence were measured under dark- and light-adapted conditions.

3.2.6. Measurements of wood vessel characteristics

The methodology adopted for this part of the research followed the same protocols as outlined in the wood structure analyses from the 'Elevated CO_2 Experiment' (see Wood structure analysis).

3.2.7. Measurements of morphological parameters

After the growth season, the following morphological parameters were assessed: plant height, stem diameter, leaf count, lead area, and biomass. Leaf area was estimated using a leaf area meter (LI-3000C, Lincoln, NE, USA). To determine fresh biomass, plants were harvested, and their roots and shoots were promptly weighed independently. Subsequently, these plant organs were subjected to air drying at room temperature for two weeks to determine the dry biomass.

3.2.8. Statistical analysis

A linear mixed-effects model was used to investigate the effects of drought progression on gas exchange parameters. In this model, the drought cycle and the interaction between treatment and time were treated as a fixed effect, while individual plants were incorporated as a random effect. A second model was constructed to evaluate the overall impact of drought conditions on leaf pigment composition, including chlorophyll, flavonols, anthocyanin, the nitrogen balance index, and chlorophyll fluorescence parameters, including Y(PSII), ETR, Fv/Fm, Y(NPQ), Y(NO) and NPQ, treating plant individuals and time as a random effect to control for temporal and plant-specific variations. The model residuals were tested for normality using the 'mcp.fnc' function, to validate the model results. Differences in the measured parameter variation over the test days were assessed using the Tukey HSD post-hoc test. The Mann-Whitney U test was used to compare differences between the treatments in the physiological and morphological parameters — namely plant height, stem diameter, biomass, leaf count, xylem vessels, and stomatal characteristics. Spearman's correlation analysis was conducted to explore the relationships between gas exchange variables and other plant traits, including stomatal characteristics, vessel characteristics, and plant dry biomass. Analysis was also conducted to assess the relationship between chlorophyll fluorescence and leaf pigment parameters. Differences were considered statistically significant at $p < 0.05$. All the statistical analyses were conducted using the R program version 4.2.1.

3.3. Experiment 3: Electrical signaling and gas exchange response of *Paulownia tomentosa* to thermal wounding and re-irrigation

Three-year-old *Paulownia tomentosa* plants were transferred from the greenhouse to the Institute for Wood Science's Laboratory of Electrophysiology, where they were subjected to natural light, temperature, and humidity fluctuations. Before the onset of the experiments, plants underwent a one-week acclimation period, allowing them to adapt to new growth conditions and avoid variations in the measured variables attributed to this process.

The electrical potentials of the plants were measured in response to burn damage and re-irrigation stimuli using both intracellular and extracellular methods.

3.3.1. Intracellular measurements

Intracellular recordings were performed using a two-electrode technique on a vibration-stabilized bench, within a Faraday cage to minimize electrical interference and noise. For the investigation of electrical signals in response to cooling and heat stimulus, shoots containing two fully expanded leaves were harvested from three-year-old *Paulownia tomentosa* trees. Subsequently, the cut end of the stem was immediately immersed in an aqueous solution consisting of 50 mM NaCl, 10 mM K_2SO_4, 4mM $CaSO_4$, and 35 mM MES buffer, with a pH of 6.0 for the maintenance of ionic stability during the recording process. The reference electrode was immersed within the same solution, and the microelectrode (Ag/AgCl-wire 0.4 mm) prefilled with a 100 mM KCl solution was inserted into a cell of the leaf basis. Cold shock with ice water (4°C) was applied approximately 5 mm near the microelectrode to test cell excitability (Figure 3-10). Heat stimulus was applied either to the leaf tip where the electrode was inserted or to the adjacent leaf.

To assess the electrical responses to re-irrigation, *P. tomentosa* trees were subjected to a drought cycle lasting approximately 11 days (point of wilting, approximately 10% of soil moisture). The reference electrode was positioned on the shoot apex (Figure 3-10B). The electric potentials were measured using a chart recorder (Sekonic SS 250 F) by amplification with a WPI model 750 (World Precision Instruments, Sarasota, FL, USA). The measured parameters included amplitude (mV), velocity (cm s^{-1}), and duration (minutes). The electrical signals were recorded independently from gas exchange measurements.
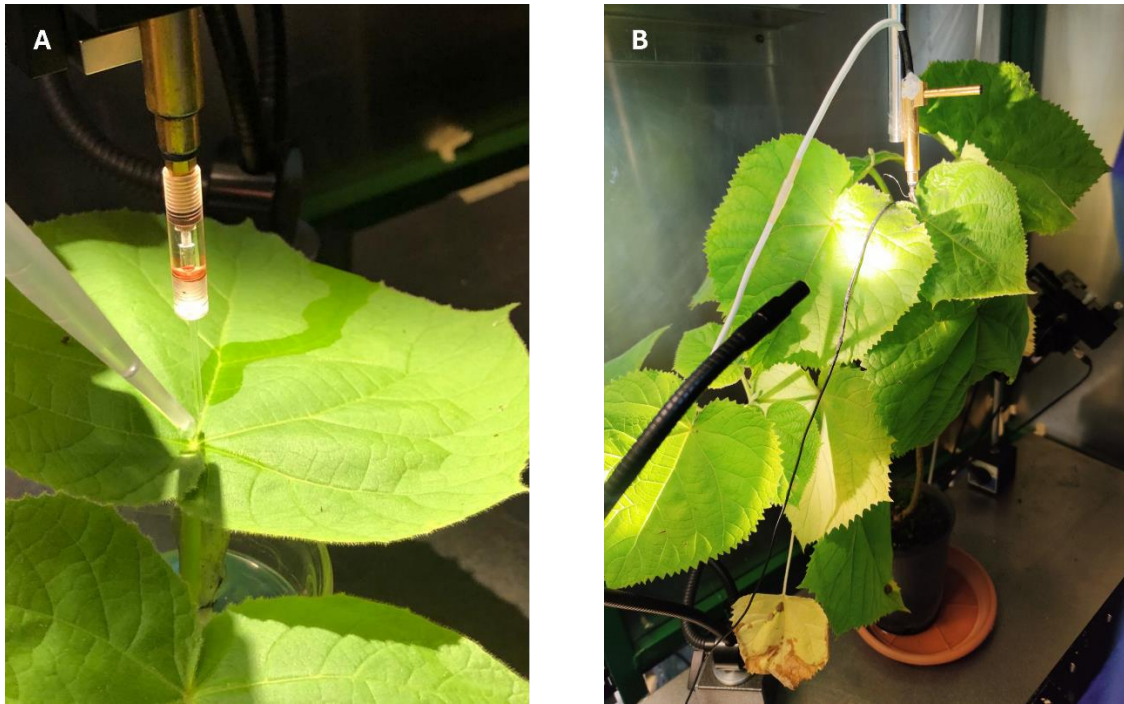
Figure 3-10 Intracellular measurements of electrical signals in *Paulownia tomentosa*. Cold shock (A) and re-irrigation (B) were applied. Microelectrodes were prefilled with 100 mM KCl and inserted into a cell located on the leaf base.

3.3.2. Extracellular measurements

Electric signals were recorded extracellularly using an electroencephalogram (Neurowerk, Berlin, Germany), equipped with a differential amplifier and a Neurowerk EEG software data acquisition system (V10.0.0.31). Data acquisition was conducted employing a three-electrode derivation method, comprising a bipolar montage using two electrodes to suit one channel connected to a high input impedance EEG equipment. Needle electrodes (15mm x 0.2mm) were inserted within the petioles of two fully expanded leaves in the canopy (spaced 3-5 cm apart), and a ground electrode was placed in the plant substrate (for electrical recordings in response to wounding) or in the shoot apex (for electrical recordings in response to re-irrigation) (Figure 3-11). The electrode configuration is set to improve the signal-to-noise ratio.

The measurements were conducted by recording the time-series voltage variation between two inserted electrodes. A selective low-pass filter with a cutoff frequency of 50 Hz was employed to minimize interference from electronic components in the environment. A low-pass digital filter of 70 Hz was also applied during data processing.

Following the insertion of electrodes, the Li-COR 6400xt chamber was installed in a leaf containing one of the inserted electrodes. Plants were subjected to a 20-minute acclimation period before initiating the simultaneous recordings. Signals and gas exchange parameters were

recorded for at least 30 minutes before and after applying the burn damage. For re-irrigation responses, signals were recorded for 30 minutes before the stimulus and 50-70 minutes after the stimulus.
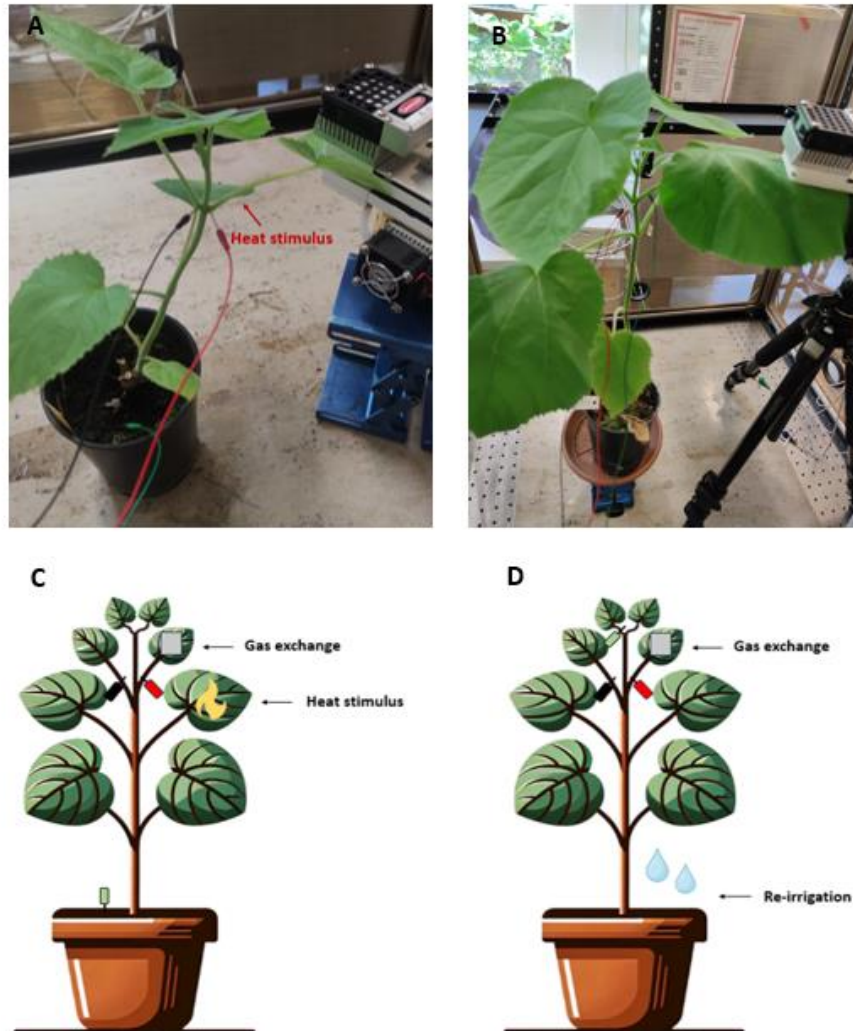
Figure 3-11 Simultaneous measurements of electrical signals using the EEG and gas exchange using the Li-COR 6400XT on three-year-old *P. tomentosa* trees. Electrodes were inserted in the petiole of two fully expanded canopy leaves, and gas exchange was measured on a leaf in which one of the electrodes was inserted. The ground electrode was inserted in the plant substrate to evaluate the response to heat stimulus (A) or in the shoot apex to avoid any interference from irrigation on the electrical recordings (B). Schematic illustration of the heat stimulus (on the neighboring leaf located approximately 10 cm below the measured leaves) (C) and irrigation (D).

3.3.3. Settings for gas exchange measurements

Net CO_2 uptake, stomatal conductance, intercellular CO_2 concentration, and transpiration were measured using the porometer (Li-Cor 6400, Lincoln, NE, USA). Data was recorded from a fully expanded leaf and acclimated for 20 minutes to allow for a steady state of the gas

exchange variables. Data points were collected every 10 seconds for 30 minutes before stimulus application. Measurements were taken during day and night cycles to study the effects of local burns on the gas exchange balance. Measurements were set at a CO_2 concentration of 415 ppm, relative humidity of about 40%, and light intensity of 1000 µmol m^{-2} s^{-1} (for day measurements), and 0.1 to 1 µmol m^{-2} s^{-1} (for dark measurements and estimation of respiration rates).

3.3.4. Chlorophyll fluorescence measurements

Chlorophyll fluorescence measurements were conducted on six Paulownia trees subjected to drought stress. Irrigation was suspended until soil moisture declined to 8.58 % ($\pm$ 4.13 SD).

Before measurements, plants underwent a 25-minute acclimation period under controlled actinic light intensity of 115.43 µmol $\pm$ 12.98 (Mean $\pm$ SD) to ensure the photosynthetic apparatus reached a steady state. Concurrently, dark adaptation clips were applied to 1-2 leaves within the canopy to facilitate dark-adapted fluorescence assessments. These measurements were performed using a modulated fluorometer (Opti-Sciences, Hudson, NH 03051, USA), with instrument settings adjusted to emit a red modulated light below 0.4 µmol, as specified by the 'AutoSet' function. The saturation pulse intensity was calibrated to 6000 µmol for 0.8 seconds, utilizing red LEDs peaking at 660nm and a cut-off filter set at 690 nm.

Data were recorded at 12-minute intervals. Five data points were collected before soil rehydration to allow for comparison. After rehydration, an additional 12 data points were collected, totalizing in a whole period of 192 minutes, by the end of which, an apparent restoration of plant turgidity was observed.

3.3.5. Data analysis of the EEG signals

For the analysis of the EEG signals, raw data were extracted from EDF files and processed using the Python programming language (version 3.8). The primary libraries utilized include Matplotlib (v3.3.4), NumPy (v1.6.0), PyEDFlib (v0.1.20), and SciPy.

The data were primarily subjected to descriptive analysis using basic statistics metrics, such as mean and ranges (minimum and maximum values), to compare amplitude variations before and after stimuli. Data were also decomposed from time to frequency domain using the Cooley-Tukey Fast Fourier Transform algorithm to analyze the dominant frequency components present in the signal. Finally, approximate entropy (ApEn) analysis was employed to evaluate

the complexity of time-series dynamics before and after the application of a stimulus. This method is adequate for analyzing chaotic time series and is commonly applied to EEG data signals to assess their predictability and irregularity (Burioka et al., 2005). Lower ApEn values indicate reduced complexity and increased predictability of the time series. Conversely, higher ApEn values signify greater randomness and decreased predictability (Delgado-Bonal & Marshal, 2019).

Approximate Entropy (ApEn) is computed using the following parameters:

- Vector length (m): Specifies the length of data sequences compared
- Filter factor (r): A threshold that determines the required similarity for two sequences to be considered equivalent.
- Total number of data points (N): This represents the entire dataset size in the time series.

ApEn is quantified through the equation:

$$\text{ApEn}(m,r,N) = \phi(m) - \phi(m+1)$$

where m is set at 2 and r at 0.2, representing 20% of the data series' standard deviation.

In this study, ApEn was calculated on data segments of equal length, each spanning 60-64 minutes, down sampled from 256 Hz (original EEG settings) to a frequency of 64 Hz, which resulted in segments containing up to 245,760 data points. Plant electrical signals are characterized by weak, low-frequency signals, with a range usually below 1 Hz (Kai et al., 2011). Simulations based on electrical models suggest that the frequency of the oscillatory bioelectric activity in plants may reach up to 15 Hz (Cabral et al., 2011). It is generally recommended to use a sampling frequency of at least twice the value of the maximum frequency to ensure accurate recording (Beniczky & Schomer, 2020), therefore a sampling frequency of 64 Hz for measuring plant signals is appropriate. The data consisted of electrical signals recorded before and after the application of localized burn treatments and re-irrigation.

To assess the significance of the differences in ApEn results, a paired T-test was performed at a significance level of $p < 0.05$. A total of 10 individual plants were subjected to the burn stimulus analysis, with measurements divided between day (five plants) and night (five plants) conditions. Additionally, five plants were evaluated under a re-irrigation stimulus.

4. RESULTS

4.1. Effects of elevated CO_2 on the physiology and wood structure of *Paulownia tomentosa*

4.1.1.   Cumulative effect of elevated CO_2 on the morphological traits

The effect of elevated CO_2 concentrations on the morphological traits of juvenile Paulownia trees is illustrated in (Figure 4-1 and Figure 4-2). The results indicate that elevated CO_2 levels markedly enhanced plant height (Mann-Whitney $U = 2$, $p < 0.05$), whereas a trend towards increased stem diameter was observed, although this did not reach statistical significance (Figure 4-1). The plants' height and diameter increased by 26.2% and 16%, respectively.

A significant increase in leaf dry biomass was also observed in response to CO_2 enrichment (Mann-Whitney $U = 2$, $p < 0.05$). Despite the root and total dry biomass remaining statistically comparable under ambient and elevated CO_2 concentrations, both growth parameters exhibited an increase of 29.6% and 70.4%, respectively, at elevated CO_2 conditions (Figure 4-2 and Figure 4-3).
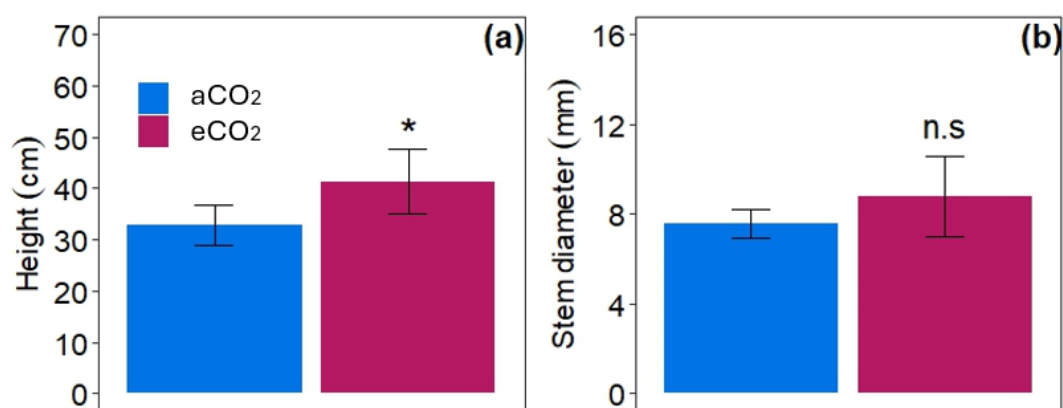
Figure 4-1. Cumulative effect of elevated CO_2 concentration on the morphological parameters. Bars represent the means (± 95% confidence interval) of the height (a) and stem diameter (b) in *Paulownia tomentosa*, measured in 'aCO_2' (410 ppm) and 'eCO_2' (950 ppm), n = 5. Stars indicate statistical significance using the Mann-Whitney U-test ($p < 0.05$). The notation 'n.s.' indicates nonstatistical variations between the means.
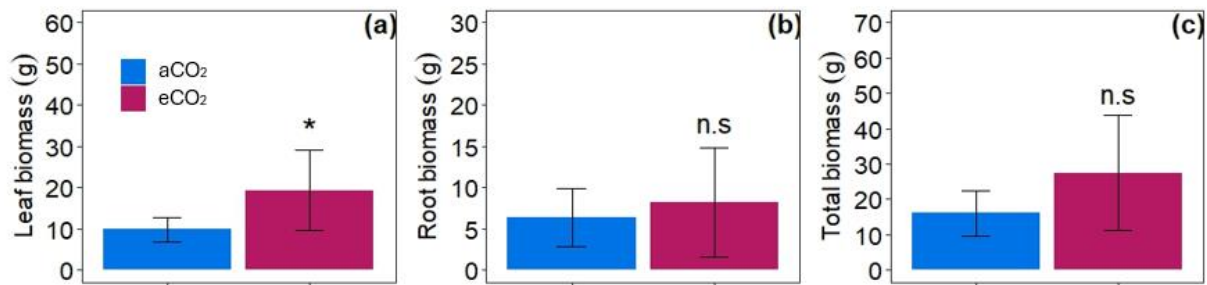
Figure 4-2. Cumulative effect of elevated CO₂ concentration on the dry biomass. Bars represent the means (± 95% confidence interval) of the leaf (a), root (b), and total dry biomass (c) in *P. tomentosa*, measured in 'aCO₂' (410 ppm) and 'eCO₂' (950 ppm), n = 5. Stars indicate statistical significance using the Mann-Whitney U-test (p < 0.05). The notation 'n.s.' indicates nonstatistical variations between the means.
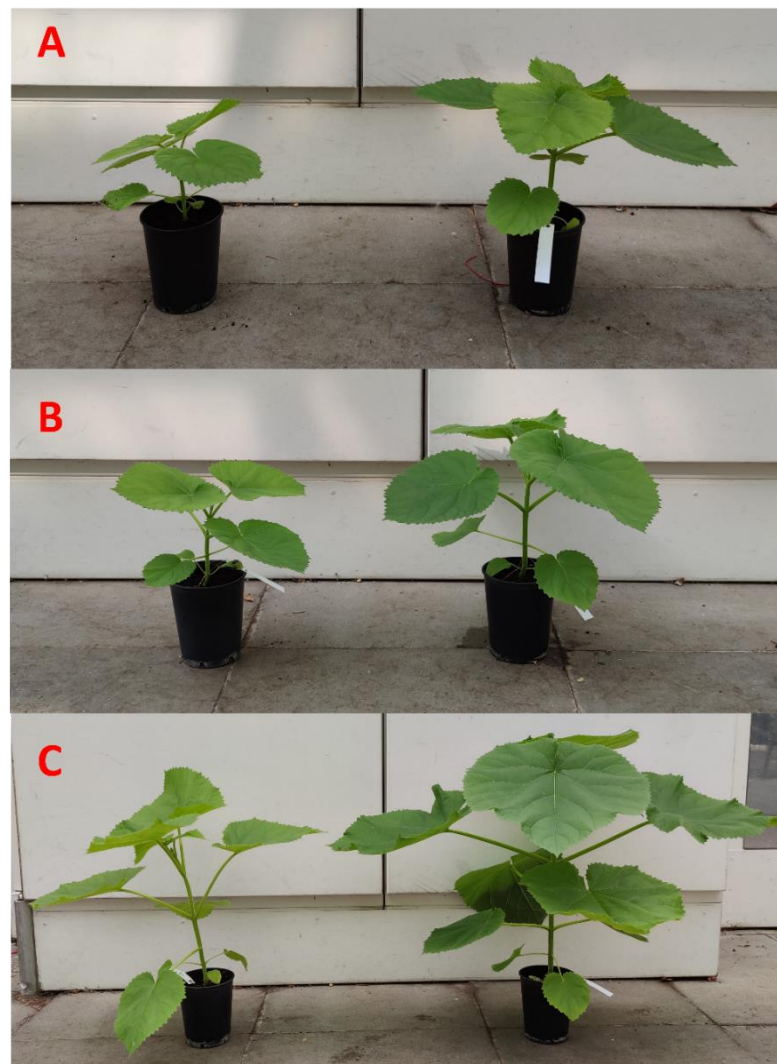
Figure 4-3. Morphological responses of *Paulownia tomentosa* to elevated CO₂. This figure compares plants grown under ambient (left) and elevated (right) CO₂ concentrations (410 ppm and 950 ppm, respectively) in three growth stages: fifth week (A), sixth week (B), and eighth week (C).

4.1.2. Seasonal effects of elevated CO_2 on the leaf gas exchange

The effect of eCO_2 on plant gas exchange parameters is delineated in Figure (Figure 4-4). The results demonstrate a significant enhancement in net CO_2 uptake (A) attributed to eCO_2 during the initial weeks of growth (Treatment effect: Anova F = 72.29, p < 0.001, Table 4-1). However, this increase in the photosynthetic activity showed a diminishing trend starting from the sixth week (Interaction effect: Anova F=7.07, p < 0.001, Table 4-1), eventually leading to statistically comparable A rates between both ambient and elevated CO_2 plants.

In parallel, the intercellular CO_2 concentration (c_i), a proxy for CO_2 availability within the leaf, fluctuated significantly throughout the study, exhibiting an evident reduction by the end of the observation period. Despite this decline, c_i values remained significantly elevated in comparison to those in plants cultivated under ambient CO_2 (aCO_2) (Interaction effect: Anova F = 6.21, p < 0.001, Table 4-1). Overall, eCO_2 consistently resulted in elevated c_i levels (Treatment effect: Anova F = 598.88, p < 0.001, Table 4-1).

Stomatal conductance (g_s) and transpiration (E) demonstrated similar trends throughout the growth season, reaching a significantly higher value only on the second week of growth compared to plants at aCO_2 (Figure 4-4). This rise may be associated with the increased photosynthetic demand observed in the same period, likely influenced by environmental fluctuations. By the fourth week, both g_s and E rates declined and reached marginally decreased values relative to plants grown in aCO_2. This result suggests that elevated CO_2 slightly reduced stomata aperture from week 4. However, in general, these variations in g_s and E did not reach statistical significance (Table 4-1).

The water use efficiency (WUE) was measured as the ratio of net CO_2 uptake to water vapor loss. The dynamic variation on WUE is shown in (Figure 4-5). Results indicate that WUE of eCO_2-treated plants was generally higher under elevated CO_2 (Treatment effect: ANOVA F = 164.61, p < 0.001, Table 4-1). A significant fluctuation in WUE was observed over the 8 weeks, with dips at weeks 2 and 4 (Interaction effect: ANOVA F = 11.28, p < 0.001, Table 4-1). The effect of elevated CO_2 on WUE was highest in the 6th week and remained constant during the final weeks of exposure, resulting from increased A values and similar E rates between plant groups grown under ambient and elevated CO_2.
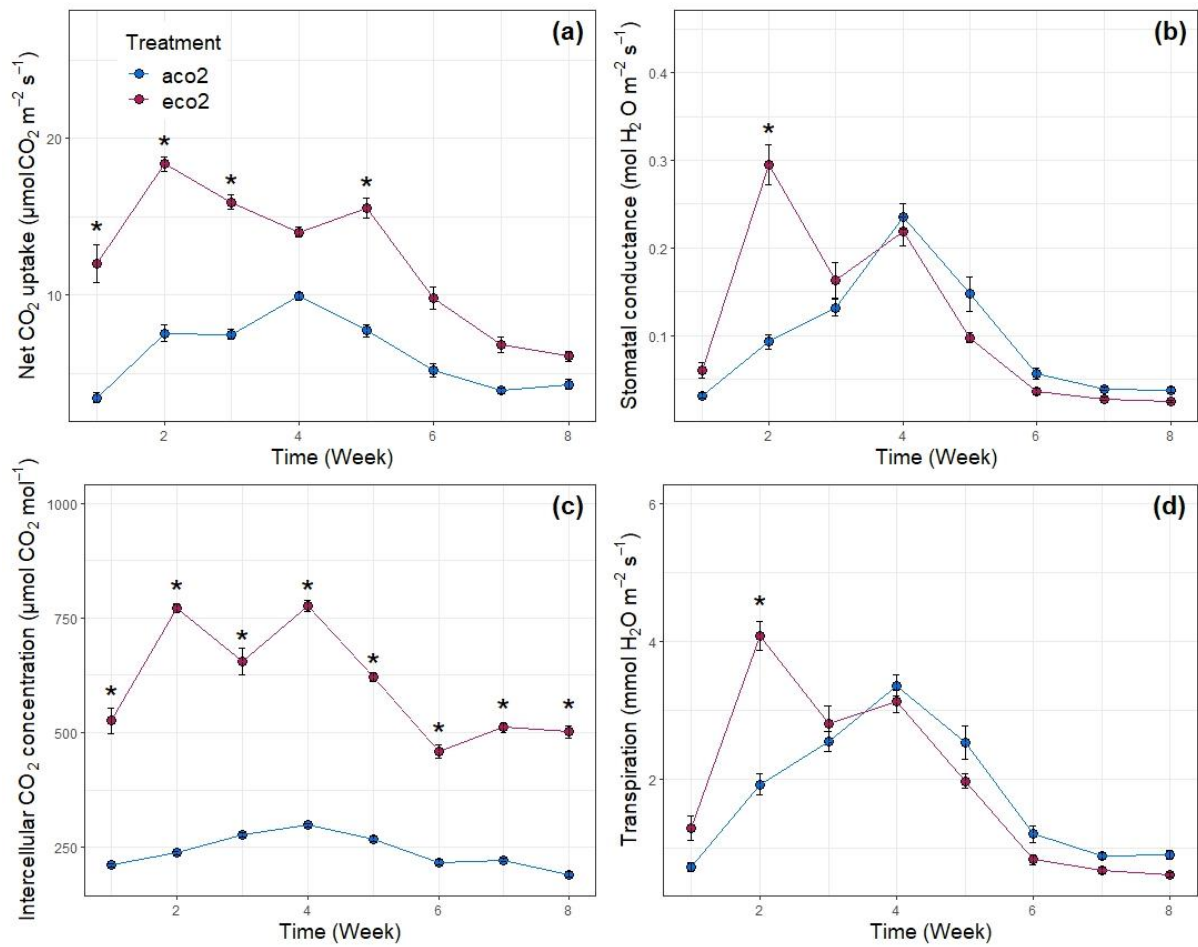
Figure 4-4. Seasonal effect of elevated CO₂ on the leaf gas exchange. Dots represent the means (± 95% confidence interval) of net CO_2 uptake (a), stomatal conductance (b), intercellular CO_2 concentration (c), and transpiration (d) in *P. tomentosa*, measured at 'aCO₂' and at 'eCO₂', n=4. Stars indicate statistical significance using the Tukey HSD post-hoc test at $p < 0.05$.
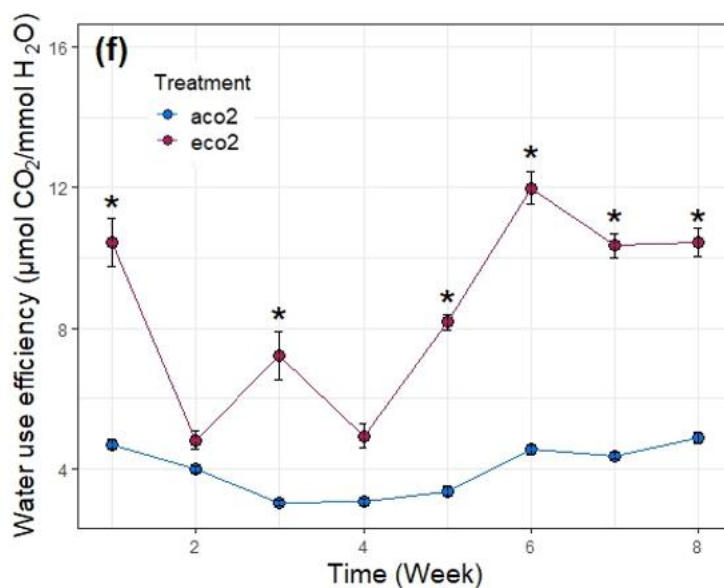
Figure 4-5. Seasonal effect of elevated CO₂ on the water use efficiency. Dots represent the means (± 95% confidence interval), measured at 'aCO₂' and at 'eCO₂', n=4. Stars indicate statistical significance using the Tukey HSD post-hoc test at p < 0.05.

Table 4-1. Statistical analysis of plant physiological responses to CO₂ treatment across different weeks. F and P-values indicate the effects of treatment and temporal changes (Weeks) on net CO_2 uptake (*A*), stomatal conductance (g_s), intercellular CO_2 concentration (c_i), on transpiration (*E*), and water use efficiency (WUE). The interaction between treatment and time (Treatment*Week) is also presented. Asterisks denote levels of statistical significance fitted with the linear mixed effect model (LME), and the analysis of variance (ANOVA) (*p < 0.05, **p < 0.01, ***p < 0.001).

Variables	Statistic	Treatment	Week	Treatment*Week
A	F	72.29	30.45	7.07
	P	0.0001553 ***	6.406e-14 ***	1.840-05***
g_s	F	1.21	17.53	4.48
	P	0.31	3.063e-10 ***	0.000967 ***
c_i	F	598.88	14.94	6.21
	P	< 2.2e-16 ***	6.786e-10 ***	4.048e-05 ***
E	F	0.46	20.99	3.51
	P	0.52	2.182e-11 ***	0.00509 **
WUE	F	164.61	11.28	5.12
	P	< 2.2e-16 ***	3.731e-08 ***	0.0002437 ***

4.1.3. Effects of elevated CO_2 on the wood structure and cross-sectional characterization

Wood cell structure was characterized using field emission scanning electron microscopy (FE-SEM) and light microscopy (Figure 4-6, Figure 4-8). The ray parenchyma tissue is characterized as multiseriate, while the axial parenchyma exhibits a paratracheal arrangement, specifically demonstrating a vasicentric or confluent pattern adjacent to the vascular tissue, and apotracheal diffuse in aggregates. Wood is ring-porous or half-ring-porous with solitary vessels, which were occasionally observed to be aggregated into multiples, comprising groups of two to three vessels.
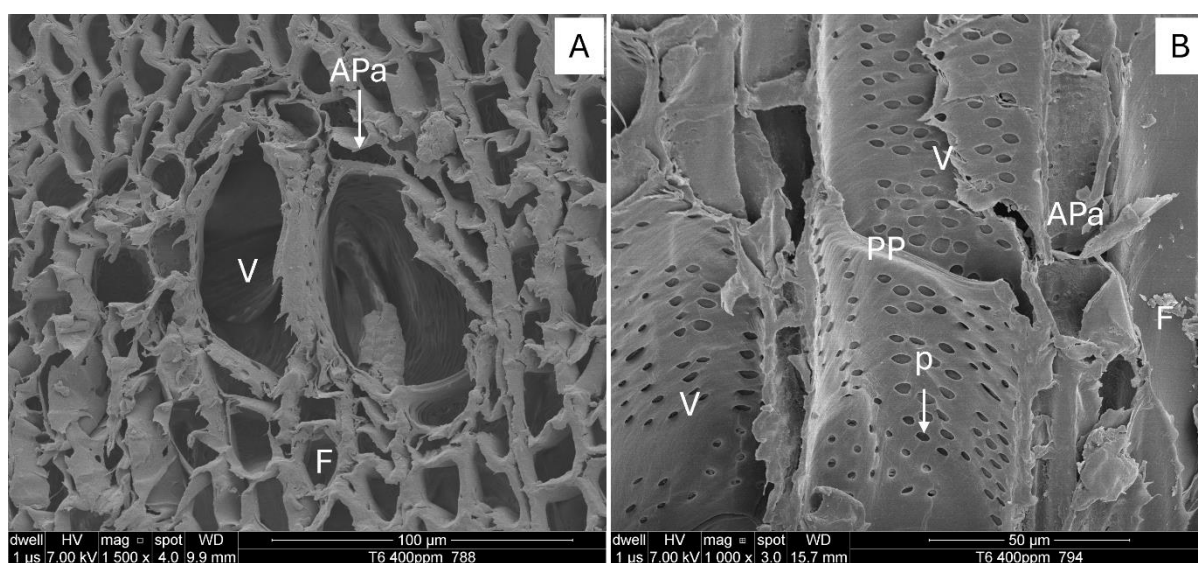
Figure 4-6. High-resolution field emission scanning electron microscope (FE-SEM) image illustrating the wood anatomy of *P. tomentosa* grown under ambient CO_2 conditions. Key structural components are labeled for clarity: 'V' indicates vessel elements; 'F' indicates fiber; 'APa' indicates the axial parenchyma; 'PP' indicates the perforation plate; and 'p' indicates the pits. Panel (A) presents a cross-sectional view of two grouped vessels. Panel (B) offers insight from the tangential perspective of the wood cells, showing two connected vessel elements by a perforation plate and axial parenchyma cells. Wood samples were coated with gold.

Major vessel characteristics were quantified to investigate the *P. tomentosa* response to elevated CO_2 in terms of hydraulic architecture. (Figure 4-8). Although the analyzed features did not statistically differ between both CO_2 concentration plant groups, elevated CO_2 increased vessel diameter by approximately 14.1% and vessel lumen area by 27.7%. Conversely, vessel frequency exhibited an 18.6% reduction (Figure 4-7), indicating an inverse relationship between both variables. The consistency in sample measurements suggests that the no significance in statistical outcomes may be attributed to restricted sample size. Nevertheless, the apparent anatomical adjustments in vessel structure indicate an adaptation likely conferring

improved hydraulic function, as supported by the premise that modest variations in vessel dimensions can have a meaningful influence on the overall plant water transport.
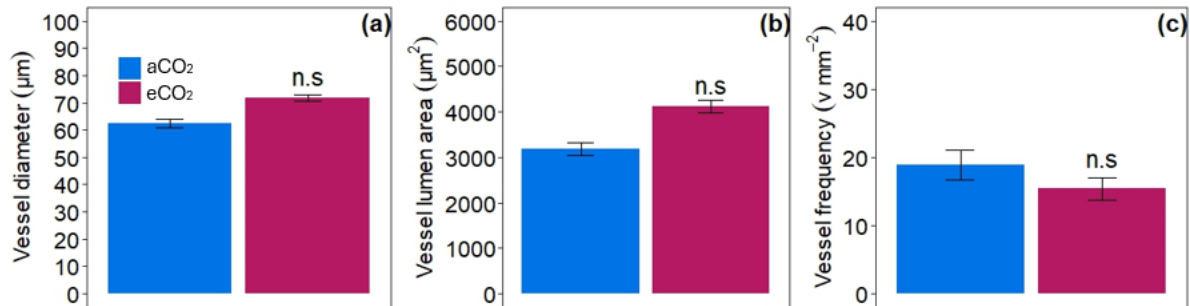
Figure 4-7. Effect of elevated CO$_2$ concentration on the vessel characteristics. Bars represent the means ($\pm$ 95% confidence interval) of the vessel diameter (a), vessel lumen area (b), and vessel frequency (c) in *Paulownia tomentosa*, measured at 'aCO$_2$' (410 ppm) and at 'eCO$_2$' (950 ppm). The notation 'n.s.' indicates nonstatistical significance between the means using the Mann-Whitney U-test at $p < 0.05$.
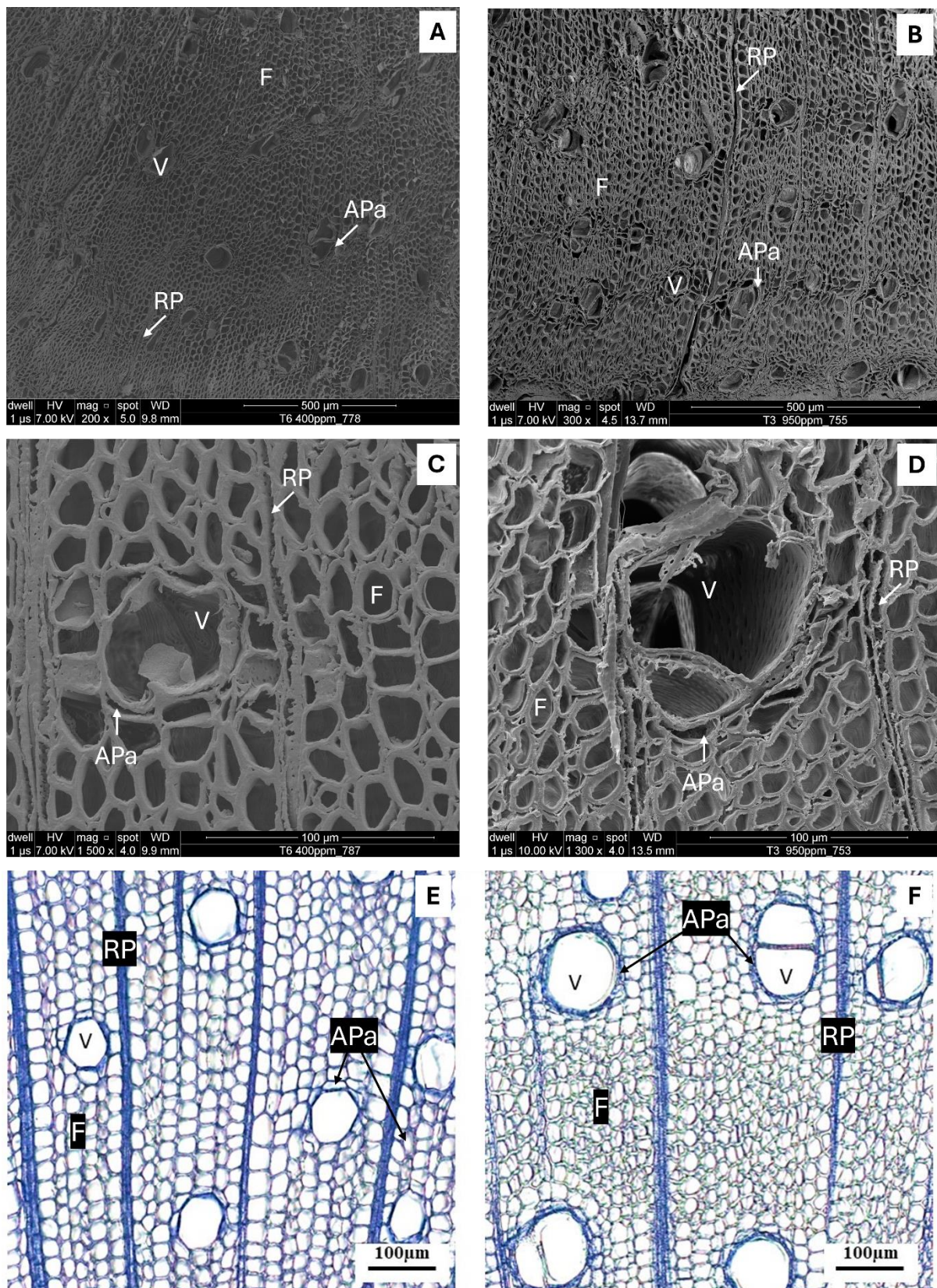
Figure 4-8. SEM and light microscopic cross-sectional images of *P. tomentosa* stem developed under ambient and elevated CO₂ concentrations. Key structural components are labeled for clarity: 'RP' indicates cells from ray parenchyma, 'APa' indicates cells from axial parenchyma, 'F' indicates the fibers, and 'v' indicates the vessel elements. (A, B, C, D) Photographs from high-resolution field emission scanning electron microscopy (FE-SEM) providing details of the xylem tissue microstructure of samples developed under ambient CO₂ (A, C) and elevated CO₂ (B, D). Wood samples were coated with gold. (E, F) Light microscopic photographs of

51

Paulownia tomentosa wood tissues developed under ambient (E) and elevated (F) CO_2 concentrations. Wood sections were stained with safranin (1%) and astra-blue (0.5%). Images were captured using an AxioCam MRC on a Zeiss Axioskop 40 microscope with 10× magnification.

4.1.4. Effect of elevated CO_2 on the elemental composition of guard cells and mesophyll chloroplasts

Analysis of essential nutrients such as magnesium (Mg), potassium (K), phosphorus (P), sulfur (S), chloride (Cl), and calcium (Ca) was performed in the guard cells (Figure 4-9 A) and chloroplasts of the mesophyll cells (Figure 4-9 B) at the end of the growth season. In guard cells, elevated CO_2 was found to significantly reduce Mg concentration by 42.3% (Student's test $T = 2.49$, $DF = 6.28$, $p = 0.045$, Figure 4-9 A). Analysis of the other minerals within guard cells revealed no statistically significant differences between plant groups grown under ambient and elevated CO_2 concentrations. Still, a decrease in K concentration by 11.6% was observed. In contrast, Cl, Ca, and P increased by 95.3%, 27.3%, and 3.3%, respectively. The S concentration remained unchanged.

In the mesophyll chloroplasts, the concentration of all the analyzed minerals did not statistically significantly differ. However, plants grown at elevated CO_2 showed decreased K and Cl concentrations by 32.9% and 54.3%, respectively. Mg, Ca, and P increased by 3.5%, 27%, and 19.5%, respectively. Sulfur levels remained comparable regardless of CO_2 concentration (Figure 4-9 B).
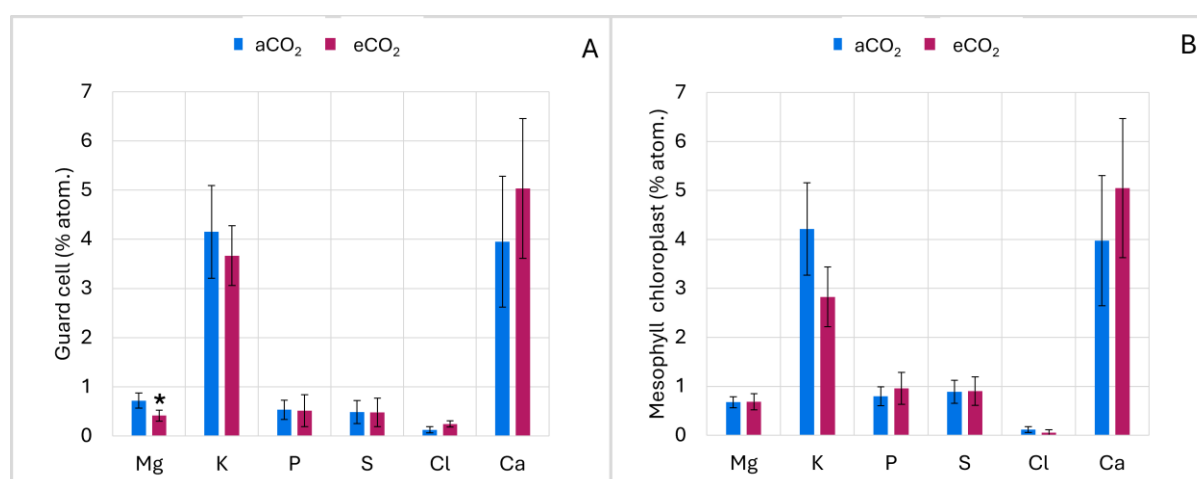
Figure 4-9. Effect of elevated CO_2 on the concentration of minerals in the leaf cells. Bars represent the means (± 95% confidence interval) of minerals in the guard cells (A) and chloroplasts of the mesophyll cells (B), measured at 'aCO_2' (410 ppm) and at 'eCO_2' (950 ppm), n=5. Stars indicate statistical variation between the means using the student's t-test at $p < 0.05$.

4.1.5. Associations between morpho-physiological traits

To elucidate the associations among gas exchange parameters, alteration in vessel characteristics, and plant performance under elevated CO_2, a Spearman correlation analysis was employed (Figure 4-10). Significant positive relationships were found between vessel diameter and both net CO_2 uptake (Spearman rho = 0.86, p < 0.05) and water use efficiency (WUE) (Spearman rho = 0.81, p < 0.05). Moreover, weak positive relationships were observed between vessel diameter and stomatal conductance (Spearman rho = 0.36, p = n.s.), as well as transpiration (Spearman rho = 0.54, p = n.s.), indicating that stomata rather than xylem conduits primarily control water transport at elevated CO_2.

Vessel diameter also positively correlated with leaf dry biomass (Spearman rho = 0.95, p = 0.0001), root dry biomass (Spearman rho = 0.81, p = 0.02), total biomass (Spearman rho = 1, p < 0.001), stem diameter (Spearman rho = 0.93, p = 0.002) and plant height (Spearman rho = 0.93, p = 0.002) (Figure 4-11). These associations suggest that CO_2-induced adjustments in xylem hydraulics also determine plant performance.

Significant correlations were identified between root and leaf biomass (Spearman rho = 0.74, p = 0.04) (Figure 4-11). A robust positive correlation was found between plant height and stem diameter (Spearman rho = 0.83, p = 0.01), leaf biomass (Spearman rho = 0.81, p = 0.02), and total biomass (Spearman rho = 0.93, p = 0.002) (Figure 4-11). Additionally, stem diameter exhibited a strong positive association with both leaf biomass (Spearman rho = 0.88, p = 0.007) and total biomass (Spearman rho = 0.88, p = 0.002) (Figure 4-11).
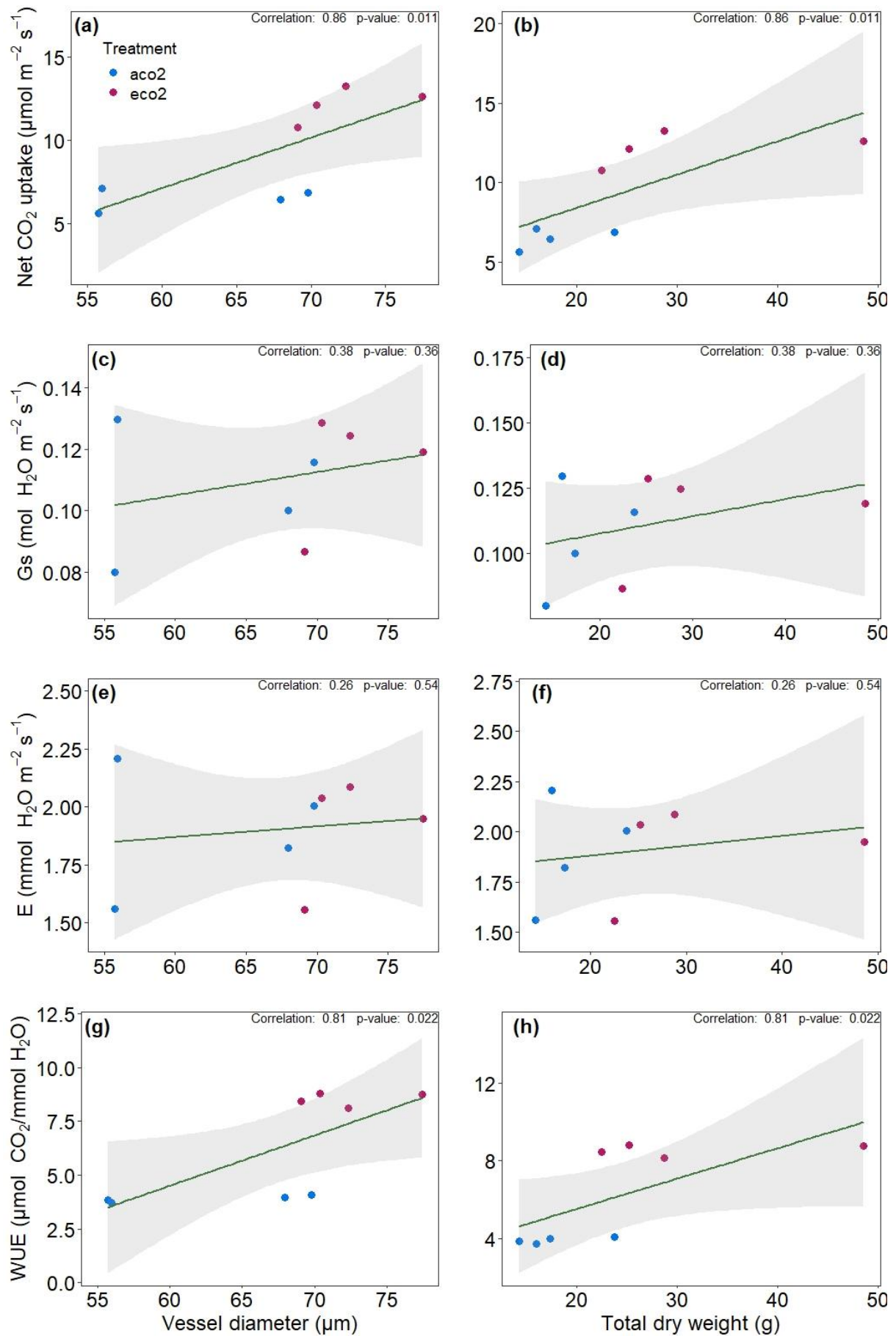
Figure 4-10. Correlations between gas exchange parameters and plant morpho-physiological traits. This figure illustrates the associations between key gas exchange metrics - net CO_2 uptake (a,b), stomatal conductance (c,d), transpiration (e,f), and water use efficiency (g,h) - with vessel diameter and total dry biomass, respectively. Each panel details the correlation coefficients and p-values, with the statistical significance of the observed relationships through Spearman's rank correlation analysis.
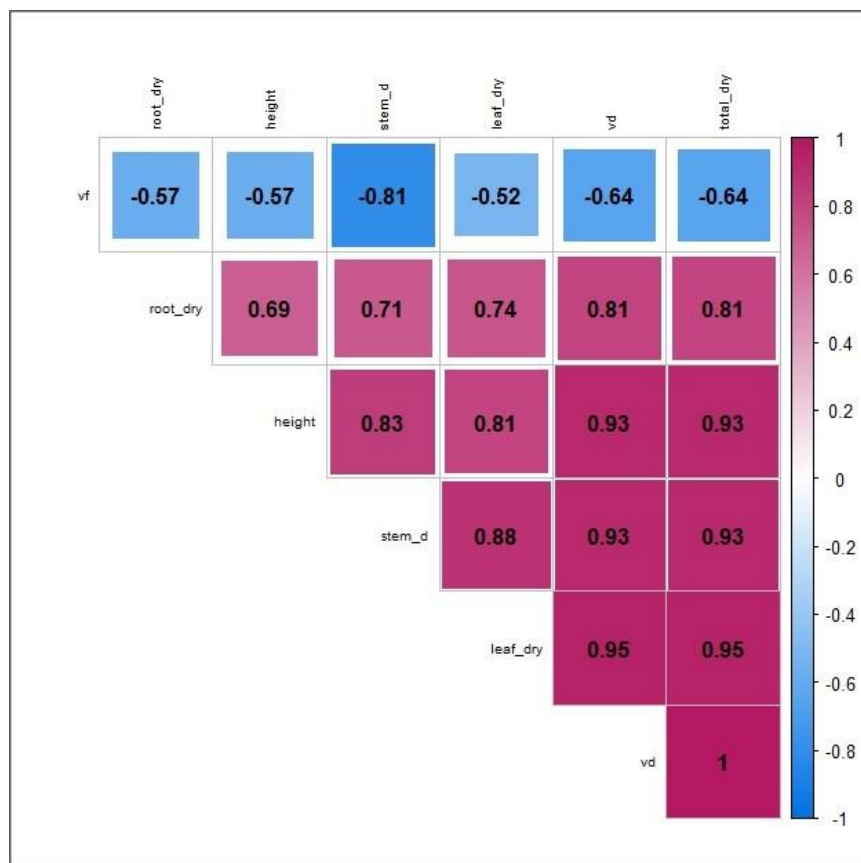
Figure 4-11 Correlation matrix showing the relationships between the vessel characteristics and morphological parameters in *P. tomentosa*. The variables are labeled for clarity: The growth indicators, root_dry, leaf_dry, total_dry, and stem_d, correspond to the root, leaf, overall dry biomass, and stem diameter, respectively). The vessel characteristics, vd, and vf, correspond to the vessel diameter and vessel frequency, respectively. The matrix details the correlation coefficients through Spearman's rank correlation analysis.

4.2. Effect of cyclic drought stress on the physiology, leaf pigment composition, and wood structure of *Paulownia tomentosa*

4.2.1. Effect of cyclic drought stress on the morphological traits

To understand the morphological adjustments of Paulownia plants to progressive drought stress, plants were harvested for analysis at the end of the growth season. This investigation followed a period during which the plants were subjected to recurrent cycles of drought stress. Thus, plants may have already started to show signs of drought adaptation. Towards the culmination of the growth season, the impact of cyclic drought was notable on the dry biomass of the root (Mann Whitney U = 0, p < 0.01), shoot (Mann Whitney U = 0, p = 0.03), and total

biomass (Mann Whitney U = 2, p = 0.01), resulting in a reduction of approximately 64.2%, 42.4%, and 56.4%, respectively (Figure 4-12).
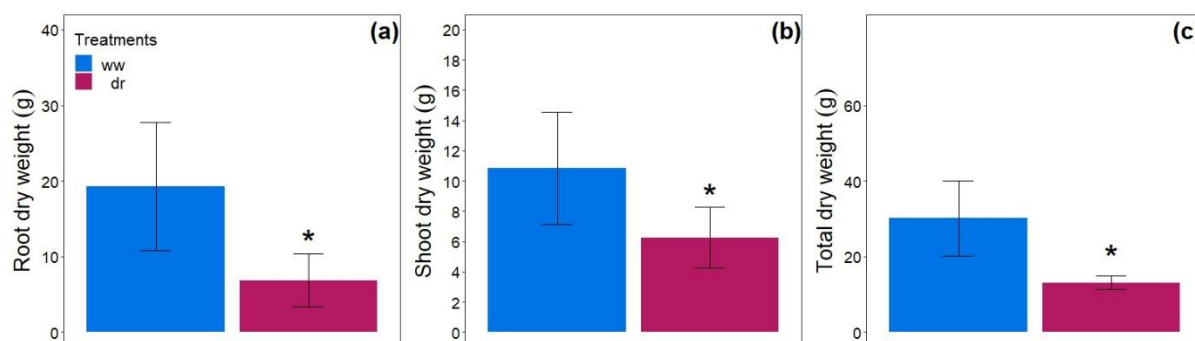
Figure 4-12. Effect of cyclic drought stress on the dry biomass of *Paulownia tomentosa*. Bars represent the means (± 95% confidence level) of the root (a), shoot (b), and total (c) biomass, measured in 'ww'= well-watered, and 'dr'= cyclic drought conditions (n=5). Star symbols indicate significant differences between treatments using the Mann-Whitney U test at p < 0.05.

A decreasing trend was observed in the stem diameter, height, total leaf area, and leaf number, even though this was not statistically significant (Figure 4-14), indicating that drought stress still exerted an influence that could culminate in substantial long-term impacts. Paulownia plants responded to drought stress by shedding older leaves with clear oxidation symptoms prior to abscission (Figure 4-13), which caused a reduction in the average leaf number by approximately 31%. Dry plants experienced losses in stem diameter, height and total leaf area of 24%, 15%, and 26%, respectively (Figure 4-14).

Figure 4-13. Paulownia plants subjected to drought stress. The red arrows point to leaves showing clear symptoms of oxidation of the chlorophylls and regions on the stem where leaves senesced. The photograph was taken when plants were under the third drought cycle.
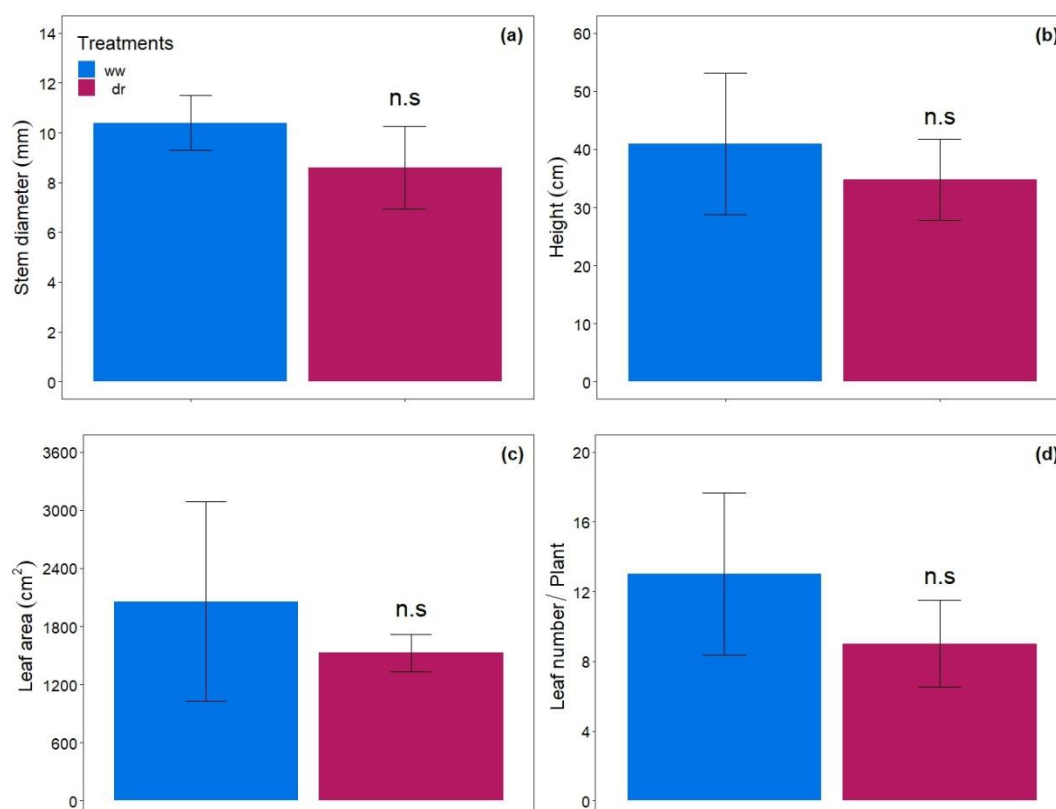
Figure 4-14. Effect of cyclic drought stress on the morphological parameters of *Paulownia tomentosa*. Bars represent the means ($\pm$ 95% confidence interval) of the stem diameter (a), height (b), leaf area (c), and leaf number (d), measured in 'ww'= well-watered, and 'dr'= cyclic drought conditions (n=5). The designation 'n.s' indicates non-significant variations between treatments using the Mann-Whitney U test at $p < 0.05$.

4.2.2. Effects of cyclic drought stress on leaf gas exchange and stomata traits

Measurements of leaf gas exchange parameters were conducted to elucidate the physiological responses of Paulownia plants to progressive drought stress. This study specifically focused on measuring net CO_2 uptake (A), stomatal conductance (g_s), intercellular CO_2 concentration (c_i), transpiration rates (E), water use efficiency (WUE), and the stomatal limitation value (Ls). These parameters were recorded at bi-daily intervals throughout two drought cycles. This frequent monitoring provided valuable insights into the dynamic changes in the mentioned physiological parameters in the Paulownia plants exposed to recurrent drought cycles.

Parameters varied significantly over the sampling days and between the treatments (Figure 4-15, Table 4-2). Gas exchange assessments revealed that plants under drought stress exhibited a comparable net CO_2 uptake to well-watered plants until the seventh day of the drought cycle. However, a reduction was evident from the ninth day (Treatment effect: Anova F =6.65, P = 0.03, Table 4-2), persisting until the conclusion of the observation period. A similar trend was observed for stomatal conductance (Treatment effect: Anova F = 22.1, P = 0.001, Table 4-2), revealing a strong positive and significant relationship with net CO_2 uptake (Spearman's rho = 0.92, p < 0.001, Figure 4-16). This correlation implies that the decline in net CO_2 uptake appears to be primarily driven by the decrease in stomatal conductance.
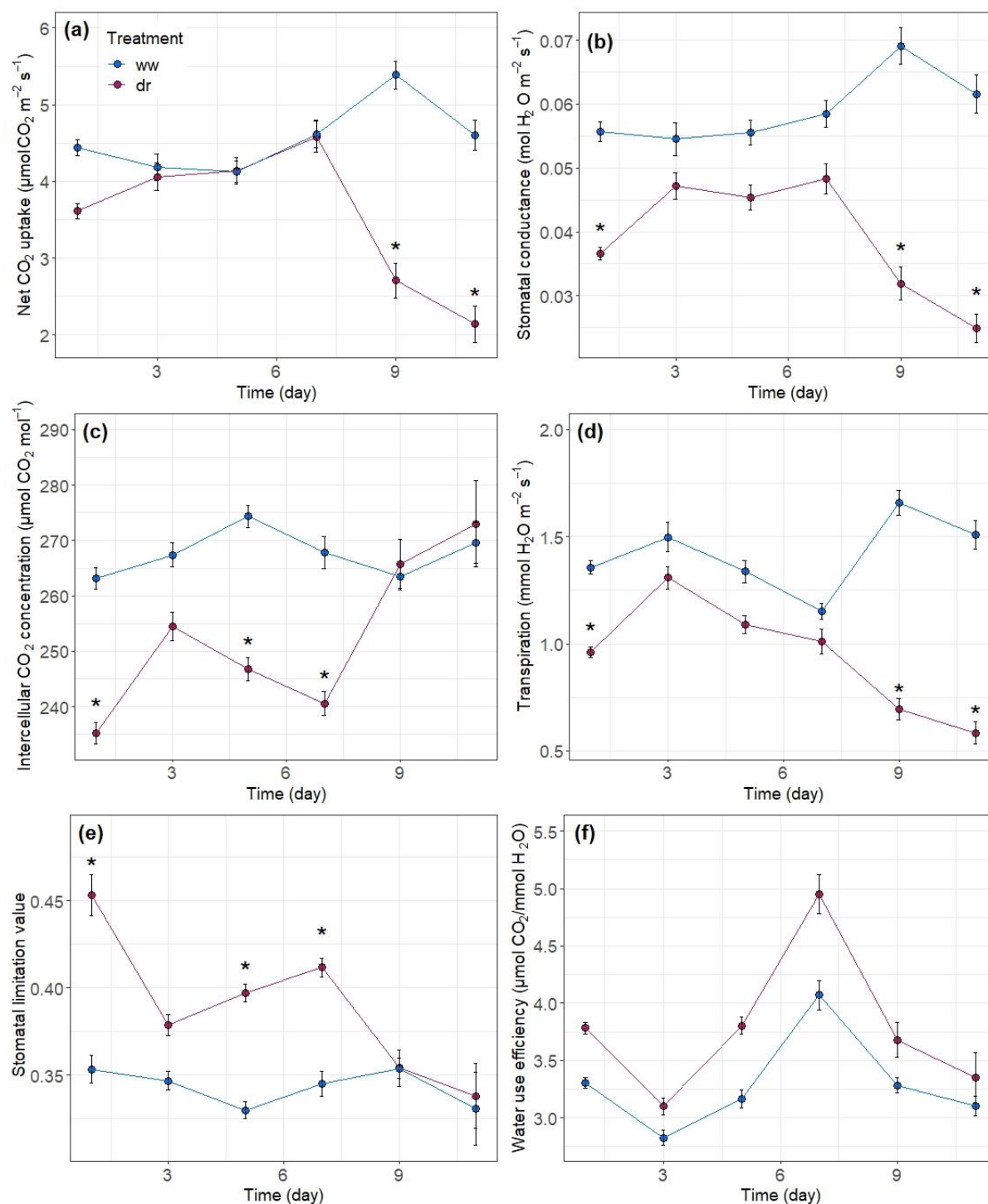
Figure 4-15. Effect of cyclic drought stress on the gas exchange parameters. Dots represent the means (± 95% confidence interval) of the net CO_2 uptake (a), stomatal conductance (b), intercellular CO_2 concentration (c), transpiration (d), stomata limitation value (e) and water use efficiency (f) in *Paulownia tomentosa* measured in 'ww'= well-watered, and 'dr'= cyclic drought conditions (n=5). Star symbols indicate significant differences between treatments using the Tukey HSD test at $p < 0.05$.

Drought-induced reductions in net CO_2 uptake rely on stomatal and non-stomatal limitations. These conditions can be assessed by observations on intercellular CO_2 concentration (c_i) and stomatal limitation value (*Ls*) parameters. Both parameters varied significantly across the days

with a stronger stomatal control on days 5 and 7 of the second drought cycle (Cycle effect on c_i: Anova F = 5.96, p = 0.01; Treatment effect: Anova F = 11.25, p = 0.008; Cycle effect on *Ls*: Anova F = 8.44, p < 0.01; Treatment effect: Anova F = 10.7, p < 0.01, Table 4-2), which finally aligned with the levels observed in well-watered plants by day 9, indicating an impairment in photosynthesis possibly caused by a combination of stomatal and enzymatic impairments.

Initial observations revealed a parallel trend in both stomatal conductance and transpiration up to the seventh day of drought exposure. Transpiration significantly varied across the days irrespective of the drought cycle (Day effect: Anova F = 2.36, p = 0.04, Table 4-2), suggesting the influence of factors beyond drought stress during this period. It is important to note that on the first day, the plants were still recovering from the effects of the preceding drought cycle, significantly impacting the early measurements. However, a marked decline in both transpiration and stomatal conductance was observed by the ninth day (Treatment effect on *E*: Anova F = 26.82, p < 0.001; Treatment effect on g_s: Anova F = 22.1, p = 0.001, Table 4-2). Interestingly, between the third and seventh day, both parameters exhibited marginally lower values in the drought-stressed plants compared to their well-watered controls. This observation suggests a potential acclimation response in stomatal behavior, modulating transpiration per the ongoing drought conditions. Paulownia plants under sufficient and lowered water conditions showed a similar trend regarding water use efficiency (WUE). However, under drought, plants tended to use the water more efficiently (Treatment effect: Anova F = 9.0529, p = 0.01, Table 4-2). Given the symmetry of the WUE response across the days and cycles, variations in both detected by the model may be caused by environmental variations during the measurements. The interaction between treatment and day did not significantly affect the plant water use efficiency, suggesting that this variable was already adjusted to the water limitation due to the pre-exposure.

Table 4-2. Statistical analysis of the gas exchange responses across the drought cycles. F and P-values indicate the effects of treatment, temporal changes (Day), and the drought cycle on Net CO_2 uptake (*A*), stomatal conductance (g_s), intercellular CO_2 concentration (c_i), transpiration (*E*), water use efficiency (WUE), and stomatal limitation value (Ls). The interaction between treatment and time (Treatment*day) is also presented. Stars denote the strength of the statistical significance fitted with the linear mixed effect model (LME), and the analysis of variance (ANOVA) (*p < 0.05, **p < 0.01, ***p < 0.001).

Variables	Statistic	Treatment	Day	Drought cycle	Treatment*day
A	F	6.65	2.88	3	7.08
	P	0.03*	0.01*	0.79	1.743e-05***
	F	22.1	1.8	0.6	5.9

g_s	P	0.001**	0.12	0.44	0.0001***
c_i	F	11.25	3.88	5.96	3.63
	P	0.008**	0.003**	0.01*	0.005**
E	F	26.82	2.36	0.06	7.45
	P	0.0006***	0.04*	0.79	9.65e-06 ***
WUE	F	9.0529	10.3333	14.4102	0.4088
	P	0.0135964 *	1.366e-07 ***	0.0002922 ***	0.8412705
Ls	F	10.7015	4.9524	8.4481	3.8757
	P	0.0097164 **	0.0005578 ***	0.0047775 **	0.0034913 **
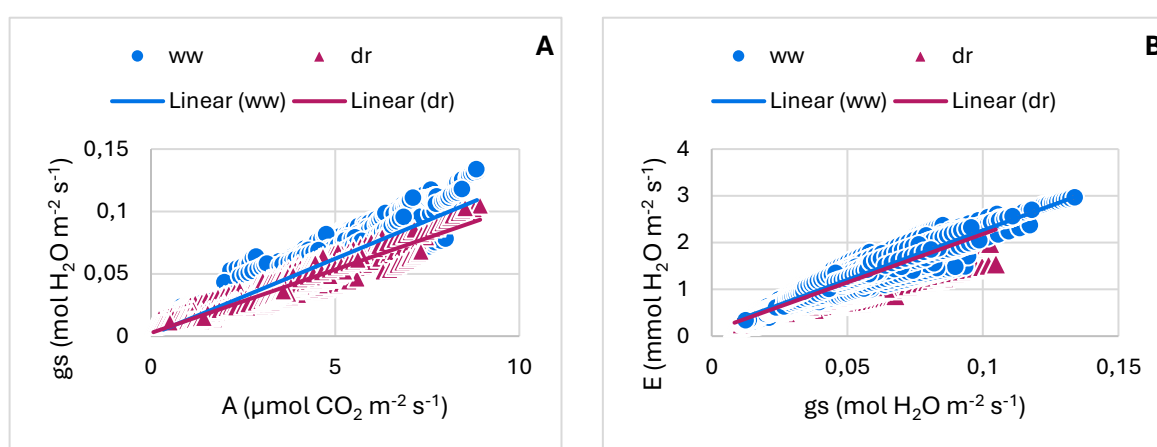
Figure 4-16. Relationship between gas exchange parameters. Stomatal conductance correlates positively with net CO_2 uptake (A) (Spearman's coefficient = 0.95, p < 0.001); and transpiration (Spearman's coefficient rho = 0.95, p < 0.001).

4.2.3. Effects of cyclic drought stress on the stomatal characteristics of Paulownia leaves

In the microscopic analysis of the effects of cyclic drought stress on stomatal characteristics, leaf samples were collected at the culmination of the growth season. Results revealed a significant impact of drought stress on stomatal size (Mann-Whitney U = 0, p < 0.01), reducing their length by 7.4%. Conversely, stomatal density did not exhibit any statistically significant changes under drought stress conditions (Figure 4-17).
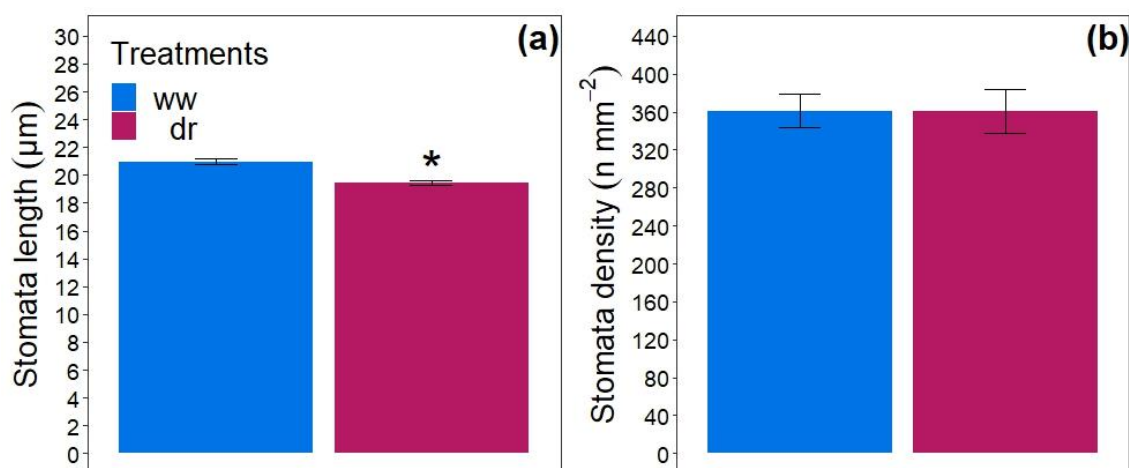
Figure 4-17. Effect of cyclic drought stress on the stomata traits. Bars represent the means (± 95% confidence interval) of the stomatal length (a), and stomatal density (b) in *Paulownia tomentosa*, measured in 'ww'= well-watered, and 'dr'= cyclic drought conditions. Star symbols indicate significant differences between treatments using the Mann-Whitney U test at p < 0.05.

4.2.4. Effect of cyclic drought stress on the chlorophyll fluorescence parameters

In this study, chlorophyll fluorescence analysis was utilized as a non-invasive method to assess the health of the photosynthetic apparatus in Paulownia plants under drought stress. The findings indicate that drought stress significantly reduced key photosynthetic efficiency parameters, including the quantum yield of photosystem II (Y(PSII)) (Anova F = 21.32, p < 0.001, Figure 4-18a) and the electron transport rate (ETR) (Anova F = 8.67, p < 0.01, Figure 4-18b). In parallel, a significant elevation was observed in both non-photochemical quenching of maximum fluorescence (NPQ) (Anova F = 5.4, p < 0.05, Figure 4-18f) and the quantum yield of regulated energy dissipation (Y(NPQ)) (Anova F = 20.3, p < 0.001, Figure 4-18e) in the light-adapted states of the plants. These results demonstrate a pronounced activation of protective mechanisms, as evidenced by the increased dissipation of absorbed light energy as heat. This enhancement in NPQ and Y(NPQ) suggests a strategic response by the plants to mitigate potential photodamage under stress, aiming at protecting the photosynthetic apparatus from excessive light exposure.

The quantum yield of non-regulated energy dissipation (Y(NO)) reflects key processes including non-radiative decay, fluorescence, and photoinhibition, while Fv/Fm represents the maximum quantum yield of the PSII in a dark-adapted state. Both parameters exhibited similar values across the different water treatment conditions, pointing to an apparent resilience of the photosynthetic apparatus in Paulownia plants under drought stress.
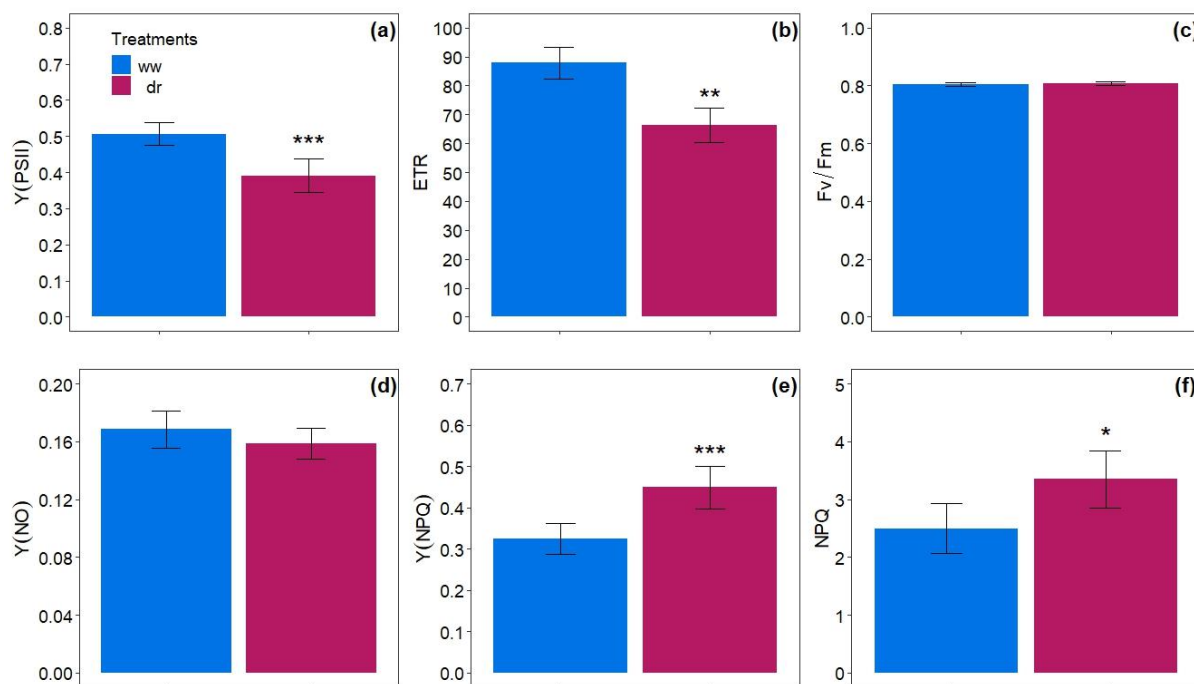
Figure 4-18. Effect of cyclic drought stress on the chlorophyll fluorescence parameters of the photosystem II. Bars represent the means (± 95% confidence interval) of operating efficiency under light-adapted state (a), the electron transport rate (b), the maximum photosynthetic efficiency (c), the quantum yield of non-regulated energy dissipation (d), the quantum yield of the non-photochemical quenching (e), and the non-photochemical quenching of maximum fluorescence, measured in 'ww'= well-watered, and 'dr'= cyclic drought conditions (n=5). Star symbols indicate significant differences between treatments using the Linear-mixed effects model. Significance codes: $p < 0.001$ '***', $p < 0.01$ '**', $p < 0.05$ '*'.

4.2.5. Effects of cyclic drought stress on the leaf pigment composition

In this study, drought stress conditions were associated with a substantial alteration in leaf pigment composition. Specifically, there was a significant increase in both chlorophyll (Anova $F = 29.27$, $p < 0.001$, Figure 4-19a) and anthocyanin (Anova $F = 40.29$, $p < 0.001$, Figure 4-19c) content across all measurements in plants subjected to drought stress. Conversely, flavonol content demonstrated a significant decrease under the same conditions (Anova $F = 103.07$, $p < 0.001$, Figure 4-19b). Interestingly, the nitrogen balance index (NBI), calculated as the ratio of chlorophyll to flavonol content in the leaves, exhibited a significant increase in plants experiencing drought stress (Anova $F = 144.08$, $p < 0.001$, Figure 4-19d).
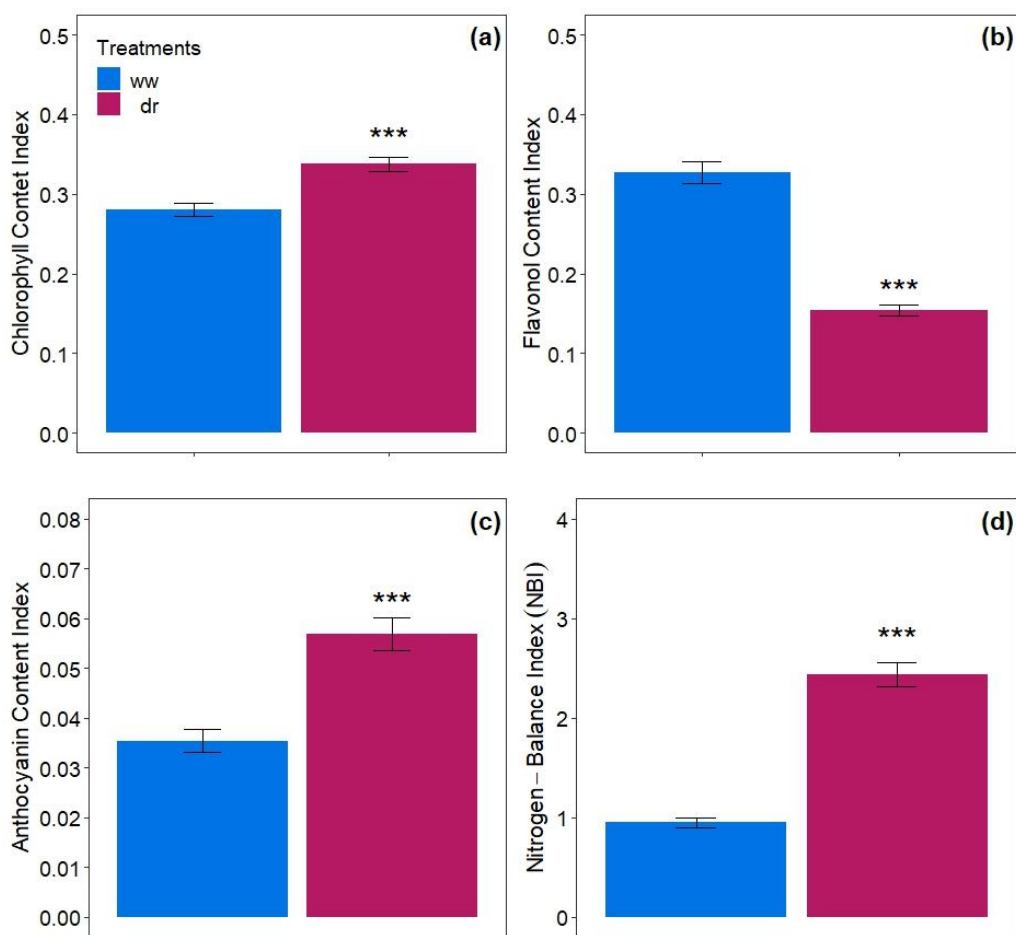
Figure 4-19 Effect of cyclic drought stress on the leaf pigment composition. Bars represent the means (± 95% confidence interval) of chlorophyll (a), flavonol (b), anthocyanin (c), and nitrogen balance index (d), measured in 'ww'= well-watered, and 'dr'= cyclic drought conditions (n=5). Star symbols indicate significant differences between treatments using the Linear-mixed effects model. Significance codes: p < 0.001 '***', p < 0.01 '**', p < 0.05 '*'.

4.2.6. Effects of cyclic drought stress on the wood structure

The anatomical adaptations of Paulownia vessels in response to drought stress are illustrated in Figure 4-20. A notable change observed was the significant reduction in vessel diameter in drought-exposed plants (Mann Whitney U = 2, p < 0.05, Figure 4-21a), leading to a corresponding decrease in lumen area by approximately 19.8% (Mann Whitney U = 2, p < 0.05, Figure 4-21b). Despite the unchanged overall vessel frequency across varying water treatments, a trend showed an approximate 8% increase in vessel density, indicating an inverse response to drought conditions.
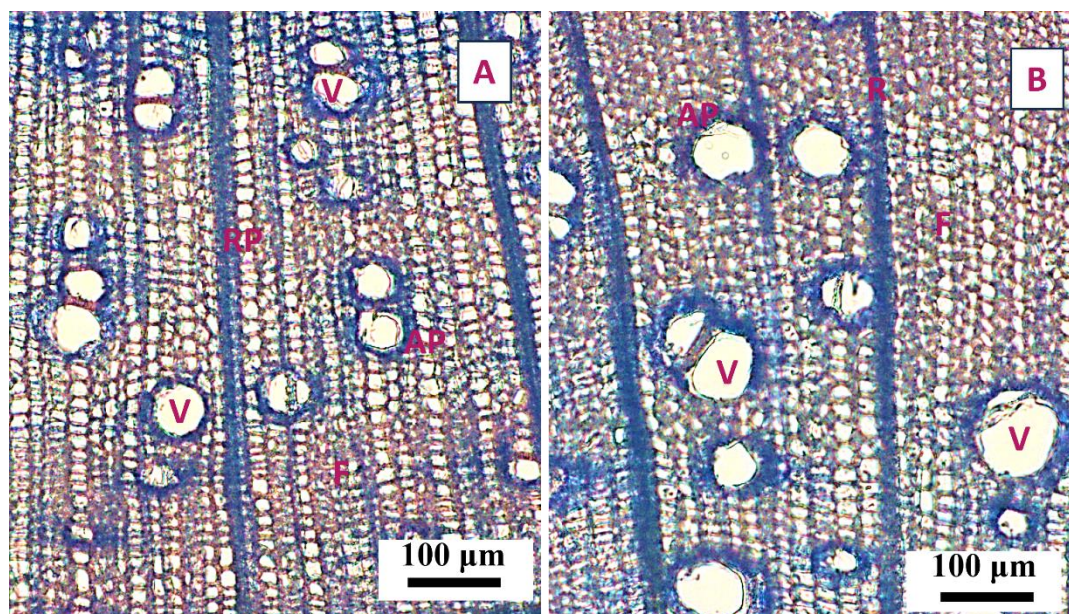
Figure 4-20.Anatomical image of the wood cross-section of well-watered and drought-stressed *P. tomentosa*. (A) cross-section of plants developed under drought stress and (B) well-watered conditions. Key cellular structures are labeled for clarity: V indicates the vessels, F indicates the fibers, AP indicates the axial parenchyma, and RP indicates the ray parenchyma. These visualizations highlight the morphological changes in xylem anatomy under drought conditions.
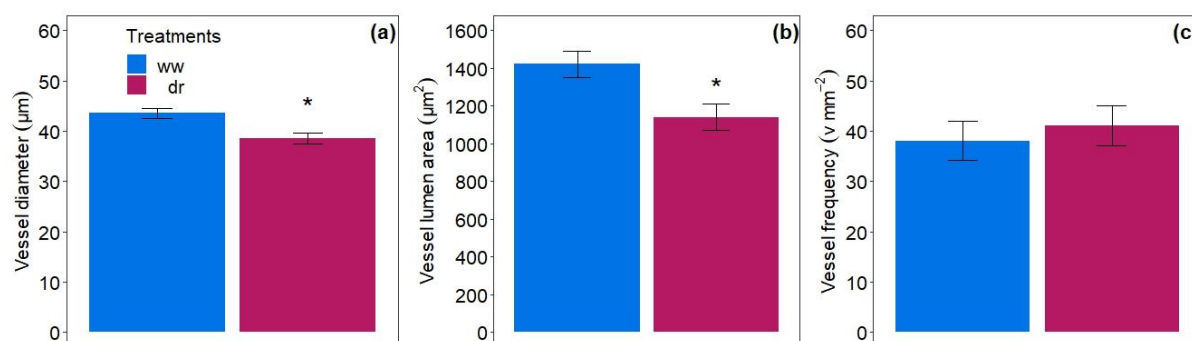
Figure 4-21 Effect of cyclic drought stress on xylem vessel characteristics. Bars represent the means (± 95% confidence interval) of vessel diameter (a), vessel lumen area (b), and vessel density (c) in *P. tomentosa*, measured in 'ww'= well-watered, and 'dr'= cyclic drought conditions (n=5). Star symbols indicate significant differences between treatments using the Mann-Whitney U test at $p < 0.05$.

4.2.7. Associations between gas exchange and stomatal characteristics

The association between gas exchange variables and stomatal length, vessel diameter, and total biomass is illustrated in Figure 4-22 and was compared using a Spearman correlation analysis. The analyses revealed that stomatal conductance (g_s) showed a significant strong positive correlation with all the three parameters mentioned above (Spearman's rho = 0.71, $p < 0.05$; Spearman's rho = 0.77, $p < 0.05$; Spearman's rho = 0.85, $p < 0,01$, respectively, Figure 4-22). A similar trend was found for transpiration (*E*) (Spearman's rho= 0,65, $p < 0.05$; Spearman's

rho = 0.67, p < 0.05; and Spearman's rho = 0,83, p < 0.01, respectively, Figure 4-22). The water use efficiency (WUE) correlated negatively with stomatal length and total dry matter (Spearman's rho = – 0.78, p < 0,05; Spearman's = – 0.71, p < 0.05, respectively, Figure 4-22), while no significant correlation was observed between WUE and vessel diameter. Finally, the net CO_2 uptake correlated positively with total dry weight (Spearman's rho = 0.7, p < 0.05, Figure 4-22), and vessel diameter (Spearman's rho = 0.71, p < 0.05, Figure 4-22), but it does not appear to correlate significantly with stomatal length.
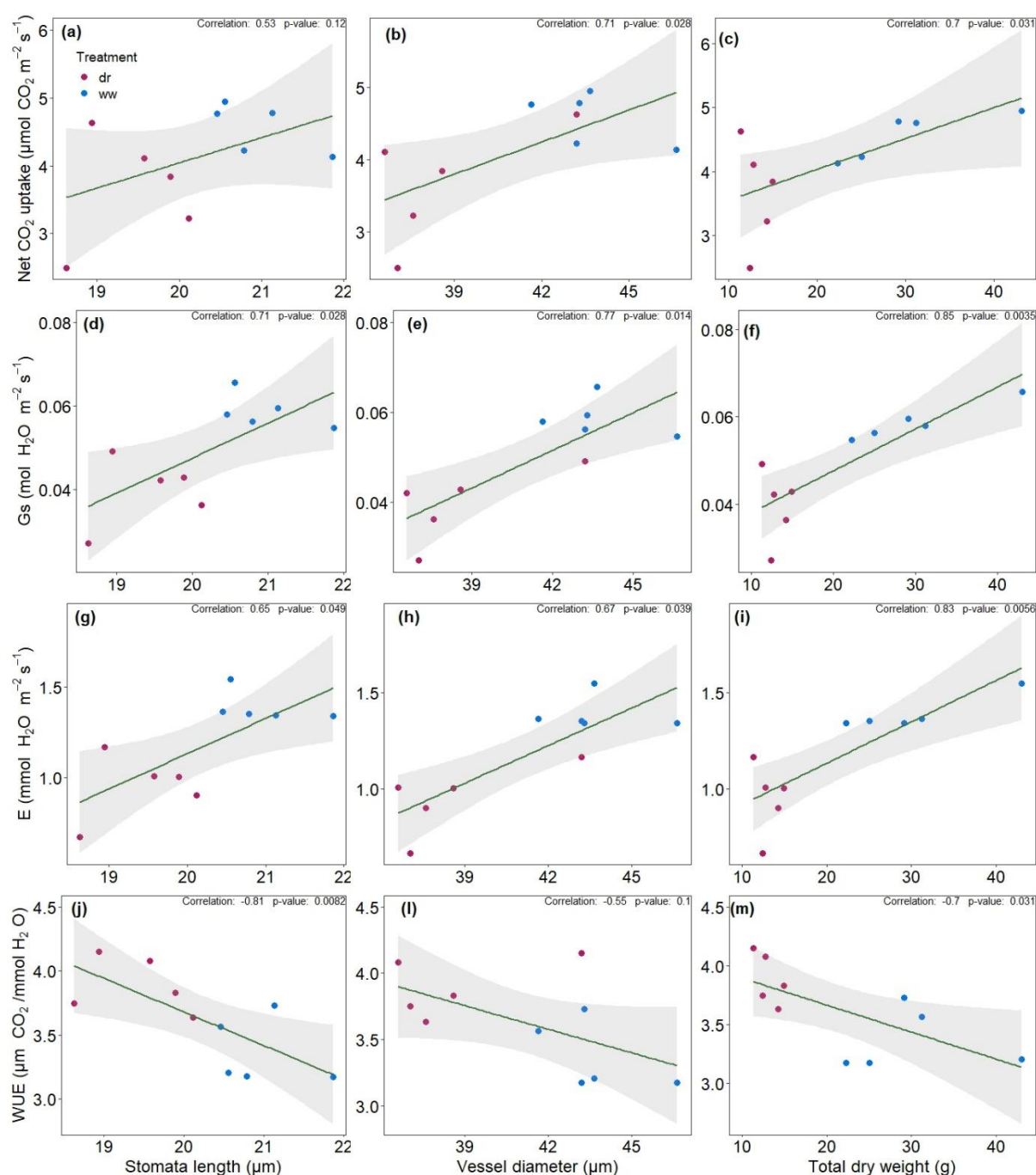
Figure 4-22. Scatter plots showing the relationships between physiological parameters and growth metrics in *Paulownia tomentosa*. The Spearman's correlation and p values are provided for (a)-(c) Net CO_2 uptake versus stomatal length, vessel diameter, and total dry weight, respectively. (d)-(f) Stomatal conductance versus stomatal length, vessel diameter, and total dry weight, respectively. (g)-(i) Transpiration rate versus stomatal length, vessel diameter, and total dry weight, respectively. (j)-(l) Water use efficiency versus stomatal length, vessel diameter, and total dry weight, respectively. Each point represents an individual plant, with treatments denoted by different colors (dry treatment in red, wet treatment in blue).

4.2.8.   Associations between chlorophyll fluorescence and leaf pigment composition

A second correlation analysis was performed to explore the relationships between the chlorophyll fluorescence parameters and the leaf pigment parameters, leaf temperature, and transpiration (Figure 4-23). Leaf temperature correlated positively with the non-photochemical quenching variables, namely Y(NPQ) (Spearman's rho = 0.72, p = 0.02) and NPQ (Spearman's rho = 0.92, p < 0.001), while it correlated negatively with the quantum yield of the PSII (Spearman's rho = − 0.65, p = 0.049). Transpiration correlated positively with Y(PSII) (Spearman rho = 0.88, p < 0.001), ETR (Spearman's rho = 0.94, p < 0.001) and flavonol content (Spearman's rho = 0.66, p =0.016), while it correlated negatively with Y(NPQ) (Spearman's rho = − 0.81, p = 0.002), chlorophyll content (Spearman's rho = − 0.77, p = 0.017) and anthocyanin content (Spearman's rho = − 0.78, p = 0.008). The Y(PSII) showed a positive correlation with ETR (Spearman's rho = 0.83, p = 0.0001) and flavonol content (Spearman rho = 0.66, p = 0.002), while it correlated negatively with the Y(NPQ) (Spearman's rho = − 0.94, p < 0.001), the chlorophyll content (Spearman's rho = − 0.75, p < 0.007), and anthocyanin content (Spearman's rho = - 0.81, p < 0.001). The ETR correlated positively with the flavonol (Spearman's rho = 0.78, p = 0.017), and negatively with the Y(NPQ) (Spearman's rho = − 0.77, p = 0.001), chlorophyll (Spearman's rho = − 0.79, p = 0.016), and anthocyanin (Spearman's rho = − 0.83, p = 0.006). The Y(NPQ) showed a positive correlation with the NPQ (Spearman coefficient = 0.88, p = 0.003), the chlorophyll (Spearman's rho = 0.71, p = 0.01), and the anthocyanin (Spearman's rho = 0.83, p = 0.002), while it correlated negatively with flavonol content (Spearman's rho = 0.70, p = 0.007). The NPQ correlated positively with the chlorophyll (Spearman's rho = 0.67, p = 0.04) and the anthocyanin (Spearman's rho = 0.76, p = 0.02). The chlorophyll correlated positively with the anthocyanins (Spearman's rho = 0.94, p < 0.001) and negatively with the flavonol content (Spearman's rho = − 0.67, p = 0.01).
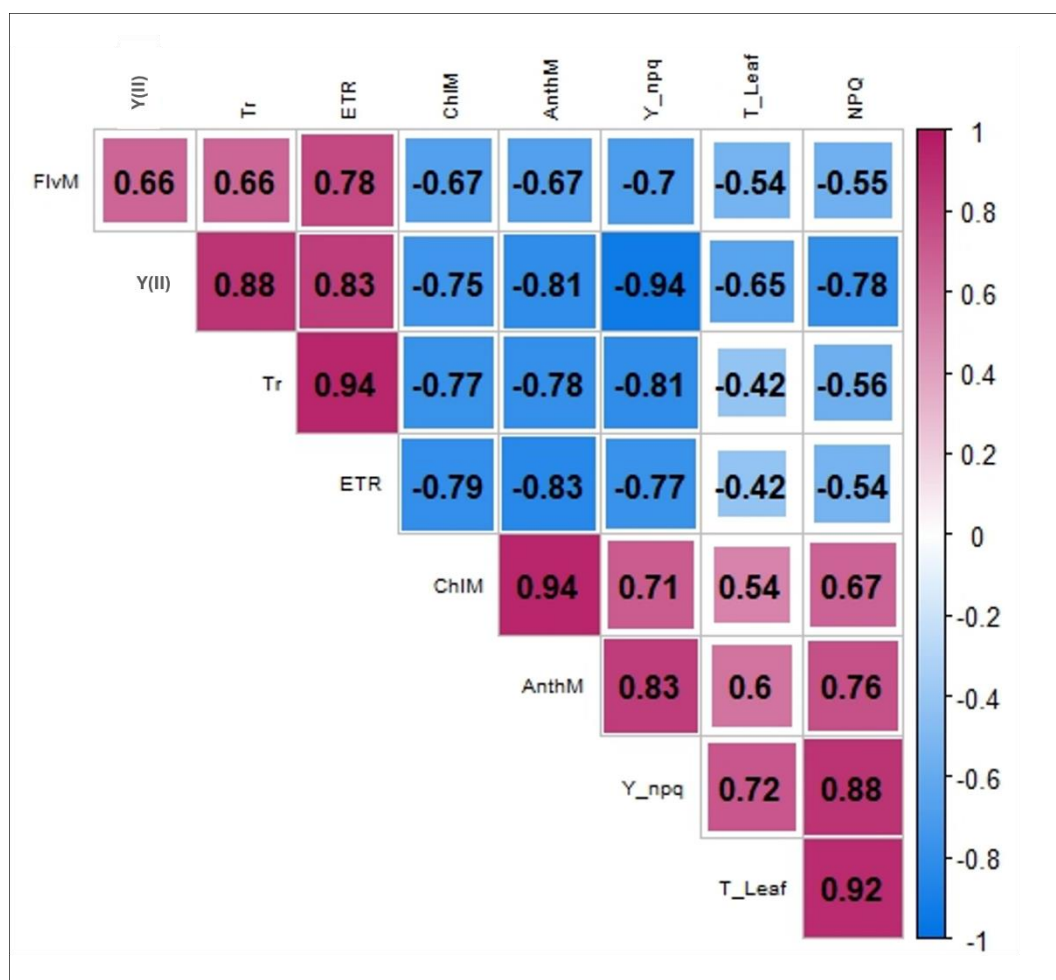
Figure 4-23 Correlation matrix showing the relationships between chlorophyll fluorescence and leaf pigments. The variables are labeled for clarity: The chlorophyll fluorescence, YII, ETR, Y_npq, and NPQ correspond to the quantum yield of the photosystem II, the electron transport chain, the quantum yield of the non-photochemical quenching, and the non-photochemical quenching, respectively. The leaf pigments ChlM, AnthM, and FlvM correspond to chlorophyll, anthocyanin, and flavonol, respectively. Tr and T_Leaf correspond to the transpiration and leaf temperature, respectively. The matrix details the coefficients through Spearman's rank correlation analysis.

4.3. Electrophysiological responses of *Paulownia tomentosa* to local burn and re-irrigation

4.3.1. Intracellular responses of the leaf cells

To verify whether plants were excitable, a cold shock stimulus was applied before local burn and re-irrigation stimuli (Figure 4-24). A transient membrane hyperpolarization was observed in response to the stimulus, with an amplitude of – 22 mV and lasting approximately 54 seconds (Table 4-3). The signal did not trigger any alterations in the gas exchange of distal leaves.
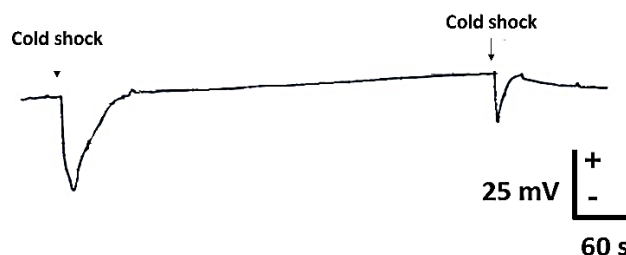
Figure 4-24 Electrical response of *P. tomentosa* to cold shock. Signals were recorded intracellularly after applying a water stimulus at 4°C, approximately 5 mm from the microelectrode.

Table 4-3. Characteristics of electrical signals elicited in *P. tomentosa* in response to cold shock. Signals were recorded intracellularly after applying a water stimulus at 4°C, approximately 5 mm from the microelectrode.

Stimulus	Amplitude (mV)		Duration (Seconds)	
	Mean	SD	Mean	SD
Cold shock	− 22.22	9.53	54.8	20.6

Following a local burn wounding, electrical signals with undefined form (Figure 4-25) were detected propagating at an approximate speed of 1.02 and 0.89 cm s^{-1} and lasting 8.7 and 7.0 minutes for the stimulus applied in the leaf tip and in the adjacent leaf, respectively (Table 4-4). The amplitude of the signal varied depending on the direction of transmission. Signals traveling acropetally induced an overall depolarization event of the plasma membrane with an average amplitude of 15.3 mV (Table 4-4). In contrast, signals transmitted basipetally, originating from a wounding event in closer proximity to the measuring electrode, resulted in overall hyperpolarization of the membrane with an average amplitude of –19.7 mV (Table 4-4). Regarding re-irrigation, a shift in amplitude towards the negative direction was observed, accounting for – 44.1 mV, with a speed of 1.5 cm s^{-1}, and a duration of 7.3 minutes (Table 4-4).
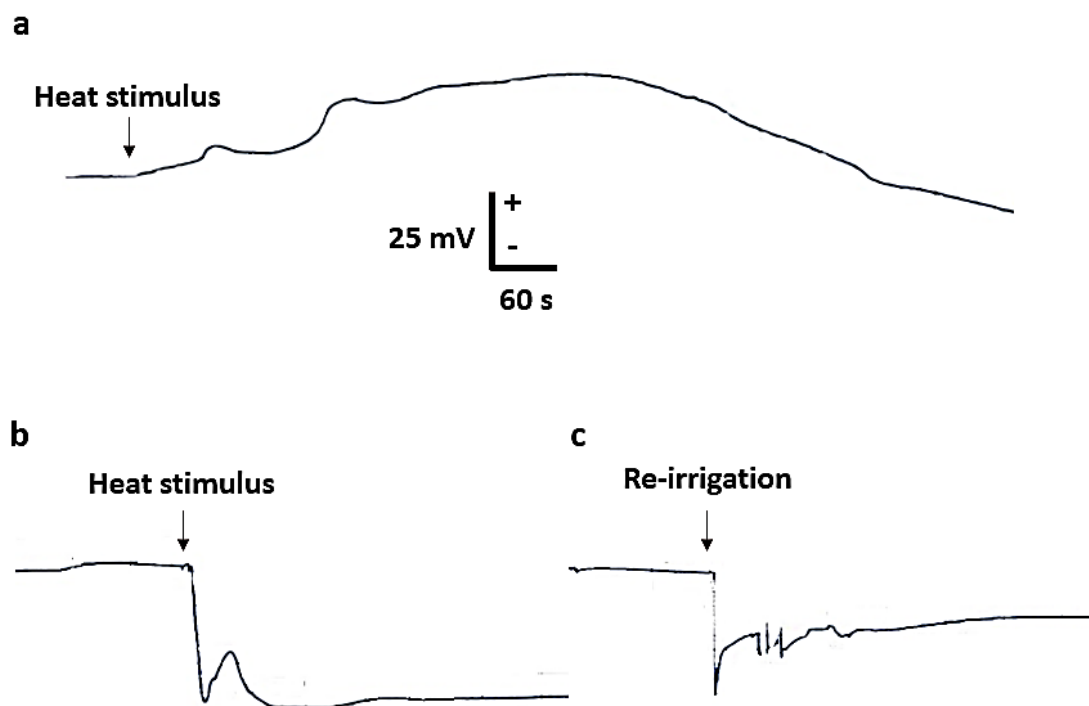
Figure 4-25. Examples of the electrical response of *P. tomentosa* to local burn and re-irrigation. The signals were recorded using the intracellular method after stimulus on the adjacent leaf leave (a), the tip of the same leaf (b), and soil rehydration (c).

Table 4-4. Characteristics of electrical signals elicited in *P. tomentosa* in response to local burn and re-irrigation. The mean values and standard deviation are detailed. Signals were recorded using the intracellular method. The designation 'Heat(tip)' corresponds to a heat stimulus applied to the tip of the leaf containing the inserted electrode (n = 6). The designation 'Heat(ad)' corresponds to a heat stimulus applied to the adjacent leaf (n = 6). Re-irrigation refers to soil rehydration upon drought (n = 3).

Stimulus	Speed (cm s^{-1})		Amplitude (mV)		Duration (min.)	
	Mean	SD	Mean	SD	Mean	SD
Heat(tip)	1,024	0,225	−19,735	17,132	8,75	5,675
Heat(ad)	0,892	0,299	15,36	20,499	7	4,123
Re-irrigation	1,5	0,433	−44,12	25,916	7,34	5,033

4.3.2. Dynamics of the extracellular electrical signals in the leaf petiole

Electrical signals induced by local burn and re-irrigation stimuli were recorded extracellularly using electroencephalogram technology (EEG) (Figure 4-26).

The extracellular electrical potential (EP) before local burn was characterized by oscillations of low voltage, reaching average peak values relative to the baseline ranging between − 49.34 µV and +71.35 µV during the light measurements and between − 18.03 µV and +31.2 µV during the dark measurements. After the burn stimulus, clear alterations in the bioelectric

dynamics were observed, with amplitude signals oscillating between – 852.7 µV and + 1604.1 µV under light, and – 268.49 µV and + 877.46 µV under dark (Table 4-5). The waves were characterized by upward and downward deflections resulting in persistent fluctuations across the baseline (Figure 4-26), apparently extending for 7.5 (light) and 16.7 (dark) minutes (Table 4-5, Figure 4-26 A, C). This irregular oscillation can be attributed to electrodes being placed in plant tissues from two distinct, equally distanced regions from the stimulus site, given that the system is engineered to enhance the signal-to-noise ratio by canceling out signals of similar amplitudes, thereby restoring the electrical potential to its baseline.

Regarding plants exposed to drought, the bioelectric activity was characterized by multiple irregular spikes of varying amplitudes up to 1.5 mV, with no observed cessation during the first 50 minutes of drought recovery (Figure 4-26 B, D). This pattern was not observed in plants under normal conditions of growth.

Table 4-5 Characteristics of the bioelectric activity of *P. tomentosa* before and after local burn. Signals were recorded under light and dark conditions for 60 minutes (30 minutes before and 30 minutes after stimulus). EEG electrodes were inserted in the petiole of two adjacent canopy leaves (n=5). The local burn stimulus was applied to a leaf below.

Stimulus	Period	Amplitude		
Local burn		Min	Max	SD
Before	Light	– 49.34	71.35	7.86
Before	Dark	– 18.04	31.17	8.5
After	Light	– 852.59	1604.11	147.719
After	Dark	– 268.49	877.46	70.34
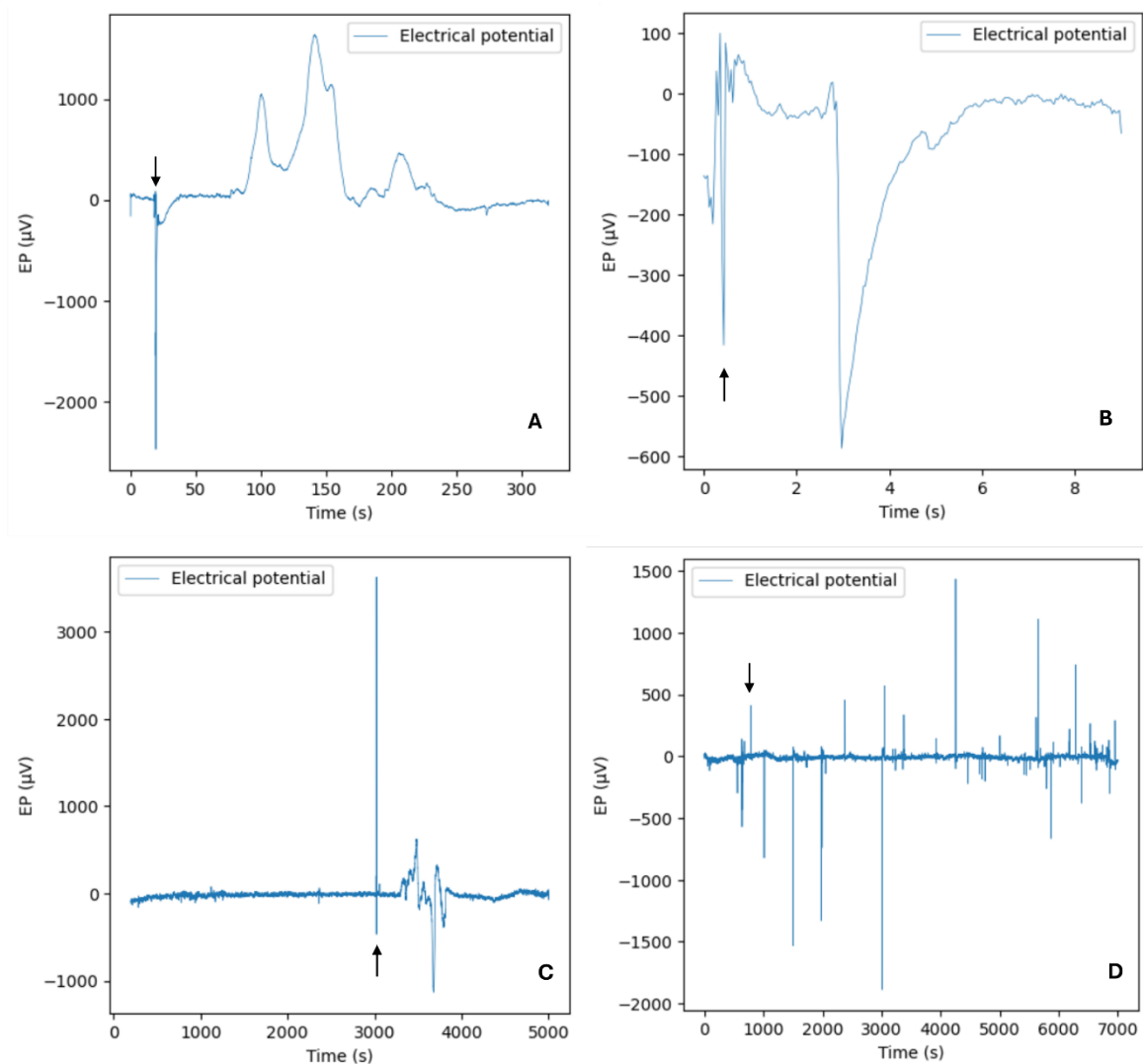
Figure 4-26. Typical electrical potentials recorded in *P. tomentosa* with EEG. Plants were subjected to local burn (A, C) and re-irrigation (B, D). Black arrows indicate the point where the stimuli were applied. Recording was conducted using the electroencephalogram (EEG), and a data acquisition software (Nerowerk EEG V10.0.0.31).

Generally, the predominant frequencies of plant electrical activity were observed between 0 and 1 Hz, exhibiting higher magnitudes between 0 and 0.2 Hz range (Figure 4-27), consistent with the frequency range of electrical signals of plants (Li et al., 2021). These magnitudes decreased sharply with increasing frequency regardless of the plant status. When subjected to both stimuli (local burn and post-drought re-irrigation), an increase in low-frequency power was observed, suggesting a dominance of slow wave activity (frequencies between 0 and 0.1 Hz) (Figure 4-27 B, D).
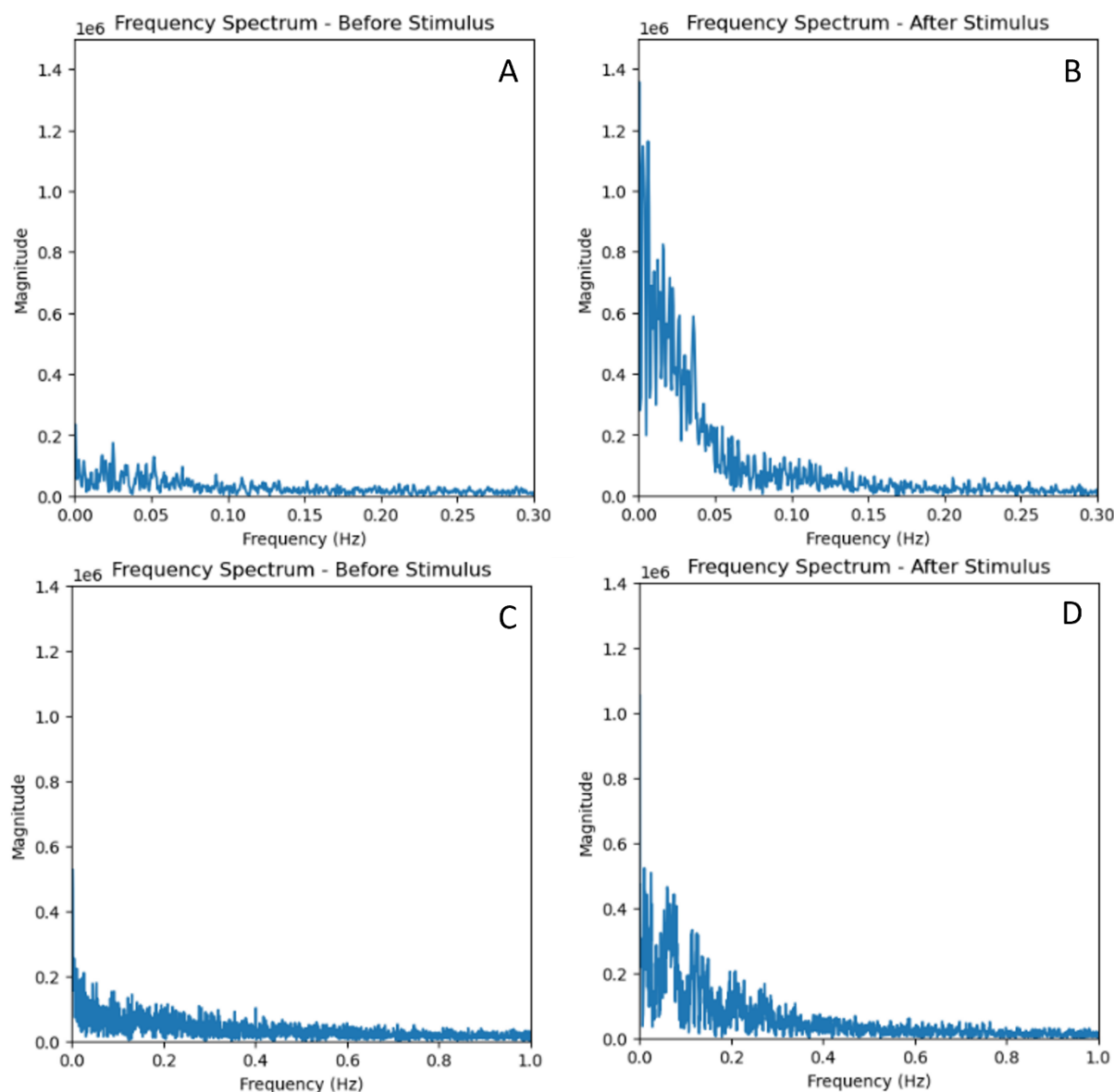
Figure 4-27. Frequency spectra of the electrical signals recorded before and after stimulus in *P. tomentosa*. Figures (A-B) show the frequency spectrum before and after local burn, and Figures (C-D) show the frequency spectrum before and after the re-irrigation stimulus.

Analysis of approximate entropy (ApEn) indicated a significant increase in signal complexity following the burn stimulus, as evidenced by higher ApEn values (Student's test T = 7.3, DF = 9, p < 0.001, Figure 4-28 B). In contrast, re-irrigation of drought-stressed plants resulted in a reduction in complexity and an increase in predictability, reflected by lower ApEn values (Student's test T = – 3.17, DF = 4, p < 0.05, Figure 4-28 A).
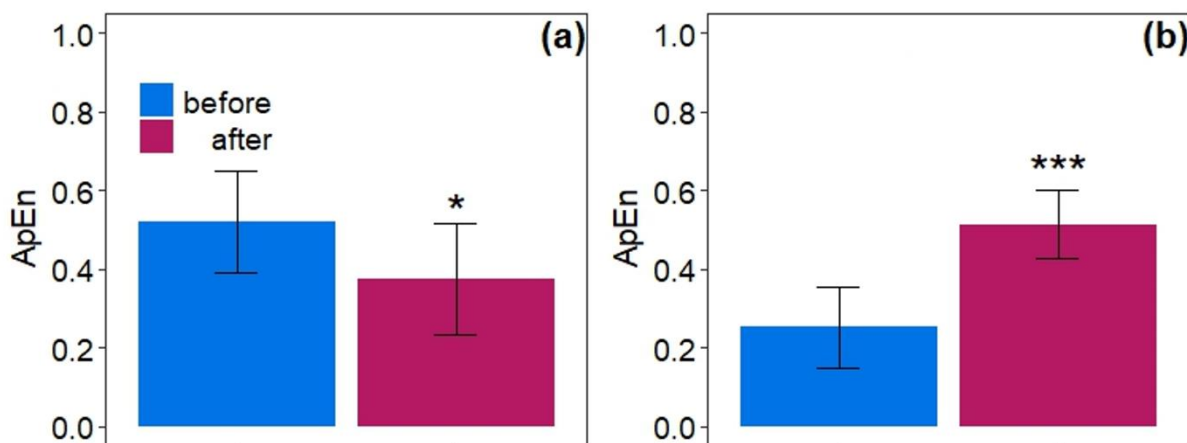
Figure 4-28. ApEn values of the EEG run before and after the stimulus in *P. tomentosa*. Bars represent the means (± 95% confidence interval) of ApEn values before and after soil rehydration after drought (n=5) (a); and before and after burn damage (n =10) (b). Star symbols indicate significant differences between treatments using the student's t-test at $p < 0.05$.

4.3.3. Photosynthetic gas exchange and chlorophyll fluorescence responses

Extracellular electrical signal measurements were carried out simultaneously with gas exchange recordings. Following the electrical signals elicited by local burn, modifications in gas exchange parameters were observed in distal undamaged leaves. Particularly, net CO_2 uptake (*A*), stomatal conductance (g_s), and transpiration (*E*) were significantly decreased, while intercellular CO_2 concentration (c_i) remained nearly constant during the day measurements (Figure 4-29 A, B, C). This indicates that the stimulus led to a systemic propagation that resulted in a partial stomata closure and partial inactivation of photosynthesis (Figure 4-29). Observations of leaf gas exchange throughout the nocturnal period revealed a transient increase in g_s and *E* after local burn, peaking at their highest rates 10 minutes post-stimulus (Figure 4-29 D, E). A concurrent decline in g_s and *E* coincided with a transient increase in net CO_2 emission and intercellular CO_2 concentration, indicating an induction of respiratory activity, with peak values reached approximately 6 minutes later (Figure 4-29 D). Interestingly, the temporal dynamics of the observed physiological events synchronized with the duration of the EP oscillations in the leaf petiole, as a decline in the rates of net CO_2 release coincided with the duration of the electrical signal (Figure 4-29 D, E, F).
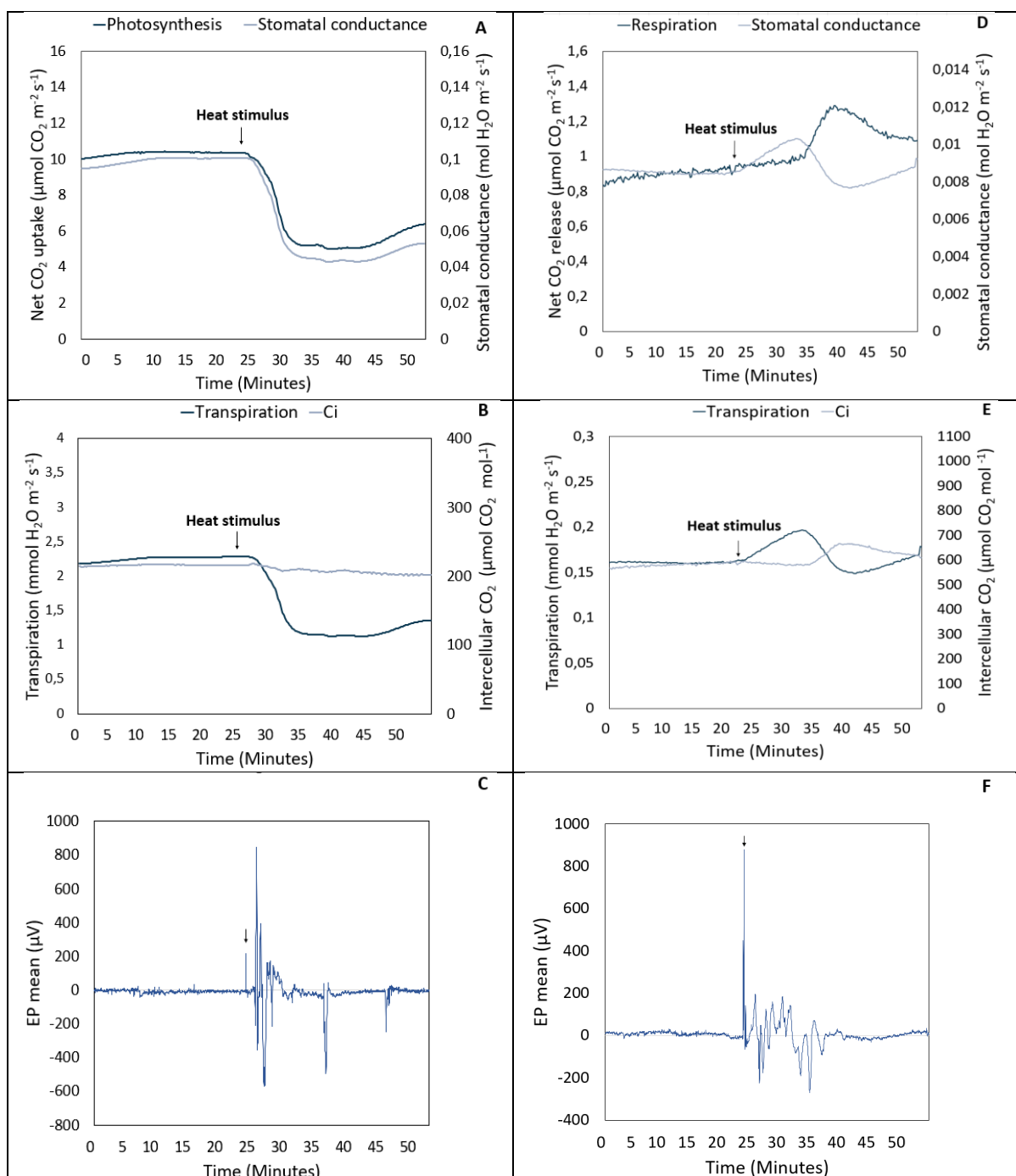
Figure 4-29. Gas exchange and bioelectric profile responses of *P. tomentosa* to local burn during light and dark. Dynamic variations on net CO_2 uptake are plotted with stomatal conductance during the day (A) and night (D); transpiration is plotted with intercellular CO_2 concentration during the day (B) and night (E); and the typical bioelectric profile of plants before and after stimulation using EEG is plotted during the day (C) and night (F). Plants were acclimated for 20 minutes before data collection. Black arrows indicate the time point of stimulation (n=5-6).

Although the re-irrigation stimulus elicited bioelectric responses in *P. tomentosa*, it appears to not substantially promptly alter net CO_2 uptake, stomatal conductance, or transpiration rates. Following the stimulus, these variables briefly stabilized before declining over the next 10 minutes. Subsequently, they gradually returned to rates comparable to those observed when the

stimulus was applied, suggesting possible enhancements in photosynthetic biochemical processes at this point (Figure 4-30). An observed increase in water use efficiency coupled with a decrease in the intercellular CO_2 concentration suggests the transition from biochemical towards stomatal constraints on photosynthesis, which may corroborate the beginning of recovery from drought (Figure 4-30B, Figure 4-31). However, these observations alone may not suffice to determine the influence of electrical signals on the photosynthetic gas exchange.

Similarly, chlorophyll fluoresce measurements were carried out to investigate whether any alterations were triggered regarding the efficiency of the photosystem II (PSII). The results demonstrated that re-irrigation did not affect the dynamics of the PSII efficiency (YPSII), electron transport rate (ETR), the yield of the non-photochemical quenching (YNPQ) and the yield of the non-regulated energy dissipation (YNO) (Figure 4-32). These results suggest that the light reactions were at sufficient rates to meet the energy requirements for the chloroplast's metabolic activity without triggering significant pH changes in the thylakoid lumen at the given water and light conditions.

The dynamics of photosynthetic processes in *P. tomentosa*, including light reactions and gas exchange dynamics, did not clearly respond to re-irrigation of the dry soil. Regarding photochemistry, future investigations should focus on chlorophyll fluorescence responses to drought at different light intensities. For gas exchange parameters, longer experimental periods may help to elucidate the role of electrical signals on the dynamics of these variables.
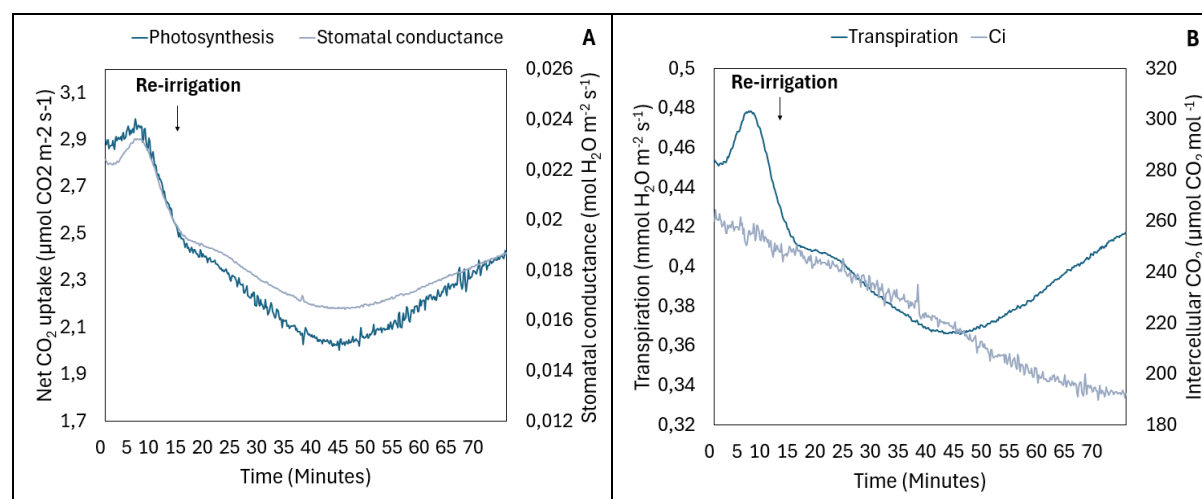
Figure 4-30. Dynamic variations on gas exchange in *P. tomentosa* in response to re-irrigation. Net CO_2 uptake was plotted with stomatal conductance (A), and transpiration was plotted with intercellular CO_2 concentration (B). Plants were acclimated for 20 minutes before data collection. Black arrows indicate the time point of stimulation (n=5).
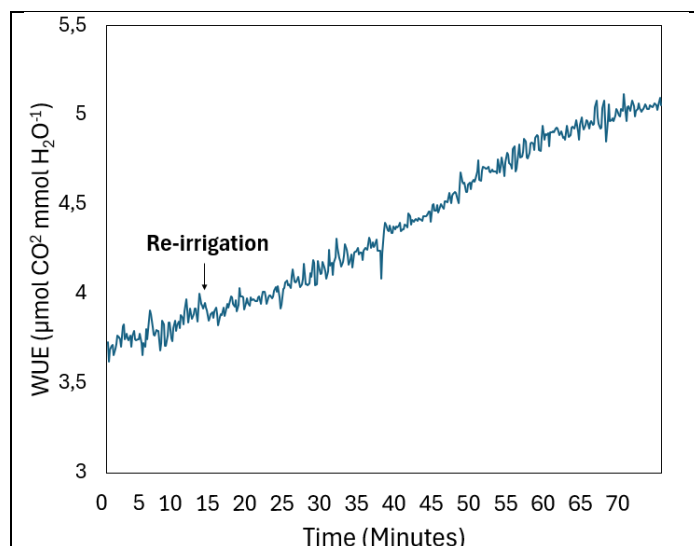
Figure 4-31. Dynamic variations on water use efficiency on *P. tomentosa* trees in response to re-irrigation. Plants were acclimated for 20 minutes before data collection. Black arrows indicate the time point of stimulation (n=5).
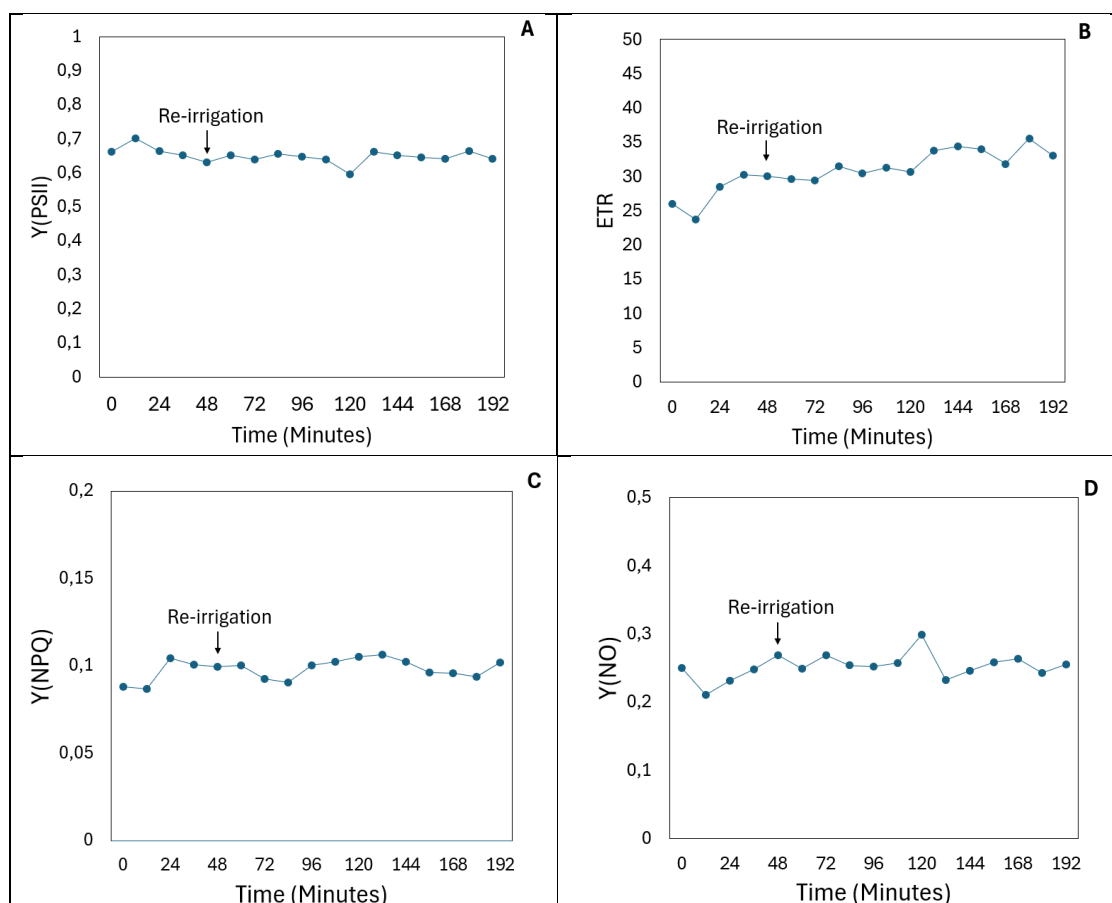
Figure 4-32. Dynamic variations on the chlorophyll fluorescence parameters in response to re-irrigation in *P. tomentosa*. Response of the (A) quantum yield of the PSII (Y(PSII)), (B) electron transport chain (ETR), (C) quantum yield of the non-photochemical quenching (Y(NPQ)), and (D) the quantum yield of the non-regulated energy dissipation (Y(NO)). Plants were acclimated for 25 minutes to light, and 5 data points were collected every 12 minutes before stimulus application (n=6).

5. DISCUSSION

5.1. Effects of elevated CO_2 on the physiology and wood structure of *Paulownia tomentosa*

The advantageous effects of atmospheric CO_2 enrichment on plant biomass performance have received empirical support. Yet, the generation of plant biomass is directly tied to the efficiency of photosynthesis, which, in turn, depends on water availability and its movement within the plant system. This denotes the significance of the plant's hydraulic properties in the process. The present study demonstrates that elevated CO_2 tended to enhance plant morphological traits, exhibiting a significant effect on the shoot biomass and height of three-years-old Paulownia trees. Furthermore, all analyzed morphological variables showed positive significant relationships with photosynthesis, which was supported by a more efficient vascular system developed under elevated CO_2.

5.1.1. Effect of elevated CO_2 on the morphological parameters

Elevated CO_2 concentrations typically enhance the accumulation of photosynthates in the leaves, promoting partitioning and resource allocation towards growth and storage at the whole-plant level. Previous studies have demonstrated varied morphological responses to elevated CO_2 (eCO_2) across different species. Hou et al. (2021) reported that eCO_2 stimulates increased investment in shoot biomass in *Brassica rapa*. Similarly, Arsić et al. (2021) observed increased above- and belowground biomass in *Quercus petraea*. A decrease in specific leaf area across both herbaceous and woody species was observed at eCO_2 (Wang et al., 2020). Moreover, Ziegler et al. (2023) noted a higher root proliferation in temperate deciduous woodlands, indicating a possible stimulation of root biomass increment under eCO_2 conditions. The results of the current study partially align with the previous findings, demonstrating that *P. tomentosa* trees respond to eCO_2 by increasing their height and leaf biomass, which confers an enhanced surface for light interception and CO_2 sequestration. Conversely, a minimal impact was observed on root biomass, which could be attributed to the spatial constraints of pot cultivation. Yet, the strong positive correlations between leaf and root biomass, stem, and height parameters indicate a synergistic relationship essential for plant function under elevated CO_2 conditions.

5.1.2. Effect of elevated CO_2 on leaf gas exchange parameters

During the initial phase of the exposure period, the leaf net CO_2 uptake responded positively to elevated CO_2 concentrations, suggesting a pronounced stimulatory influence on Rubisco enzymatic activity. As the exposure progressed into the latter half of the growth season, the extent of this stimulatory effect gradually declined. A corresponding decrease was noted in stomatal conductance, suggesting that the CO_2-induced enhancement of photosynthesis was at least partially limited by seasonal regulation of stomatal pores, which limited the entry of CO_2 in the leaf. Yet, the internal CO_2 concentration remained significantly elevated, indicating that the downregulation of photosynthesis at elevated CO_2 extended to biochemical constraints. This phenomenon termed the CO_2 acclimation effect, is frequently observed across plant species; however, its comprehensive understanding remains elusive. Typically, exposure to elevated CO_2 enhances carbohydrate and biomass production, reducing the concentration of essential nutrients in the plant tissue, a phenomenon known as the 'dilution effect'. Previous investigations have associated photosynthetic acclimation with reduced nitrogen assimilation stemming from reduced photorespiratory activity in *Arabidopsis thaliana* (Krämer et al., 2022). In forest, cropland, and grassland ecosystems, the acclimation to elevated CO_2 has been associated with soil N supply (Peng et al., 2022). This relationship posits N availability as an important factor underlying the observed decrement in the efficiency of Rubisco at elevated CO_2 over time. Here, the underlying mechanisms driving potential photosynthetic acclimation were not investigated. Nonetheless, the overall effect of elevated CO_2 highly benefited the development of *Paulownia tomentosa*.

Regarding stomatal responses, a range of research indicates that elevated CO_2 levels reduce stomatal aperture, resulting in decreased stomatal conductance (g_s) and transpiration (E) rates. These physiological adjustments, in turn, contribute positively to plant water use efficiency (WUE) by optimizing the ratio between water loss and CO_2 fixation (Cao & Liu, 2022; Lammertsma et al., 2011; Wei et al., 2022). In the present study, the overall variation on g_s and *E* was not substantial in plants cultivated at elevated CO_2. Yet, both variables tended to decrease during the latter half of the experimental period compared to plants at ambient CO_2, contributing to the optimization of plant water use efficiency (WUE). However, the observed weak correlations between net CO_2 uptake and both stomatal conductance and transpiration rates observed in this study suggest that the predominant factor enhancing WUE is the increased atmospheric CO_2 partial pressure, which directly strengthens the driving force for CO_2 diffusion and facilitates CO_2 uptake, even with slight variations in stomatal aperture.

5.1.3. Effect of elevated CO_2 on the elemental composition of the guard cells and mesophyll chloroplasts

In this study, the guard cells of plants developed at elevated CO_2 presented significantly lower magnesium (Mg^{2+}) content, while potassium (K^+) content tended to decrease. Recent research revealed that, like K^+, Mg^{2+} ions participate in stomata opening in *Arabidopsis thaliana*. The study highlighted that the movement of Mg^{2+} ions is mediated by a tonoplast transporter that is ineffective at low Mg^{2+} concentrations (Inoue et al., 2022). Here, alteration in the concentration of these two ions was coupled with slight reductions in transpiration rates observed from the second half of the growth season, suggesting that stomata opening tended to decrease at elevated CO_2 concentration. Additionally, a reduction in Mg^{2+} may indicate lower chlorophyll content and Rubisco activity, given that Mg^{2+} is required for Rubisco activation. Photosynthesis in guard cells contributes to the energy needed for stomata functioning and has been deemed essential for turgor production and stomata opening in *Arabidopsis thaliana* (Azouly-Shemer et al., 2015). Given that guard cells can import accumulated sugars from their apoplast (Misra et al., 2015), and CO_2 fixed in the mesophyll is facilitated under elevated CO_2 conditions without full stomata opening, it may imply that elevated CO_2 decreases the photosynthetic activity in the guard cells of *Paulownia tomentosa*. Additionally, active sites of enzymes involved in cell metabolism are specific for binding with Mg^{2+} complexes (A. Lal, 2018), which may suggest that eCO_2 decreases the overall metabolism of the guard cells. The observed decrease in K^+ under elevated CO_2 conditions could also result from nutrient dilution associated with increased biomass accumulation, similar to findings reported for winter wheat (Wang et al., 2023).

Concurrently, elevated CO_2 led to an increase in calcium (Ca^{2+}) concentration in both guard cells and chloroplasts. Considering the multiple roles of Ca^{2+} in plant functionality, this observation permits a range of interpretations. For instance, free Ca^{2+} ions are important for cell signaling, regulating several biochemical processes, including photosynthesis and stomata movement. Given that an increase in Ca^{2+} in the guard cells leads to activation of ion channels involved in turgidity regulation, this observation could support the decreased rates of the stomatal conductance observed in the second half of the growth season. On the other hand, elevation of free Ca^{2+} in the chloroplast stroma could cause downregulation of important enzymes of the CBB cycle (Hochmal et al., 2015), which does not align with the increased photosynthetic activity at elevated CO_2 presented in this study. On this basis, an increase in Ca^{2+} content may imply, at the cellular level, an increase of Ca^{2+}-associated molecules, such

as the pectin in the cell wall. This hypothesis arises from previous research findings, which have indicated that elevated CO_2 levels stimulate pectin biosynthesis in the leaves of rice plants (Zhu et al., 2019). Additionally, an increase in the ratio of pectin relative to cellulose and hemicellulose has been shown to increase cell wall hydrophilicity, which in turn improves the mesophyll conductance to CO_2 and facilitates its diffusion from the substomatal cavities to the carboxylation sites (Carriquí et al., 2020). This leads to an inquiry regarding the effect of CO_2 enrichment on the chemical composition of the cell wall in the leaves. Future research may help to elucidate whether elevated CO_2 elicits such alterations and how they relate to photosynthesis and plant traits, enhancing our understanding of how *Paulownia tomentosa* adapts to rising atmospheric CO_2 concentrations.

The concentration of phosphorus (P) was similar in guard cells regardless of the CO_2 treatment, while in the mesophyll cells, a slight increase in P was observed, which may indicate an accumulation of high-energy biomolecules, such as ATP and carbohydrates, resulting from the higher net CO_2 uptake rates.

5.1.4. Effect of elevated CO_2 on the wood structure

Increasing leaf biomass and area elevates hydraulic needs due to the direct link between water availability and biomass production. Furthermore, larger leaf areas amplify transpiration rates, increasing the plant water requirements. The speed at which water moves through a segment of stem results from the interaction of various elements, with the diameter of the vessels being considered the predominant factor determining the effectiveness of the water transport and the tree's water usage rate. In this study, while vessel characteristics did not statistically differ under elevated CO_2 exposure, a 14.1% enlargement in vessel diameter suggests an improvement in the hydraulic conductivity in *Paulownia tomentosa*, given that hydraulic conductivity increases proportionally to the fourth power of the vessel diameter (Janssen et al., 2020), leading to a more efficient water supply to the leaves. This inference is supported by the strong correlation between vessel diameter and indicators of overall plant performance, such as net CO_2 uptake and overall biomass production.

Vessel development usually varies across species. For instance, it has been previously demonstrated that eCO_2 induced the formation of wider vessels in *Eucalyptus grandis* (Costa et al., 2023), and *Phaseolus vulgaris* (Medeiros et al., 2013). Contrarily, smaller vessel sizes were observed in the stem of *Helianthus annuus* exposed to eCO_2, associated with a fortified

cell wall and likely to a decreased water demand compared to sub-ambient CO_2 concentration (Rico et al., 2013). These different adjustments imply different strategies regarding the hydraulic function in response to the changing atmospheric CO_2 conditions.

Although wider vessels generally lead to improved hydraulic conductivity, they are often associated with thinner and porous pit membranes, which may increase the vulnerability to air seeding and embolism (Hacke et al., 2001). This could be particularly critical during severe fluctuations in water availability, as predicted for future climate scenarios, given that vessels are unable to adapt to environmental shifts once developed. In this context, elevated CO_2 might enhance tree longevity when water availability is sufficient to keep the xylem vessels within sustainable tension thresholds. Further research into how elevated CO_2 affects cavitation susceptibility may help to better predict the vulnerability of *Paulownia tomentosa* to embolism under anticipated climatic conditions.

5.2. Effects of cyclic drought stress on the morphology, physiology, and leaf pigment composition and wood structure of *Paulownia tomentosa*

Physiological parameters such as gas exchange rates, chlorophyll fluorescence, leaf pigment concentration, and hydraulic traits are vital indicators of plant health. These metrics not only reflect a plant's current condition but also its stress tolerance and adaptability, which have direct implications for growth. This study investigates young *Paulownia tomentosa* grown in pots, subjected to two distinct irrigation regimes: a consistent, well-watered treatment and a variable, drought-inducing treatment with progressively decreasing water availability. Plants were pre-exposed to recurrent drought cycles and monitored over two additional cycles to gain insights into the trees' adaptive mechanisms to changing water conditions.

5.2.1. Effects of drought stress on the morphology of *Paulownia tomentosa*

In this study, exposure to cyclic drought caused several morphological responses in Paulownia plants, including a significant reduction in leaves, root, and total biomass increment and a decreasing trend in stem diameter, height, leaf size, and leaf number per plant, corroborating previously documented growth patterns in other species under drought stress (Koch et al., 2019; Skirycz et al., 2009). The modulation of leaf structure in terms of size and number represents crucial adaptative responses to mitigate the detrimental impacts of drought since both inducing

leaf abscission and reducing leaf surface can allow for redistribution of resources that often become scarce under stress conditions, and prevent dehydration by reducing transpiring surface (Skirycz et al., 2009). Additionally, leaf shedding was associated with higher resistance to xylem cavitation in *Grayia spinosa* and *Tetradymia glabrata* (Hacke & Pitternann, 2000). This observation suggests that Paulownia plants shed their older leaves as a mechanism to reduce the soil-plant-atmosphere continuum, eventually protecting the stem hydraulic integrity since cuticle transpiration can continue to increase xylem tension beyond the point of stomatal closure (Cardoso et al., 2020). Therefore, shedding older leaves might be beneficial in enhancing the water status of the remaining foliage that is more exposed to solar irradiance, hence improving cellular metabolism and photosynthesis, and increasing plant survival (Holloway-Phillips, 2020; McDowell et al., 2008). In this study, a significant correlation was observed between the number of leaves and both root biomass and the total biomass of individual Paulownia plants. This suggests that leaf adaptive responses are associated with quantifiable growth costs, possibly due to reduced light interception area and subsequent lower photosynthesis.

5.2.2.   Effects of drought stress on gas exchange and stomata of *Paulownia tomentosa*

Regulation of stomata is the first line of physiological response to increasing vapor pressure deficit (Luo & Wang, 2022). On the other hand, diminishing the stomata aperture to prevent excessive water loss is considered a key limiting factor for photosynthesis since CO_2 diffusion into the leaves is also restricted, directly affecting carboxylation reactions (Wang et al., 2018). In line with previous gas exchange investigations (Dubey at al., 2023; Song et al., 2020), drought stress caused an overall decrease in net CO_2 uptake (A), stomatal conductance (g_s), intercellular CO_2 concentration (c_i) and transpiration (E) during the drought cycles. A decrease in A appeared to be primarily driven by stomatal conductance over biochemical limitations in the early stages of drought, indicated by comparable values of net CO_2 uptake, which coincided with significantly lower intercellular CO_2 concentrations between the treatment and control groups. This suggests that plants acclimated to the early stages of drought by optimizing carbon gain through stomata regulation and metabolic adjustments. This may include an increased photorespiratory activity, which, despite reducing Rubisco carboxylation efficiency, can enhance photosynthetic CO_2 uptake by promoting carbon fixation as amino acids (Busch et al., 2017). Photorespiration-derived amino acids may contribute to glycine- and serine-enriched dehydrins, enhancing plant drought resistance (Busch et al., 2017). Moreover, photorespiratory

metabolism can prevent the over-reduction of chloroplasts by consuming electrons, thereby reducing the risk of photoinhibition under low CO_2 availability due to stomata closure (Eisenhut et al., 2017).

Herein, a further increase in stress intensity caused a substantial decline in g_s, E, and A, indicating that stomata pores declined to minimal apertures to preserve hydraulic integrity over photosynthetic requirements (Hu et al., 2023). Overall, sustaining the rates of A while decreasing E led to an increase in water use efficiency (WUE) in drought-stressed Paulownia plants. Similar responses on WUE were reported for *P. dulcis* (Rouhi & Damme., 2007) *Juglans mandshurica* Maxim. and *Junglans regia* L. (Liu et al., 2019). The ability of plants to increase the ratio between CO_2 assimilation in relation to water loss is associated with stress tolerance and ascribe competitive advantage in dry environments (Bi et al., 2022; Huang & Zhai., 2023). Many plants adjust their stomata characteristics to modulate the rates of gas exchange when exposed to varying levels of stress. For instance, an increase in stomata density and a decrease in stomata length were observed on a cotton drought-tolerant cultivar and associated with WUE (Dubey et al., 2023). Here, drought did not impact stomata density, while a decrease in stomata length was observed. Stomata length correlated negatively with the WUE and positively with stomata conductance, indicating that these adjustments of the stomata pores contributed to enhanced resistance to transpiration. Consequently, young *Paulownia tomentosa* trees demonstrated a remarkable acclimative response to repeated episodes of drought stress, particularly in terms of gas exchange mechanisms by maintaining photosynthetic function with reduced water loss when the trees were subjected to moderate stress under the conditions of this experiment.

5.2.3. Effect of drought stress on leaf pigment composition

In this study, drought-exposed plants exhibited increased chlorophyll content, suggesting an enhanced leaf nitrogen balance. Typically, water scarcity limits nutrient absorption in roots, even in nutrient-rich soils (Javaid et al., 2022); hence, the rise in leaf nitrogen concentration under drought was unexpected. However, a similar response has been observed in species from low-rainfall environments, which maintain higher leaf nitrogen per unit area compared to species in high-rainfall sites (Wright & Westoby, 2003). Additionally, increase in leaf nitrogen has been linked to a functional optimization of nitrogen economy as an acclimative response to water stress in *Quercus suber* and *Salix* spp. (Lobo-do-vale et al., 2019; Weih et al., 2011). Therefore, an increase in leaf nitrogen may indicate nutrient resorption from senescent to

younger leaves to supply metabolic requirements and increase the survival rate in *P. tomentosa* plants under periods of low water availability. Furthermore, the increase in chlorophyll content might represent an adaptive strategy to enhance light absorption and photosynthetic efficiency, especially relevant as the plants were grown indoors with primarily moderate irradiance exposure. This adaptation could help sustain photosynthetic efficiency in the initial stages of drought stress, as indicated by the similar CO_2 uptake levels compared to well-watered plants, specifically observed from days 3 to 7 post-irrigation.

On the other hand, when drought intensifies, a rise in chlorophyll concentration can disrupt photosynthetic balance, especially under higher light intensities. This disruption may stem from an imbalance in NADPH and ATP synthesis relative to their use in CO_2 assimilation, leading to decreased available oxidized pheophytin and increased triplet-state chlorophyll. This condition favors the formation of singlet oxygen molecules, which are highly reactive and can inflict damage on the D1 protein in the photosynthetic apparatus (A. Lal, 2018; Blankenship, 2021). This study had a significant negative correlation between total chlorophyll content and key photosynthetic processes, such as the quantum yield of PSII and the electron transport rate. In contrast, chlorophyll positively correlated with the quantum yield of non-photochemical quenching. The chlorophyll fluorescence variables recorded on day 7 post-irrigation suggest that moderate light becomes excessive when accompanied by an increase in chlorophyll content and drought under the experimental setup of this study.

Several photoprotective mechanisms are induced in plants to minimize the detrimental effects of excessive light interception. For instance, it has been recently suggested that the accumulation of anthocyanins reduces leaf light perception due to their ability to partially absorb irradiance (Cirillo et al., 2021). Accumulation of leaf anthocyanins was demonstrated to be upregulated by reactive oxygen species (ROS) in *Arabidopsis thaliana*, generating a protective feedback mechanism through scavenging excess ROS (Xu & Rothstein., 2018). In this study, an increase in the fluorescence ratio at 660 nm and 525 nm indicates a higher anthocyanin accumulation in response to drought stress, consistent with the results of a recent meta-analysis from 102 studies datasets, showing that drought stress increased anthocyanin content by 41.9% in several plant species (Yan et al., 2022). A previous study on Arabidopsis anthocyanin-deficient mutants also suggested that anthocyanins may play a role in protecting from high temperatures (Shao et al., 2007). Inhere, leaf temperature tended to increase under drought, which could result from a reduced cooling effect due to diminished transpiration and increased energy dissipated as heat through non-photochemical quenching. Anthocyanin content

correlated negatively with transpiration, suggesting that the plants experienced heat stress because of drought.

Moreover, flavonols, derived from a distinct branch of the same biosynthetic pathway as anthocyanins (phenylpropanoid pathway), exhibited enhanced accumulation in the leaves of well-irrigated *Paulownia tomentosa*. A key function of flavonols is to shield plants from the stresses of environmental fluctuations (Daryanavard et al., 2023). A previous study has shown that flavonol accumulation partially prevents stomatal closure by scavenging H_2O_2 in *Arabidopsis thaliana* guard cells (An et al., 2016), allowing for photosynthetic CO_2 uptake under transiently suboptimal conditions (i.e. light fluctuation). Anthocyanins and flavonols, sharing subcellular locations and biosynthetic substrates, may compete for these substrates, with the regulation of this competition still being explored (Zhong et al., 2020). In this study, drought stress channeled the biosynthesis of flavonoids primarily into anthocyanin on the leaves of *Paulownia tomentosa*, which likely contributed to the desiccation defense by preventing excess damage caused by ROS, thereby helping to maintain photosynthetic activity (Xu & Rothstein., 2018).

5.2.4. Effect of drought stress on chlorophyll fluorescence parameters

Non-photochemical quenching is another protective mechanism that promotes overexcitation energy dissipation into heat (Ruban & Wilson, 2020; Nosalewicz & Skotupka, 2022). In Paulownia, limited water availability led to an overall increase in the non-photochemical quenching parameters, indicating an effective energy dissipation as heat through the xanthophyll cycle (Shin et al., 2021). On the other hand, the quantum yield of PSII, and the electron transport chain (ETR) declined, showing an impairment on the photochemical reactions. Similar results were demonstrated in lettuce seedlings exposed to progressive drought stress (Shin et al., 2021). Fv/Fm represents the maximum quantum yield of the PSII when non-photochemical quenching is inactivated. Previous studies have indicated that drought conditions lead to a reduction in the Fv/Fm ratio in various species, such as *Cucumis sativus L.* (Zhuang et al., 2020) and *Glycyrrhiza uralensis* (Gao et al., 2022), implying potential closure of reaction centers and impairment of PSII. In contrast, in Paulownia, the Fv/Fm ratio remained at similar values compared to the controls. The same response was observed in *Phaseolus vulgaris L.* (Mathobo et al., 2017). In lettuce seedlings, a reduction in Fv/Fm was only noted on the last day of drought exposure, which coincided with an increase in Y(NO) (Shin et al., 2021). The Y(NO) represents a lake model quenching parameter in which higher

values can indicate photoinhibition. Y(NO) remained unchanged in Paulownia during the measurements, indicating that the integrity of the PSII was not severely affected by photoinhibition. These different responses might rely on plant species and their susceptibility to drought stress under different experimental conditions (Shin et al., 2021). However, it is important to consider that in this study, chlorophyll fluorescence parameters were measured only on the 7th day of drought progression, offering insight into how PSII was impacted at this specific stage of drought stress. Conducting further experiments with increased temporal resolution will help to elucidate better the dynamic changes in chlorophyll fluorescence variables under varying levels of drought stress in Paulownia plants.

5.2.5. Effect of drought stress on wood formation

The current study revealed that young Paulownia trees exposed to drought stress conditions exhibited a slight increase in the proliferation of conduit cells. Concurrently, a pronounced decrease in the vessel's diameter was observed, which, together with the lower radial increment, indicates an impact of the water deprivation on both cell division and expansion of the cambial derivatives. This response is consistent with the one observed in Poplar (Yu et al., 2021; Fichot et al., 2009) and *Chukrasia tabularis* (Islam & Bräuning, 2019).

The xylem formation is a complex process that adapts to environmental changes (Fichot et al., 2009). Drought conditions affect the cellular energy status and activate defense signaling pathways, involving the elevation of active abscisic acid (ABA) levels. In Poplar, a decrease in vessel size and an increase in frequency were accompanied by an upregulation of genes associated with ABA biosynthesis in response to drought stress (Yu et al., 2021). ABA acts antagonistically to auxins, and auxins are required for H^+-ATPase activation, apoplastic acidification, and activation of cell wall-loosening proteins to mediate cell wall relaxation. Additionally, a hyperpolarization caused by the activation of H^+-ATPase is needed to activate voltage-dependent K^+ inward channels, contributing to the hydrostatic pressure required to drive cell expansion, ultimately determining the cell diameter (Lin et al., 2021; Rodriguez-Zaccaro & Groover., 2019; Bhatla & Lal; 2018; Balducci et al., 2016). ABA has been documented to inhibit the activity of H^+-ATPase by dephosphorylating its penultimate residue, dampening hypocotyl elongation in *Arabidopsis thaliana* (Hayashi et al., 2014). Considering the established roles of H^+-ATPase and the regulatory effects of ABA on plant physiology and growth responses as documented in previous studies, these mechanisms may be the molecular

basis underlying the observed drought-induced alterations in the xylogenesis of *Paulownia tomentosa* reported in the present study.

Here, vessel diameter negatively correlated with vessel frequency, suggesting a compensatory adaptation to counteract reduced hydraulic conductance from smaller vessel sizes (Fichot et al., 2009). Moreover, associations between vessel size and growth performance suggest that these anatomical modifications resulted in a less efficient vascular system, which was also evidenced by a significant reduction in vessel lumen area. This may be perceived as an adverse response from a commercial perspective, but the broader ecological and physiological implications must be considered. For instance, vessel diameter has been widely correlated with resistance to embolism across different tree species (Isasa et al., 2023). Levanic et al. (2011) also observed that Oak trees that succumbed to drought exhibited larger vessels than those that survived. Tomasella et al. (2019) showed that a reduction in transpiring area and xylem hydraulic conductivity may help European beech trees to survive further drought events, despite growth impairments. Therefore, these observed anatomical adjustments may imply an increased resistance to embolism in *Paulownia tomentosa*. Finally, vessel diameter was associated with stomatal conductance and transpiration rates, suggesting that wood acclimation is an important aspect of the resilience of *P. tomentosa* to drought, reducing water consumption and delaying extreme conditions of stress (Joshi & Prentice, 2020), which may suggest prioritizing long-term survival over short-term performance (Gessler et al., 2020).

5.3. Plant electrical signaling and photosynthetic regulation in response to localized damage and soil rehydration upon intensive drought stress

5.3.1. Intracellular electrical signals

Electrical signals are an early event following stimulus perception, comprising a key component of the plant systemic signaling network, which plays a crucial role in quickly transmitting information that initiates protective mechanisms to induce systemic acclimation in plant tissues (Li et al., 2021). This study demonstrates that both local burning and re-irrigation stimuli induced electrical signals detected intracellularly in *Paulownia tomentosa*. Local burn triggered depolarization (VP-like signal) and hyperpolarization (SP-like signal) on the plasma membrane of the leaf cells. The depolarization response was predominantly noted during long-distance signaling events, while the hyperpolarization response appeared primarily

in short-distance signaling. These observations are consistent with the findings of Lautner et al. (2005), who observed similar responses in Poplar trees.

While VP-like signals are well documented as regulators of physiological adaptations in response to stress, the mechanisms underlying the activation and roles of SP-like signals are currently under investigation. In Poplar, the hyperpolarization response was associated with a transient opening of the plasma membrane K^+ channels (Lautner et al., 2005). More recently, it has been proposed that the concentration of cytoplasmic Ca^{2+} may also be a key determinant of the type of electrical signal generated, wherein significantly elevated levels induce depolarization, while moderately elevated levels trigger hyperpolarization events (Sukhova et al., 2023). The hypothesis is grounded in observations that slight elevations in cytosolic Ca^{2+} levels prompt the activation of the H^+-ATPase in wheat plants (Grinberg et al., 2022), a process regarded as a possible mechanism involved in system potential generation (Sukhova et al., 2023).

Regarding their roles, stressors have been reported to induce SP-like signals in wheat, poplar, and maize, causing similar physiological adjustments to those observed in depolarization responses (Lautner et al., 2005; Vuralhan-Eckert et al., 2018; Yudina et al., 2023). In contrast, depolarizing and hyperpolarizing potentials triggered opposite photosynthetic adjustments in drought-stressed pea plants after damage (Yudina et al., 2022). These converging responses highlight that the physiological adjustments triggered by electrical signals rely on the plant status and may also vary with growth conditions, repeated stress exposure, and duration (Sukhova et al., 2023).

In this study, although gas exchange measurements were not paired with intracellular measurements of electrical signals, applying a local burn to adjacent and distal leaves was associated with depolarization and hyperpolarization in the membranes of cells within undamaged leaves. The consistent observation that local burn led to detectable changes in the dynamics of leaf gas exchange suggests that these events may trigger similar responses in *P. tomentosa*, as reported for Poplar (Lautner et al., 2005). However, further experimental investigations are required to elucidate the specificity of the hyperpolarization signals and to compare their physiological impacts relative to VP-like signals in the stress responses of *P. tomentosa*.

Regarding re-irrigation, hyperpolarization signals were observed on leaf cells upon soil rehydration after severe drought exposure, which appeared to have minimal effects on leaf gas exchange. The next subsections discuss possible involved mechanisms.

5.3.2. Extracellular electrical signals

Plants continuously adapt to environmental stimuli, the intensity and nature of which can vary across different regions of the organism due to factors such as shading, physical barriers, and other localized environmental conditions. This implies that basal electrical activity varies across different regions of a plant, leading to localized adaptations that do not necessarily impact distal areas significantly. Thus, high-impact stimuli may lead to systemic responses since the magnitude of the response positively correlates with the signal's amplitude (Sukhov et al., 2014b). This bioelectric activity of plants has been referred to "plant electrome" and comprises the totality of bioelectric activity occurring in a plant (required for cellular functionality and system integration under environmental fluctuations).

In this study, oscillatory waves were recorded in the petiole of undamaged leaves following the burn stimulation. These waves were characterized by irregular upward and downward deflections of higher amplitudes compared to the baseline signal, extending for several minutes. This response could be observed in the FFT results, which showed an induction of higher power on the low-frequency waves. Similar results were reported by Costa et al. (2023), whose investigations included the effects of localized damage on untouched leaflets of common beans.

Differently, drought-stressed Paulownia exhibited a pattern of electrical activity characterized by spikes of varying amplitudes distributed over time, which persisted at least for the following minutes upon rehydration. This pattern was also observed in soybeans exposed to osmotic stress, as reported by Saraiva et al. (2017). In soybeans, spikes followed a power law distribution, which may characterize a self-organized system under a critical state. This suggests that tension accumulated from drought stress is released through bursts of electrical currents, stabilizing the system under stress conditions (Saraiva et al., 2017). Although the descriptive analysis showed no difference in the bioelectric activity before and after soil rehydration, FFT results demonstrated that most plants were sensitive to the stimulus and increased the power of the low-frequency waves, suggesting strong ion movement to allow the signal to reach distant tissues.

Approximated entropy (ApEn) analysis is widely used in chaotic time series data to determine the degree of the signal's disorder. It is widely recognized that healthy biological systems display electrical signals with high complexity, whereas degrading systems tend to be more regular and predictable (Sun et al., 2018). Indeed, previous research has shown a decrease in signal complexity in response to osmotic stress in soybeans (Saraiva et al., 2017), which was

interpreted as a synchronization of signals, aimed at improving the efficiency of information transmission under stress. In contrast, increasing ApEn values were noted in tomato plants following fungal inoculation (Simmi et al., 2020). In common beans, the ApEn increased upon wounding (Costa et al., 2023), suggesting the signals are more irregular and less predictable under specific stress conditions. Here, elevated ApEn values characterized the bioelectric activity of Paulownia under stress conditions, such as drought stress and localized burn.

These divergent results suggest that different species, or even individual plants, may adopt unique strategies at the bioelectric level to cope with stress. Consequently, these variations manifest as distinct behaviors of bioelectric activity. In Paulownia, under burn stimulus, sudden and transient alterations in the bioelectrical potential appear to reflect a higher complexity of the ion movements, possibly resulting from the cell's attempts to restore its previous ionic state. Moreover, the higher ApEn value under drought stress may stem from the gradual decrease of water availability, leading to a dynamic adaptation to the new stress condition. The observed increase in irregularity may reflect a spectrum of low-amplitude signals originating from nearby regions, likely resulting from distinct biochemical responses to drought stress. For instance, the selective senescence of older leaves to preserve younger ones could contribute to this increased irregularity. Finally, a decrease in ApEn values upon soil rehydration suggests a more homogenized response, where quick and transient ionic shifts are minimized, allowing the uptake of water to initiate recovery processes.

5.3.3. Gas exchange responses to electrical signals induced by local burn

Photosynthesis exhibits a high sensitivity to environmental stresses, with stress conditions resulting in a marked decrease in its efficiency (Wang et al., 2019). Previous studies have documented the influence of localized burning on plant bioelectric activity and its respective effects on photosynthetic activity and stomatal movement. For instance, Lautner et al. (2005) observed that local damage triggered an electrical signal followed by a reduction in net CO_2 uptake in Poplar leaves. This was concurrent with a decline in the quantum yield of the PSII, while stomatal behavior remained unaffected, as indicated by the consistent stomatal conductance. Further research demonstrated that both photosynthetic activity and stomata dynamics were influenced by burn-induced electrical signals, with maize plants exhibiting a marked decrease in stomatal conductance (Vuralhan-Eckert et al., 2018) and pea plants experiencing a sustained reduction in transpiration rates (Yudina et al., 2019). In the present study, local damage induced changes in plant bioelectric activity and a substantial decrease in

net CO_2 uptake, stomatal conductance, and transpiration on intact leaves. The internal CO_2 concentration remained relatively stable, suggesting that the limitations to photosynthetic reactions were not primarily attributed to stomatal resistance to CO_2 diffusion. Instead, biochemical constraints appear to play a more predominant role. The exact mechanism by which electrical signals regulate the cellular metabolism in plants is not fully elucidated. It possibly involves a network that includes cellular alterations in pH, cytosolic Ca^{2+}, and downstream signaling events. In a previous investigation, electrical signals were associated with the activity of Ca^{2+} channels in *Arabidopsis thaliana* (Bialasek et al., 2017), and elevated cytosolic Ca^{2+} ions were observed in sieve elements of *Vicia faba* (Furch et al., 2009). An increase in cytosolic Ca^{2+} concentration entails the transport from the apoplast and internal stores, like vacuoles and chloroplasts. Chloroplasts store substantial amounts of Ca^{2+} within the negatively charged thylakoid membrane and Ca^{2+}-binding proteins throughout the photoperiod, therefore contributing to the regulation of resting Ca^{2+} levels in stroma – required for CO_2 fixation – and in the cytosol, required for cellular function (Hochmal et al., 2015). It was recently revealed that cMCU, a chloroplast homolog of the mitochondrial calcium uniporter (MCU) family, mediates Ca^{2+} flux into the chloroplast in vivo, thus playing a role in sensing osmotic stress in *Arabidopsis thaliana* (Teardo et al., 2019). Therefore, since electrical signals in response to local burn can result in increased Ca^{2+} concentration in the cytosol and their effect is mainly linked to the dark photosynthetic reactions (Surova et al., 2016; Pavlovic et al., 2011), it is proposed that alterations in gas exchange may be due to the translocation of Ca^{2+} ions from the apoplast and their subsequent leakage into the chloroplast stroma, leading to the downregulation of the CBB cycle (Krupenina et al., 2008). Given the feedback mechanism of photochemistry and CO_2 assimilation processes, the decrease in net CO_2 uptake observed in this study suggests alterations in the photochemical activity. Typically, decreased $NADP^+$ availability redirects electrons toward the plastoquinone pool (A. Lal, 2018), and an increase in ATP to ADP ratio can reduce the activity of the H^+-ATP synthase due to substrate limitation (Sukhov et al., 2014a; Sukhov et al., 2011), both leading to the acidification of the thylakoid lumen. Declining pH in the thylakoid lumen induces the release of Ca^{2+} from PSBO (Honchmal et al., 2015), impairing oxygen evolution, contributing to cyclic electron flow, and finally triggering NPQ mechanisms to protect the photosynthetic apparatus against photodamage (Hochmal et al., 2015). In *Arabidopsis thaliana*, heat-induced electrical signals caused a rapid increase in non-photochemical quenching (NPQ) and a decrease in PSII operating efficiency (Bialasek et al., 2017). In pea plants, a reduction in net CO_2 uptake was associated with lowering activity of PSI and PSII (Sukhov et al., 2014b). Additionally, Yudina

et al. (2023) showed that moderate stressors induce membrane hyperpolarization in wheat plants, detrimentally affecting photochemistry and enhancing NPQ.

An alternative hypothesis is that VP-induced proton accumulation in the cytoplasm, followed by its influx into the chloroplast, inactivates pH-dependent enzymes of the CBB cycle, disrupts light reactions, and enhances NPQ (Sukhov et al., 2014a). Electrical signals have also been demonstrated to decrease the mesophyll conductance to CO_2 in soybeans. However, the metabolic mechanism requires additional investigation (Gallé et al., 2012).

In this study, the steady intercellular CO_2 concentration also implies that metabolic processes responsible for CO_2 release, such as respiration, were sustained at a constant rate or stimulated. This inference is supported by the observed enhancement in respiratory activity during dark gas exchange, as documented in the current study. This response aligns with the findings of Surova et al. (2016) and Sukhov et al. (2014a), where the downregulation of photosynthetic activity and an upregulation of respiratory activity were linked to electrical signals in pea plants. Lautner et al. (2013) also reported similar physiological responses in their investigation of the underlying reasons for the knockout of photosynthesis in *Mimosa pudica*. Their research concluded that increased respiration rates partially contribute to the observed decline in net CO_2 uptake. Therefore, an increase in respiratory activity may have also influenced the net CO_2 balance observed in *P. tomentosa* during the photoperiod.

Moreover, in dark conditions, local burn transiently elevated stomatal conductance and transpiration before observable alterations in respiratory activity, which may result from pressure buildup from gases and intracellular media released from damaged cells (Mudrilov et al., 2021), leading to hydro-passive stomata opening (Lautner et al., 2013). Additionally, the results imply that an electric signal generated by the damage may trigger stomatal opening, possibly enhancing oxygen uptake for cellular respiration. However, further research is needed to clarify the molecular mechanisms through which *P. tomentosa* perceive low O_2 levels and regulate stomatal movements in response.

In a previous report, Khlopkov et al. (2021) proposed that the observed respiration increase in pea plants, induced by VP, is associated with calcium-activated rotenone-insensitive alternative NADPH dehydrogenase in mitochondria, which accelerates the tricarboxylic acid cycle and CO_2 release. Another study by Surova et al. (2016) demonstrated that ATP accumulates in pea plants following burn damage, which may result from the inactivation of photosynthesis and the increase of respiration. Therefore, the observed stimulation in respiratory activity may be

attributed to an increased ATP demand, which powers ion pumps to restore the previous ionic state of the cell. An increase in respiration may also support the synthesis of stress-response molecules. This hypothesis arises from the observation that injury-induced electrical signals enhance ethylene production in the receiving tissues of *Vicia faba* seedlings (Dziubińska et al., 2003). Similarly, in tobacco plants, burn-induced electrical signals coincide with elevated levels of abscisic acid (ABA) and jasmonic acid (JA) in distal leaves (Hlaváčková et al., 2006). Furthermore, electrical signaling has been shown to trigger jasmonate biosynthesis in distal leaves of *Arabidopsis thaliana* following wounding (Mousavi et al., 2013).

This study presents evidence that burn damage in *Paulownia tomentosa* initiates the propagation of VP and signals with characteristics of SP to distal undamaged leaf cells, thereby regulating photosynthetic and respiratory metabolism in young trees. These signals were detected extracellularly, characterized by oscillatory electrical potential in the group of petiole cells. Further research is needed to elucidate the roles of ions and defense molecules within a complex systemic signaling network, which facilitates both cell-to-cell and organ-to-organ communication in *Paulownia tomentosa* under stress conditions.

5.3.4. Gas exchange responses to electrical signals induced by re-irrigation

The mechanism by which electrical signals contribute to the recovery from drought stress is still under investigation. Prior studies have documented an increase in stomatal conductance, transpiration, and net CO_2 uptake occurring within minutes following soil rehydration and electrical signal emission in plants such as microtomato (Silva et al., 2020) and maize (Vuralhan-Ercket et al., 2018). These findings indicate the recovery onset of photosynthetic activity and stomatal parameters, suggesting an association between electrical signals and recovery of plant physiological processes when drought is alleviated. Here, upon increasing soil moisture levels, a hyperpolarization response was observed in the leaf cells of *Paulownia tomentosa*, consistent with the characteristics of a system potential (SP). Observable recovery of plant turgidity, marked by the resolution of wilting, initiated within minutes post soil rehydration (Figure 8-1). This response may indicate enhanced activity of the H^+-ATPase and inward-rectifying K^+ channels, which drive essential solute transport for osmotic adjustment (Silva et al., 2020). Despite that, the plants showed little response in leaf gas exchange during the first fifth-minute interval, which may be insufficient to discern the initial dynamics of rehydration on these parameters. However, this suggests that the observed electrical signal did

not immediately affect the functioning of the guard cells. This converging observed response is probably dependent on the species' strategy to cope with intensive drought exposure. In this study, plants were severely water-stressed, which might require a longer period for the cell to reduce abscisic acid (ABA) levels, which highly accumulate under drought conditions. Nevertheless, the decrease in intercellular CO_2 concentrations and increase in WUE during the observation period could indicate a gradual enhancement in the CBB cycle, since the response of stomata is generally slower than that of photosynthetic events (Murchie & Lwason, 2013).

Regarding the chlorophyll fluorescence parameters, the quantum yield of the PSII Y(PSII), the electron transport rate (ETR), and both regulated (Y(NPQ)) and non-regulated (Y(NO)) energy dissipation remained steady pre- and post- irrigation. The higher values of Y(PSII) compared to Y(NO) and Y(NPQ) indicate that most of the absorbed light was used for photochemical reactions, and electrons were not excessive to highly activate the photoprotection mechanisms. This indicates that drought stress did not highly impact the photosynthetic apparatus at the specific light intensity used in this experiment.

Additional experiments are needed to elucidate the mechanism of drought recovery in *Paulownia tomentosa*. This study demonstrates a clear bioelectric response to soil rehydration, recorded intracellularly, without apparent or little effect on photosynthesis and stomata movement. A prior study examining severely drought-stressed *Vitis vinifera* suggested that ABA restricts leaf gas exchange over extended periods, preventing the reopening of stomata upon soil rehydration to favoring embolism repair and water conservation during repeated drought events, since repairing vessels requires their isolation from tension (Tombesi et al., 2015). In moderately water-stressed seedlings of *Fraxinus chinensis* stomata reopening following re-irrigation was constrained by the phytohormone ethylene and plant hydraulics, and this response favored plant water use efficiency in early recovering periods (Bi et al., 2022). On this basis, it is proposed that the recurrent hyperpolarization of the cell membranes observed on the leaves following re-watering may play a more pivotal role in restoring turgidity, relieving the drought-induced tension, and repairing the plant hydraulics rather than immediately opening the stomata for photosynthetic CO_2 uptake in the short term. Furthermore, maintaining a lower transpiration rate upon rehydration is possibly one of the key mechanisms contributing to the notable resilience observed in Paulownia species. Future studies should aim to bridge the biochemical gap between electrical signaling and gas exchange responses during drought recovery of *Paulownia tomentosa*.

6. CONCLUSION

6.1. General conclusions from experiment 1: Effects of elevated CO_2 on the physiology of *P. tomentosa*

Elevated CO_2 generally enhanced photosynthetic performance in *Paulownia tomentosa* with minimal impact on stomatal behavior, maintaining transpiration rates similar to plants grown at current atmospheric CO_2 levels. This response improved the water use efficiency and enhanced overall plant growth, aligning with the initial hypothesis of this study. Adjustments in hydraulic architecture accompanied these physiological responses, characterized by wider and less frequent vessels. This modification suggests a coordinated development of a more efficient vascular system in response to elevated CO_2, supporting the second hypothesis of this study. These findings highlight the benefits of CO_2 enrichment for young *P. tomentosa* trees under semi-controlled conditions. However, the implications for mineral concentrations in leaf cells remain uncertain. For instance, elevated CO_2 was associated with increased calcium levels, which could indicate higher pectin content, while potassium levels decreased, which has been previously associated with nutrient dilution. The observed increase in leaf biomass and area points to an increased demand for resources, which might be constrained under natural conditions. Therefore, future studies should consider interactions with nutrients and other factors, such as drought, temperature, and competition. Additionally, the development of larger vessels prompts a question of whether Paulownia trees will be more prone to suffer from embolism under future climate scenarios. Further research should also explore additional anatomical adaptations, such as cell wall structure, inter-vessel pit characteristics, and the trade-offs between hydraulic efficiency and safety. Overall, the results suggest that elevated CO_2 will likely benefit *P. tomentosa* in environments with few limiting factors, by enhancing photosynthesis, water use efficiency, and vessel features, leading to improved biomass accumulation.

6.2. General conclusions from experiment 2: Effects of cyclic drought stress on the physiology of *P. tomentosa*

Paulownia tomentosa exhibited adaptive responses to enhance survival under drought conditions, occurring at the cost of reduced growth. As such, stomata modulation caused a greater reduction in transpiration related to net CO_2 uptake, ultimately enhancing the water use

efficiency, especially in the early stage of soil water decline, supporting the first hypothesis of this study.

Upon rehydration of the soil, net CO_2 assimilation in *Paulownia tomentosa* bounced back to levels observed in well-watered plants; however, stomatal conductance did not fully recover, suggesting that this species implements strategies to (1) remain semi-conservative in water use even in post-drought periods, preparing the plant for subsequent water shortages and (2) optimize photosynthetic activity under drought conditions. The second interpretation is further supported by elevated chlorophyll levels in the leaves, suggesting an adaptive mechanism to compensate for the diminished photosynthetic surface resulting from increased leaf senescence. This response was accompanied by an increase in the anthocyanins, presumably to protect the photosynthetic apparatus from harmful ROS due to chlorophyll overexcitation under high light intensity and low water availability, supporting the second hypothesis of this study. Furthermore, shedding old leaves and reducing vessel size appear to be key strategies to decrease the risk of lethal xylem tensions by reducing the evaporating surface, conserving water in the soil, improving water use efficiency, and possibly minimizing vulnerability to hydraulic failure, supporting the third hypothesis.

This study provides valuable information on the adaptative mechanisms of *Paulownia tomentosa* to drought stress, enhancing our understanding of its resilience to climate change. Future studies should investigate unresolved questions, such as whether the observed adaptations influence plant performance in subsequent growing seasons, if wood acclimation encompasses additional modifications, such as alterations in the cell wall structure and pit pore morphology, and whether these changes contribute to enhanced resistance to cavitation. Furthermore, field experiments may provide insights into the commercial implications of reduced growth rates under severe drought conditions. Finally, research should explore how *Paulownia tomentosa* responds to concurrent climate factors, like drought, temperature variations, and increased CO_2 levels, to fully understand its adaptation to global climate change.

6.3. General conclusions from Experiment 3: Electric signaling and photosynthetic regulation

Results demonstrate that electrical signals triggered in response to burn damage induce rapid and systemic physiological adjustments in the cells of healthy leaves of *P. tomentosa*. At the

cellular level, electrical responses manifest as both depolarization and hyperpolarization of the plasma membrane. Major physiological adjustments observed include the partial closure of stomata and a reduction in photosynthetic activity during the day. Additionally, under dark conditions, these electrical signals elicited transient stomatal opening and increased respiratory activity, as evidenced by an increased g_s, E, and net CO_2 release.

The modulation of photosynthetic and respiratory rates by electrical signals in *Paulownia tomentosa* demonstrates the species' capacity to adjust its energy balance dynamically in response to stress. These findings imply a complex intercellular communication mechanism that likely contributes to stress mitigation, thereby supporting the hypotheses of this study.

Re-irrigation following an extended drought period induced hyperpolarization responses in the leaf cells, suggesting the onset of recovery mechanisms. However, this response does not appear to significantly impact the stomata's behavior, which may indicate a semi-conservative strategy prioritizing hydraulic repair over CO_2 uptake for photosynthesis. An observed decrease in c_i and WUE may indicate a gradual improvement in photosynthetic activity. However, different experimental setups must be tested to confirm these interpretations and understand the physiological responses under drought recovery.

In this study, extracellular measurements revealed that the bioelectric activity of *Paulownia tomentosa* became increasingly complex and less predictable when subjected to burn damage, coinciding with physiological responses observed during both light and dark periods. Furthermore, plants subjected to extreme drought stress demonstrated increased approximate entropy, which subsequently decreased upon soil rehydration. This pattern suggests that bioelectric activity in *P. tomentosa* shifts toward more complex states under stress conditions and normalizes with the alleviation of the stress. These results can be particularly useful to monitor plant responses to environmental stresses, which may help to ensure tree health and improve cultivation practices. Future research should focus on additional experimental setups, involving extended monitoring periods in response to a range of stress conditions.

By characterizing the electrical signaling, this research contributes to a broader comprehension of the biology of *P. tomentosa*.

7. REFERENCES

Adach, W., Żuchowski, J., Moniuszko-Szajwaj, B., Szumacher-Strabel, M., Stochmal, A., Olas, B., & Cieslak, A. (2020). Comparative phytochemical, antioxidant, and hemostatic studies of extract and four fractions from Paulownia clone in vitro 112 leaves in human plasma. *Molecules*, *25*(19), 4371. https://doi.org/10.3390/molecules25194371

Agurla, S., Gahir, S., Munemasa, S., Murata, Y., & Raghavendra, A. S. (2018). Mechanism of stomatal closure in plants exposed to drought and cold stress. *Advances in Experimental Medicine and Biology*, 215–232. https://doi.org/10.1007/978-981-13-1244-1_12

A. Lal, M. (2018). Photosynthesis. *Plant Physiology, Development and Metabolism*, pp. 159–226. https://doi.org/10.1007/978-981-13-2023-1_5

Alemu, S. T. (2020). Photosynthesis limiting stresses under climate change scenarios and role of chlorophyll fluorescence: A review article. *Cogent Food & Agriculture*, *6*(1), 1785136. https://doi.org/10.1080/23311932.2020.1785136

An, Y., Feng, X., Liu, L., Xiong, L., & Wang, L. (2016). Ala-induced flavonols accumulation in guard cells is involved in scavenging H_2O_2 and inhibiting stomatal closure in Arabidopsis cotyledons. *Frontiers in Plant Science*, *7*. https://doi.org/10.3389/fpls.2016.01713

Arend, M., Link, R. M., Patthey, R., Hoch, G., Schuldt, B., & Kahmen, A. (2021). Rapid hydraulic collapse as cause of drought-induced mortality in conifers. *Proceedings of the National Academy of Sciences*, *118*(16). https://doi.org/10.1073/pnas.2025251118

Aroca, A., García-Díaz, I., García-Calderón, M., Gotor, C., Márquez, A. J., & Betti, M. (2023). Photorespiration: Regulation and new insights on the potential role of persulfidation. *Journal of Experimental Botany*, *74*(19), 6023–6039. https://doi.org/10.1093/jxb/erad291

Arsić, J., Stojanović, M., Petrovičová, L., Noyer, E., Milanović, S., Světlík, J., Horáček, P., & Krejza, J. (2021a). Increased wood biomass growth is associated with lower wood density in Quercus petraea (Matt.) Liebl. saplings growing under elevated CO2. *PLOS ONE*, *16*(10). https://doi.org/10.1371/journal.pone.0259054

Ates, S., Ni, Y., Akgul, M., & Tozluoglu, A. (2008). *Characterization and evaluation of Paulownia elongota as a raw material for paper production. African Journal of Technology, 7(22), 4143-4158.*

Azoulay-Shemer, T., Palomares, A., Bagheri, A., Israelsson-Nordstrom, M., Engineer, C. B., Bargmann, B. O., Stephan, A. B., & Schroeder, J. I. (2015). Guard cell photosynthesis is critical for stomatal turgor production, yet does not directly mediate CO_2- and ABA-induced stomatal closing. *The Plant Journal*, *83*(4), 567–581. https://doi.org/10.1111/tpj.12916

Balducci, L., Cuny, H. E., Rathgeber, C. B., Deslauriers, A., Giovannelli, A., & Rossi, S. (2016). Compensatory mechanisms mitigate the effect of warming and drought on wood formation. *Plant, Cell & Environment*, *39*(6), 1338–1352. https://doi.org/10.1111/pce.12689

Bandurska, H. (2022). Drought stress responses: Coping strategy and resistance. *Plants*, *11*(7), 922. https://doi.org/10.3390/plants11070922

Barbu, M. C., Buresova, K., Tudor, E. M., & Petutschnigg, A. (2022). Physical and mechanical properties of *Paulownia tomentosa* x *elongata* sawn wood from Spanish, Bulgarian and Serbian plantations. *Forests*, *13*(10), 1543. https://doi.org/10.3390/f13101543

Bastos, A., & Fleischer, K. (2021). Effects of rising CO_2 levels on carbon sequestration are coordinated above and below ground. *Nature*, *591*(7851), 532–534. https://doi.org/10.1038/d41586-021-00737-1

Beerling, D. J., & Franks, P. J. (2010). The hidden cost of transpiration. *Nature*, *464*(7288), 495–496. https://doi.org/10.1038/464495a

Beniczky, S., & Schomer, D. L. (2020). Electroencephalography: Basic biophysical and technological aspects important for clinical applications. *Epileptic Disorders*, *22*(6), 697–715. https://doi.org/10.1684/epd.2020.1217

Bhatla, S. C. (2018). Water and solute transport. *Plant Physiology, Development and Metabolism*, 83–115. https://doi.org/10.1007/978-981-13-2023-1_3

Bi, M.-H., Jiang, C., Brodribb, T., Yang, Y.-J., Yao, G.-Q., Jiang, H., & Fang, X.-W. (2022). Ethylene constrains stomatal reopening in *fraxinus chinensis* post moderate drought. *Tree Physiology*, *43*(6), 883–892. https://doi.org/10.1093/treephys/tpac144

Białasek, M., Górecka, M., Mittler, R., & Karpiński, S. (2017). Evidence for the involvement of electrical, calcium and Ros signaling in the systemic regulation of non-photochemical quenching and photosynthesis. *Plant and Cell Physiology*, *58*(2), 207–215. https://doi.org/10.1093/pcp/pcw232

Blankenship, R. E. (2023). Molecular Mechanisms of Photosynthesis (3rd ed.). Wiley.

Brodersen, C. R., McElrone, A. J., Choat, B., Matthews, M. A., & Shackel, K. A. (2010). The dynamics of embolism repair in xylem: In vivo visualizations using high-resolution computed tomography. *Plant Physiology*, *154*(3), 1088–1095. https://doi.org/10.1104/pp.110.162396

Burioka, N., Miyata, M., Cornélissen, G., Halberg, F., Takeshima, T., Kaplan, D. T., Suyama, H., Endo, M., Maegaki, Y., Nomura, T., Tomita, Y., Nakashima, K., & Shimizu, E. (2005). Approximate entropy in the electroencephalogram during wake and sleep. *Clinical EEG and Neuroscience*, *36*(1), 21–24. https://doi.org/10.1177/155005940503600106

Busch, F. A., Sage, R. F., & Farquhar, G. D. (2017). Plants increase CO_2 uptake by assimilating nitrogen via the photorespiratory pathway. *Nature Plants*, *4*(1), 46–54. https://doi.org/10.1038/s41477-017-0065-x

Busch, F. A., Ainsworth, E. A., Amtmann, A., Cavanagh, A. P., Driever, S. M., Ferguson, J. N., Kromdijk, J., Lawson, T., Leakey, A. D., Matthews, J. S., Meacham-Hensold, K., Vath, R. L., Vialet-Chabrand, S., Walker, B. J., & Papanatsiou, M. (2024). A guide to photosynthetic gas exchange measurements: Fundamental principles, best practice and potential pitfalls. *Plant, Cell & Environment*. https://doi.org/10.1111/pce.14815

Cabral, E. F., Pecora, P. C., Arce, A. I., Tech, A. R., & Costa, E. J. (2011). The oscillatory bioelectrical signal from plants explained by a simulated electrical model and tested using Lempel–Ziv Complexity. *Computers and Electronics in Agriculture*, *76*(1), 1–5. https://doi.org/10.1016/j.compag.2010.12.001

Cao, Q., Li, G., & Liu, F. (2022). Elevated CO_2 enhanced water use efficiency of wheat to progressive drought stress but not on maize. *Frontiers in Plant Science*, *13*. https://doi.org/10.3389/fpls.2022.953712

Cao, Y., Sun, G., Zhai, X., Xu, P., Ma, L., Deng, M., Zhao, Z., Yang, H., Dong, Y., Shang, Z., Lv, Y., Yan, L., Liu, H., Cao, X., Li, B., Wang, Z., Zhao, X., Yu, H., Wang, F., … Fan, G. (2021). Genomic insights into the fast growth of Paulownias and the formation of Paulownia Witches' broom. *Molecular Plant*, *14*(10), 1668–1682. https://doi.org/10.1016/j.molp.2021.06.021

Caparros, S., Diaz, M., Ariza, J., Lopez, F., & Jimenez, L. (2008). New Perspectives for Paulownia Fortunei L. valorisation of the autohydrolysis and pulping processes. *Bioresource Technology*, *99*(4), 741–749. https://doi.org/10.1016/j.biortech.2007.01.028

Cardoso, A. A., Billon, L., Fanton Borges, A., Fernández-de-Uña, L., Gersony, J. T., Güney, A., Johnson, K. M., Lemaire, C., Mrad, A., Wagner, Y., & Petit, G. (2020). New developments in understanding plant water transport under drought stress. *New Phytologist*, *227*(4), 1025–1027. https://doi.org/10.1111/nph.16663

Carriquí, M., Nadal, M., Clemente-Moreno, M. J., Gago, J., Miedes, E., & Flexas, J. (2020). Cell wall composition strongly influences mesophyll conductance in Gymnosperms. *The Plant Journal*, *103*(4), 1372–1385. https://doi.org/10.1111/tpj.14806

Christman, M. A., Sperry, J. S., & Adler, F. R. (2009). Testing the 'Rare Pit' hypothesis for xylem cavitation resistance in three species of *acer*. *New Phytologist*, *182*(3), 664–674. https://doi.org/10.1111/j.1469-8137.2009.02776.x

Choat, B., Brodribb, T. J., Brodersen, C. R., Duursma, R. A., López, R., & Medlyn, B. E. (2018). Triggers of tree mortality under drought. *Nature*, *558*(7711), 531–539. https://doi.org/10.1038/s41586-018-0240-x

Cirillo, V., D'Amelia, V., Esposito, M., Amitrano, C., Carillo, P., Carputo, D., & Maggio, A. (2021). Anthocyanins are key regulators of drought stress tolerance in tobacco. *Biology*, *10*(2), 139. https://doi.org/10.3390/biology10020139

Costa, Á. V., Oliveira, T. F., Posso, D. A., Reissig, G. N., Parise, A. G., Barros, W. S., & Souza, G. M. (2023). Systemic signals induced by single and combined abiotic stimuli in common bean plants. *Plants*, *12*(4), 924. https://doi.org/10.3390/plants12040924

Costa, L.d.S.; Vuralhan-Eckert, J.; Fromm, J. Effect of Elevated CO_2 and Drought on Biomass, Gas Exchange and Wood Structure of Eucalyptus grandis. Plants 2023, 12, 148. https://doi.org/10.3390/plants12010148

Daryanavard, H., Postiglione, A. E., Mühlemann, J. K., & Muday, G. K. (2023). Flavonols modulate plant development, signaling, and stress responses. *Current Opinion in Plant Biology*, *72*, 102350. https://doi.org/10.1016/j.pbi.2023.102350

Daszkowska-Golec, A., & Szarejko, I. (2013). Open or close the Gate – stomata action under the control of phytohormones in drought stress conditions. *Frontiers in Plant Science*, *4*. https://doi.org/10.3389/fpls.2013.00138

Delgado-Bonal, A., & Marshak, A. (2019). Approximate entropy and sample entropy: A comprehensive tutorial. *Entropy*, *21*(6), 541. https://doi.org/10.3390/e21060541

de Oliveira, R. F., Macedo, F. da C. O., da Silva, F. B., Daneluzzi, G. S., Silva, A. R., & Capelin, D. (2020). O que é neurobiologia de plantas? Uma abordagem além da biologia vegetal. . *Rev. Helius*, *v. 3*(n.2), 247–290.

de Toledo, G. R., Parise, A. G., Simmi, F. Z., Costa, A. V., Senko, L. G., Debono, M.-W., & Souza, G. M. (2019). Plant Electrome: The Electrical Dimension of Plant Life. *Theoretical and Experimental Plant Physiology*, *31*(1), 21–46. https://doi.org/10.1007/s40626-019-00145-x

Doelman, J. C., Stehfest, E., van Vuuren, D. P., Tabeau, A., Hof, A. F., Braakhekke, M. C., Gernaat, D. E., van den Berg, M., van Zeist, W., Daioglou, V., van Meijl, H., & Lucas, P. L. (2019). Afforestation for climate change mitigation: Potentials, risks and trade-offs. *Global Change Biology*, *26*(3), 1576–1591. https://doi.org/10.1111/gcb.14887

Domínguez, E., Romaní, A., Domingues, L., & Garrote, G. (2017). Evaluation of strategies for second generation bioethanol production from fast growing biomass paulownia within a Biorefinery Scheme. *Applied Energy*, *187*, 777–789. https://doi.org/10.1016/j.apenergy.2016.11.114

Douthe, C., Gago, J., Ribas-Carbó, M., Núñez, R., Pedrol, N., & Flexas, J. (2018). Measuring photosynthesis and respiration with infrared gas analysers. *Advances in Plant Ecophysiology Techniques*, 51–75. https://doi.org/10.1007/978-3-319-93233-0_4

Dubey, R., Pandey, B. K., Sawant, S. V., & Shirke, P. A. (2023). Drought stress inhibits stomatal development to improve water use efficiency in Cotton. *Acta Physiologiae Plantarum*, *45*(2). https://doi.org/10.1007/s11738-022-03511-6

Drzewiecka, K., Gąsecka, M., Magdziak, Z., Budzyńska, S., Szostek, M., Niedzielski, P., Budka, A., Roszyk, E., Doczekalska, B., Górska, M., & Mleczek, M. (2021). The possibility of using *Paulownia elongata* S. Y. Hu × *Paulownia Fortunei* hybrid for

phytoextraction of toxic elements from post-industrial wastes with biochar. *Plants*, *10*(10), 2049. https://doi.org/10.3390/plants10102049

Dziubinska, H., Filek, M., Koscielniak, J., & Trebacz, K. (2003). Variation and action potentials evoked by thermal stimuli accompany enhancement of ethylene emission in distant non-stimulated leaves of *Vicia faba* minor seedlings. *Journal of Plant Physiology*, *160*(10), 1203–1210. https://doi.org/10.1078/0176-1617-00914

Eckert, C., Sharmin, S., Kogel, A., Yu, D., Kins, L., Strijkstra, G.-J., & Polle, A. (2019). What makes the wood? exploring the molecular mechanisms of xylem acclimation in hardwoods to an ever-changing environment. *Forests*, *10*(4), 358. https://doi.org/10.3390/f10040358

Eisenhut, M., Bräutigam, A., Timm, S., Florian, A., Tohge, T., Fernie, A. R., Bauwe, H., & Weber, A. P. M. (2017). Photorespiration is crucial for dynamic response of photosynthetic metabolism and stomatal movement to altered CO_2 availability. *Molecular Plant*, *10*(1), 47–61. https://doi.org/10.1016/j.molp.2016.09.011

El-showk, S., & El-showk, N. (2003). Paulownia Tree an Alternative for Sustainable Forestry. (2013). Retrieved from https://energia.bio/wordpress/wp-content/uploads/2019/10/PaulowniaBooklet.pdf

Ellsworth, D. S., Thomas, R., Crous, K. Y., Palmroth, S., Ward, E., Maier, C., DeLucia, E., & Oren, R. (2011). Elevated CO_2 affects photosynthetic responses in canopy pine and subcanopy deciduous trees over 10 years: A synthesis from duke face. *Global Change Biology*, *18*(1), 223–242. https://doi.org/10.1111/j.1365-2486.2011.02505.x

Ezquer, I., Salameh, I., Colombo, L., & Kalaitzis, P. (2020). Plant Cell Walls Tackling Climate Change: Biotechnological strategies to improve crop adaptations and photosynthesis in response to global warming. *Plants*, *9*(2), 212. https://doi.org/10.3390/plants9020212

Forster, E. J., Healey, J. R., Dymond, C., & Styles, D. (2021). Commercial afforestation can deliver effective climate change mitigation under multiple decarbonisation pathways. *Nature Communications*, *12*(1). https://doi.org/10.1038/s41467-021-24084-x.

Fichot, R., Laurans, F., Monclus, R., Moreau, A., Pilate, G., & Brignolas, F. (2009). Xylem anatomy correlates with gas exchange, water-use efficiency and growth performance under contrasting water regimes: Evidence from *Populus deltoides* x *Populus nigra* hybrids. *Tree Physiology*, *29*(12), 1537–1549. https://doi.org/10.1093/treephys/tpp087

Fromm, J. (2006). Long-distance electrical signaling and physiological functions in higher plants. *Plant Electrophysiology*, 269–285. https://doi.org/10.1007/978-3-540-37843-3_12

Fromm, J., & Bauer, T. (1994). Action potentials in maize sieve tubes change phloem translocation. *Journal of Experimental Botany*, *45*(4), 463–469. https://doi.org/10.1093/jxb/45.4.463

Fromm, J., & Lautner, S. (2006). Electrical signals and their physiological significance in plants. *Plant, Cell & Environment*, *30*(3), 249–257. https://doi.org/10.1111/j.1365-3040.2006.01614.x

Fu, X., Gregory, L. M., Weise, S. E., & Walker, B. J. (2022). Integrated Flux and pool size analysis in plant central metabolism reveals unique roles of glycine and serine during photorespiration. *Nature Plants*, *9*(1), 169–178. https://doi.org/10.1038/s41477-022-01294-9

Furch, A. C. U., van Bel, A. J. E., Fricker, M. D., Felle, H. H., Fuchs, M., & Hafke, J. B. (2009). Sieve element Ca^{2+} channels as relay stations between remote stimuli and sieve tube occlusion in *Vicia faba*; *The Plant Cell*, *21*(7), 2118–2132. https://doi.org/10.1105/tpc.108.063107

Gallé, A., Lautner, S., Flexas, J., Ribas-Carbo, M., Hanson, D., Roesgen, J., & Fromm, J. (2012). Photosynthetic responses of soybean (*glycine max* L.) to heat-induced electrical signalling are predominantly governed by modifications of mesophyll conductance for CO_2. *Plant, Cell & Environment*, *36*(3), 542–552. https://doi.org/10.1111/j.1365-3040.2012.02594.x

Gallé, A., Lautner, S., Flexas, J., Fromm, J. (2015). Environmental stimuli and physiological responses: The current view on electrical signalling. *Environmental and Experimental Botany, 114(), 15–21.* https://doi:10.1016/j.envexpbot.2014.06.013

Gamage, D., Thompson, M., Sutherland, M., Hirotsu, N., Makino, A., & Seneweera, S. (2018). New insights into the cellular mechanisms of plant growth at elevated atmospheric carbon dioxide concentrations. *Plant, Cell & Environment*, *41*(6), 1233–1246. https://doi.org/10.1111/pce.13206

Gao, H., Bai, N., Zhang, Y., Zhang, X. H., Zhang, Y. J., Wang, L., Wang, E. J., Tian, Y. Y., Guo, Y. Y., Yan, F., Li, Y. H., & Zhang, H. (2022). Drought stress alters gas exchange, chlorophyll fluorescence, and antioxidant enzyme activities in *Glycyrrhiza uralensis* in the Hexi Corridor, China. *Russian Journal of Plant Physiology*, *69*(6). https://doi.org/10.1134/s102144372206005x

Gardner, A., Jiang, M., Ellsworth, D. S., MacKenzie, A. R., Pritchard, J., Bader, M. K., Barton, C. V., Bernacchi, C., Calfapietra, C., Crous, K. Y., Dusenge, M. E., Gimeno, T. E., Hall, M., Lamba, S., Leuzinger, S., Uddling, J., Warren, J., Wallin, G., & Medlyn, B. E. (2022). Optimal stomatal theory predicts CO_2 responses of stomatal conductance in both gymnosperm and angiosperm trees. *New Phytologist*, *237*(4), 1229–1241. https://doi.org/10.1111/nph.18618

Gessler, A., Bottero, A., Marshall, J., & Arend, M. (2020). The way back: Recovery of trees from drought and its implication for acclimation. *New Phytologist*, *228*(6), 1704–1709. https://doi.org/10.1111/nph.16703

Ghazzawy, H. S., Bakr, A., Mansour, A. T., & Ashour, M. (2024). Paulownia trees as a sustainable solution for CO_2 mitigation: Assessing progress toward 2050 climate goals. *Frontiers in Environmental Science*, *12*. https://doi.org/10.3389/fenvs.2024.1307840

Grinberg, M., Mudrilov, M., Kozlova, E., Sukhov, V., Sarafanov, F., Evtushenko, A., Ilin, N., Vodeneev, V., Price, C., & Mareev, E. (2022). Effect of extremely low-frequency magnetic fields on light-induced electric reactions in wheat. *Plant Signaling & Behavior*, *17*(1). https://doi.org/10.1080/15592324.2021.2021664

Gupta, A., Rico-Medina, A., & Caño-Delgado, A. I. (2020). The physiology of plant responses to drought. *Science*, *368*(6488), 266–269. https://doi.org/10.1126/science.aaz7614.

Hacke, U. G., Sperry, J. S., & Pittermann, J. (2000). Drought experience and cavitation resistance in six shrubs from the Great Basin, Utah. *Basic and Applied Ecology*, *1*(1), 31–41. https://doi.org/10.1078/1439-1791-00006

Hacke, U. G., & Sperry, J. S. (2001). Functional and ecological xylem anatomy. *Perspectives in Plant Ecology, Evolution and Systematics*, *4*(2), 97–115. https://doi.org/10.1078/1433-8319-00017

Hampshire-Waugh, M. (2021). Climate change and the road to net-zero: *Science, technology, economics, politics*. Crowstone Publishing.

Han, X., Zhou, G., Luo, Q., Ferlian, O., Zhou, L., Meng, J., Qi, Y., Pei, J., He, Y., Liu, R., Du, Z., Long, J., Zhou, X., & Eisenhauer, N. (2023). Plant biomass responses to elevated CO_2 are mediated by phosphorus uptake. *Science of The Total Environment*, *863*, 160775. https://doi.org/10.1016/j.scitotenv.2022.160775

Hayashi, Y., Takahashi, K., Inoue, S., & Kinoshita, T. (2014). Abscisic acid suppresses hypocotyl elongation by dephosphorylating plasma membrane H^+-ATPase in Arabidopsis thaliana. *Plant and Cell Physiology*, *55*(4), 845–853. https://doi.org/10.1093/pcp/pcu028

He, T., Vaidya, B., Perry, Z., Parajuli, P., & Joshee, N. (2016). Paulownia as a medicinal tree: Traditional uses and current advances. *European Journal of Medicinal Plants*, *14*(1), 1–15. https://doi.org/10.9734/ejmp/2016/25170

Hemati, A., Moghiseh, E., Amirifar, A., Mofidi-Chelan, M., & Asgari Lajayer, B. (2022). Physiological effects of drought stress in plants. *Plant Stress Mitigators*, 113–124. https://doi.org/10.1007/978-981-16-7759-5_6

Hlaváčková, V., Krchňák, P., Nauš, J., Novák, O., Špundová, M., & Strnad, M. (2006). Electrical and chemical signals involved in short-term systemic photosynthetic responses of tobacco plants to local burning. *Planta*, *225*(1), 235–244. https://doi.org/10.1007/s00425-006-0325-x

Hochmal, A. K., Schulze, S., Trompelt, K., & Hippler, M. (2015). Calcium-dependent regulation of photosynthesis. *Biochimica et Biophysica Acta (BBA) - Bioenergetics*, *1847*(9), 993–1003. https://doi.org/10.1016/j.bbabio.2015.02.010

Holloway-Phillips, M. (2020). Variation in xylem resistance to cavitation explains why some leaves within a canopy are more likely to die under water stress. *Plant Physiology*, *182*(1), 450–452. https://doi.org/10.1104/pp.19.01394

Hou, L., Shang, M., Chen, Y., Zhang, J., Xu, X., Song, H., Zheng, S., Li, M., & Xing, G. (2021). Physiological and molecular mechanisms of elevated CO_2 in promoting the growth of Pak Choi (brassica rapa ssp. chinensis). *Scientia Horticulturae*, *288*, 110318. https://doi.org/10.1016/j.scienta.2021.110318

Hu, Y., Sun, Z., Zeng, Y., Ouyang, S., Chen, L., Lei, P., Deng, X., Zhao, Z., Fang, X., & Xiang, W. (2023). Tree-level stomatal regulation is more closely related to xylem hydraulic traits than to leaf photosynthetic traits across diverse tree species. *Agricultural and Forest Meteorology*, *329*, 109291. https://doi.org/10.1016/j.agrformet.2022.109291

Huang, M., & Zhai, P. (2023). Impacts of extreme droughts on ecosystem water use efficiency diverge between forest and grassland. *Journal of Meteorological Research*, *37*(5), 710–721. https://doi.org/10.1007/s13351-023-3022-9

Huber, A. E., & Bauerle, T. L. (2016). Long-distance plant signaling pathways in response to multiple stressors: The Gap in Knowledge. *Journal of Experimental Botany*, *67*(7), 2063–2079. https://doi.org/10.1093/jxb/erw099

Icka, P., Damo, R., & Icka, E. (2016). *Paulownia Tomentosa, a Fast-Growing Timber. Annals "Valahia" University of Targoviste - Agriculture, 10(1), 14–19.* doi:10.1515/agr-2016-0003

Inoue, S., Hayashi, M., Huang, S., Yokosho, K., Gotoh, E., Ikematsu, S., Okumura, M., Suzuki, T., Kamura, T., Kinoshita, T., & Ma, J. F. (2022). A tonoplast-localized magnesium transporter is crucial for stomatal opening in Arabidopsis under high Mg^{2+} conditions. *New Phytologist*, *236*(3), 864–877. https://doi.org/10.1111/nph.18410

IPCC, 2014: Climate Change 2014: Synthesis report. Contribution of working groups I, II, and III to the Fifth Assessment Report of the intergovernmental Panel on Climate Change [Core Writinf Team, R.K. Pachuari and L.A. Meyer (eds.)]. IPCC, Geneva, Switzerland, 151 pp.

IPCC, 2021: Climate Change 2021: The Physical Science Basis. Contribution of Working Group I to the Sixth Assessment Report of the Intergovernmental Panel on Climate Change [Masson-Delmotte, V., P. Zhai, A. Pirani, S.L. Connors, C. Péan, S. Berger, N. Caud, Y. Chen, L. Goldfarb, M.I. Gomis, M. Huang, K. Leitzell, E. Lonnoy, J.B.R. Matthews, T.K. Maycock, T. Waterfield, O. Yelekçi, R. Yu, and B. Zhou (eds.)]. Cambridge University Press, Cambridge, United Kingdom and New York, NY, USA, 2391 pp. doi:10.1017/9781009157896.

IPCC, 2023: Sections. In: Climate Change 2023: Synthesis Report. Contribution of Working Groups I, II and III to the Sixth Assessment Report of the Intergovernmental Panel on Climate Change [Core Writing Team, H. Lee and J. Romero (eds.)]. IPCC, Geneva, Switzerland, pp. 35–115, doi: 10.59327/IPCC/AR6-9789291691647.

Islam, M., Rahman, M., & Bräuning, A. (2019). Impact of extreme drought on tree-ring width and vessel anatomical features of *Chukrasia tabularis*. *Dendrochronologia*, *53*, 63–72. https://doi.org/10.1016/j.dendro.2018.11.007

Isasa, E., Link, R. M., Jansen, S., Tezeh, F. R., Kaack, L., Sarmento Cabral, J., & Schuldt, B. (2023). Addressing controversies in the xylem embolism resistance–vessel diameter relationship. *New Phytologist*, *238*(1), 283–296. https://doi.org/10.1111/nph.18731

Ivanova, K., Geneva, M., Anev, S., Georgieva, T., Tzvetkova, N., Stancheva, I. & Markovska, Y. (2018). Effect of soil salinity on morphology and gas exchange of two Paulownia hybrids. *Agroforestry Systems*. https://doi:10.1007/s10457-018-0186-x

Jakubowski, M. (2022). Cultivation potential and uses of Paulownia Wood: A Review. *Forests*, *13*(5), 668. https://doi.org/10.3390/f13050668

Jaleel, C. A., Manivannan, P., Wahid, A., Farooq, M., Al-Juburi, H. J., Somasundaram, R., & Panneerselvam, R. (2009). Drought stress in plants: A review on morphological characteristics and pigments composition. International Journal of Agriculture and Biology, 11, 100-105.

Janssens, I. A., Beemster, G. T. S., & Asard, H. (2014). Physiological, biochemical, and genome-wide transcriptional analysis reveals that elevated CO_2 mitigates the impact of combined heat wave and drought stress in *Arabidopsis thaliana* at multiple organizational levels. *Global Change Biology*, *20*(12), 3670–3685. https://doi.org/10.1111/gcb.12626

Janssen, T. A., Hölttä, T., Fleischer, K., Naudts, K., & Dolman, H. (2020). Wood allocation trade-offs between fiber wall, fiber lumen, and axial parenchyma drive drought resistance in Neotropical trees. *Plant, Cell and Environment*, 43(4), 965–980. https://doi.org/10.1111/pce.13687

Javaid, M. H., Khan, A. R., Salam, A., Neelam, A., Azhar, W., Ulhassan, Z., & Gan, Y. (2022). Exploring the adaptive responses of plants to abiotic stresses using transcriptome data. *Agriculture*, *12*(2), 211. https://doi.org/10.3390/agriculture12020211

Jensen, J.B. An Investigation into the Suitability of Paulownia as an Agroforestry Species for UK & NW European Farming Systems. Master's Dissertation, Coventry University, Coventry, UK, 2016.

Joshi, J., Dieckmann, U., & Prentice, I. C. (2020). Towards a Unified Theory of Plant Photosynthesis and Hydraulics. https://doi.org/10.5194/egusphere-egu2020-9687

Kai, L., Gang, X., Lin-lin, F., Xiao-li, M., Xiang, G., & Qing, L. (2011). The changes of electrical signals in corn at different temperatures. *Procedia Environmental Sciences*, *10*, 39–44. https://doi.org/10.1016/j.proenv.2011.09.008

Kalra, G., & Bhatla, S. C. (2018). Abscisic acid. *Plant Physiology, Development and Metabolism*, 629–641. https://doi.org/10.1007/978-981-13-2023-1_18

Kathpalia, R., & Bhatla, S. C. (2018). Plant water relations. *Plant Physiology, Development and Metabolism*, 3–36. https://doi.org/10.1007/978-981-13-2023-1_1

Kooyers, N. J. (2015). The evolution of drought escape and avoidance in natural herbaceous populations. *Plant Science*, *234*, 155–162. https://doi.org/10.1016/j.plantsci.2015.02.012

Krämer, K., Kepp, G., Brock, J., Stutz, S., & Heyer, A. G. (2022). Acclimation to elevated CO_2 affects the C/N balance by reducing de novo n-assimilation. *Physiologia Plantarum*, *174*(1). https://doi.org/10.1111/ppl.13615

Khlopkov, A., Sherstneva, O., Ladeynova, M., Grinberg, M., Yudina, L., Sukhov, V., & Vodeneev, V. (2021). Participation of calcium ions in induction of respiratory response caused by variation potential in pea seedlings. *Plant Signaling & Behavior*, *16*(4), 1869415. https://doi.org/10.1080/15592324.2020.1869415

Kirschbaum, M. U. F., Cowie, A. L., Peñuelas, J., Smith, P., Conant, R. T., Sage, R. F., Brandão, M., Cotrufo, M. F., Luo, Y., Way, D. A., & Robinson, S. A. (2024). Is tree planting an effective strategy for climate change mitigation? *Science of The Total Environment*, *909*, 168479. https://doi.org/10.1016/j.scitotenv.2023.168479.

Koch, G., Rolland, G., Dauzat, M., Bédiée, A., Baldazzi, V., Bertin, N., Guédon, Y., & Granier, C. (2019). Leaf production and expansion: A generalized response to drought stresses from cells to whole leaf biomass—a case study in the tomato compound leaf. *Plants*, *8*(10), 409. https://doi.org/10.3390/plants8100409

Kollist, H., Nuhkat, M., & Roelfsema, M. R. (2014). Closing gaps: Linking elements that control stomatal movement. *New Phytologist*, *203*(1), 44–62. https://doi.org/10.1111/nph.12832

Krupenina, N. A., Bulychev, A. A., Roelfsema, M. R., & Schreiber, U. (2008). Action potential in Chara cells intensifies spatial patterns of photosynthetic electron flow and non-photochemical quenching in parallel with inhibition of ph banding. *Photochemical & Photobiological Sciences*, *7*(6), 681–688. https://doi.org/10.1039/b802243g

Lamers, J., van der Meer, T., & Testerink, C. (2020). How plants sense and respond to stressful environments. *Plant Physiology*, *182*(4), 1624–1635. https://doi.org/10.1104/pp.19.01464

Lammertsma, E. I., Boer, H. J., Dekker, S. C., Dilcher, D. L., Lotter, A. F., & Wagner-Cremer, F. (2011). Global CO_2 rise leads to reduced maximum stomatal conductance in Florida vegetation. *Proceedings of the National Academy of Sciences*, *108*(10), 4035–4040. https://doi.org/10.1073/pnas.1100371108

Lautner, S., Grams, T. E., Matyssek, R., & Fromm, J. (2005). Characteristics of electrical signals in Poplar and responses in photosynthesis. *Plant Physiology*, *138*(4), 2200–2209. https://doi.org/10.1104/pp.105.064196

Lautner, S., Stummer, M., Matyssek, R., Fromm, J., & Grams, T. E. (2013). Involvement of respiratory processes in the transient knockout of net CO_2 uptake in *Mimosa pudica*

upon heat stimulation. *Plant, Cell & Environment*, *37*(1), 254–260. https://doi.org/10.1111/pce.12150

Levanic, T., Cater, M., & McDowell, N. G. (2011). Associations between growth, Wood Anatomy, carbon isotope discrimination and mortality in a *Quercus robur* forest. *Tree Physiology*, *31*(3), 298–308. 6

Levesque, M., Andreu-Hayles, L., & Pederson, N. (2017). Water availability drives gas exchange and growth of trees in northeastern US, not elevated CO_2 and reduced acid deposition. *Scientific Reports*, *7*(1). https://doi.org/10.1038/srep46158

Li, J.-H., Fan, L.-F., Zhao, D.-J., Zhou, Q., Yao, J.-P., Wang, Z.-Y., & Huang, L. (2021). Plant Electrical Signals: A Multidisciplinary Challenge. *Journal of Plant Physiology*, *261*, 153418. https://doi.org/10.1016/j.jplph.2021.153418

Liang, X., Wang, D., Ye, Q., Zhang, J., Liu, M., Liu, H., Yu, K., Wang, Y., Hou, E., Zhong, B., Xu, L., Lv, T., Peng, S., Lu, H., Sicard, P., Anav, A., & Ellsworth, D. S. (2023). Stomatal responses of terrestrial plants to Global Change. *Nature Communications*, *14*(1). https://doi.org/10.1038/s41467-023-37934-7.

LI-COR. (2012). Using the LI-6400/LI-6400XT portable photosynthesis system, version 6. Lincoln, NE, USA: LI-COR Biosciences. https://www.licor.com/env/support/LI-6400/manuals.html

Lima, V. F., Medeiros, D. B., Dos Anjos, L., Gago, J., Fernie, A. R., & Daloso, D. M. (2018). Toward multifaceted roles of sucrose in the regulation of stomatal movement. *Plant Signaling & Behavior*, 1–8. https://doi.org/10.1080/15592324.2018.1494468

Lin, W., Zhou, X., Tang, W., Takahashi, K., Pan, X., Dai, J., Ren, H., Zhu, X., Pan, S., Zheng, H., Gray, W. M., Xu, T., Kinoshita, T., & Yang, Z. (2021). TMK-based cell-surface auxin signalling activates cell-wall acidification. *Nature*, *599*(7884), 278–282. https://doi.org/10.1038/s41586-021-03976-4

Liu, B., Liang, J., Tang, G., Wang, X., Liu, F., & Zhao, D. (2019). Drought stress affects on growth, water use efficiency, gas exchange and chlorophyll fluorescence of juglans rootstocks. *Scientia Horticulturae*, *250*, 230–235.

Liu, Q., Liu, Y., Gao, L., Wang, Y., Yang, M., & Wang, G. (2023). Vessel, Intervessel Pits and vessel-to-fiber pits have significant impact on hydraulic function under different drought conditions and re-irrigation. *Environmental and Experimental Botany*, *214*, 105476. https://doi.org/10.1016/j.envexpbot.2023.105476

Llano-Sotelo, J. M., Alcaraz, L., & Castellanos, A. E. (2009). Gas exchange in Paulownia species growing under different soil moisture conditions in the field. *Journal of environmental biology, 31(4), 497-502.*

Lobo-do-Vale, R., Kurz Besson, C., Caldeira, M. C., Chaves, M. M., & Pereira, J. S. (2019). Drought reduces tree growing season length but increases nitrogen resorption efficiency in a Mediterranean ecosystem. *Biogeosciences*, *16*(6), 1265–1279. https://doi.org/10.5194/bg-16-1265-2019

López, F., Pérez, A., Zamudio, M. A. M., De Alva, H. E., & García, J. C. (2012). Paulownia as raw material for solid biofuel and Cellulose Pulp. *Biomass and Bioenergy*, *45*, 77–86. https://doi.org/10.1016/j.biombioe.2012.05.010

Lugli, L., Mezzalira, G., Lambardi, M., Zhang, H., & La Porta, N. (2023). Paulownia spp.: A bibliometric trend analysis of a global multi-use tree. *Horticulturae*, *9*(12), 1352. https://doi.org/10.3390/horticulturae9121352

Luo, D., Wang, C., Jin, Y., Li, Z., & Wang, Z. (2022). Different hydraulic strategies under drought stress between *Fraxinus mandshurica* and *Larix gmelinii* seedlings. *Journal of Forestry Research*, *34*(1), 99–111. https://doi.org/10.1007/s11676-021-01438-1

Ma, X., & Bai, L. (2021). Elevated CO_2 and reactive oxygen species in stomatal closure. *Plants*, *10*(2), 410. https://doi.org/10.3390/plants10020410

Macedo, F. da, Daneluzzi, G. S., Capelin, D., Barbosa, F. da, da Silva, A. R., & de Oliveira, R. F. (2021). Equipment and protocol for measurement of extracellular electrical signals, gas exchange and turgor pressure in plants. *MethodsX*, *8*, 101214. https://doi.org/10.1016/j.mex.2021.101214

Macdonald, F. D., & Buchanan, B. B. (1987). Chapter 8 carbon dioxide assimilation. *New Comprehensive Biochemistry*, 175–197. https://doi.org/10.1016/s0167-7306(08)60139-8

MacRobbie, E. A. C. (2006). Control of volume and Turgor in stomatal guard cells. *Journal of Membrane Biology*, *210*(2), 131–142. https://doi.org/10.1007/s00232-005-0851-7

Magar, L. B., Khadka, S., Joshi, J. R., Pokharel, U., Rana, N., Thapa, P., Sharma, K. R., Khadka, U., Marasini, B. P., & Parajuli, N. (2018). Total biomass carbon sequestration ability under the changing climatic condition by Paulownia Tomentosa Steud. *International Journal of Applied Sciences and Biotechnology*, *6*(3), 220–226. https://doi.org/10.3126/ijasbt.v6i3.20772.

Mamirova, A., Baubekova, A., Pidlisnyuk, V., Shadenova, E., Djansugurova, L., & Jurjanz, S. (2022). Phytoremediation of soil contaminated by organochlorine pesticides and toxic trace elements: Prospects and limitations of Paulownia tomentosa. *Toxics*, *10*(8), 465. https://doi.org/10.3390/toxics10080465

Malnoë, A. (2018). Photoinhibition or photoprotection of photosynthesis? update on the (newly termed) sustained quenching component qh. *Environmental and Experimental Botany*, *154*, 123–133. https://doi.org/10.1016/j.envexpbot.2018.05.005

Manzoni, S., Vico, G., Katul, G., Palmroth, S., Jackson, R. B., & Porporato, A. (2013). Hydraulic limits on maximum plant transpiration and the emergence of the safety–efficiency trade-off. *New Phytologist*, *198*(1), 169–178. https://doi.org/10.1111/nph.12126

Mathobo, R., Marais, D., & Steyn, J. M. (2017). The effect of drought stress on yield, leaf gaseous exchange and chlorophyll fluorescence of dry beans (*Phaseolus vulgaris* L.).

Agricultural Water Management, *180*, 118–125.
https://doi.org/10.1016/j.agwat.2016.11.005

Maxwell, K., & Johnson, G. N. (2000). Chlorophyll fluorescence—a practical guide. *Journal of Experimental Botany*, *51*(345), 659–668. https://doi.org/10.1093/jxb/51.345.659

McDowell, N., Pockman, W. T., Allen, C. D., Breshears, D. D., Cobb, N., Kolb, T., Plaut, J., Sperry, J., West, A., Williams, D. G., & Yepez, E. A. (2008). Mechanisms of plant survival and mortality during drought: Why do some plants survive while others succumb to drought? *New Phytologist*, *178*(4), 719–739. https://doi.org/10.1111/j.1469-8137.2008.02436.x

McElrone, A. J., Choat, B., Gambetta, G. A., & Brodersen, C. R. (2013). Water Uptake and Transport in Vascular Plants. *Nature Education Knowledge, 4(5):6*. Retrieved from https://www.nature.com/scitable/knowledge/library/water-uptake-and-transport-in-vascular-plants-103016037/

Medeiros, J. S., & Ward, J. K. (2013). Increasing atmospheric [co2] from glacial to future concentrations affects drought tolerance via impacts on leaves, xylem and their integrated function. *New Phytologist, 199(3), 738–748*. https://doi.org/10.1111/nph.12318

Medlyn, B. E., Barton, C. V., Broadmeadow, M. S., Ceulemans, R., De Angelis, P., Forstreuter, M., Freeman, M., Jackson, S. B., Kellomäki, S., Laitat, E., Rey, A., Roberntz, P., Sigurdsson, B. D., Strassemeyer, J., Wang, K., Curtis, P. S., & Jarvis, P. G. (2001). Stomatal conductance of forest species after long-term exposure to elevated CO_2 concentration: A synthesis. *New Phytologist*, *149*(2), 247–264. https://doi.org/10.1046/j.1469-8137.2001.00028.x

Menga, M. (2023, October 2). *The future of droughts: Living on a drier planet*. Foresight. https://www.climateforesight.eu/articles/the-ipcc-focus-on-drought/

Misra, B. B., Acharya, B. R., Granot, D., Assmann, S. M., & Chen, S. (2015). The guard cell metabolome: Functions in stomatal movement and Global Food Security. *Frontiers in Plant Science*, *6*. https://doi.org/10.3389/fpls.2015.00334

Moreno, J. L., Bastida, F., Ondoño, S., García, C., Andrés-Abellán, M., & López-Serrano, F. R. (2017). Agro-forestry management of Paulownia plantations and their impact on soil biological quality: The effects of fertilization and irrigation treatments. *Applied Soil Ecology*, *117–118*, 46–56. https://doi.org/10.1016/j.apsoil.2017.05.001.

Mousavi, S. A., Chauvin, A., Pascaud, F., Kellenberger, S., & Farmer, E. E. (2013). Glutamate receptor-like genes mediate leaf-to-leaf wound signalling. *Nature*, *500*(7463), 422–426. https://doi.org/10.1038/nature12478

Mudrilov, M., Ladeynova, M., Grinberg, M., Balalaeva, I., & Vodeneev, V. (2021). Electrical signaling of plants under abiotic stressors: Transmission of stimulus-specific information. *International Journal of Molecular Sciences*, *22*(19), 10715. https://doi.org/10.3390/ijms221910715

Murchie, E. H., & Lawson, T. (2013). Chlorophyll fluorescence analysis: A guide to good practice and understanding some new applications. *Journal of Experimental Botany*, *64*(13), 3983–3998. https://doi.org/10.1093/jxb/ert208

National Oceanic and Atmospheric Administration (NOAA). (2024). *Trends in atmospheric carbon dioxide*. Global Monitoring Laboratory. Retrieved September 18, 2024, from https://gml.noaa.gov/ccgg/trends/

Nevo, R., Charuvi, D., Tsabari, O., & Reich, Z. (2012). Composition, architecture and dynamics of the photosynthetic apparatus in higher plants. *The Plant Journal*, *70*(1), 157–176. https://doi.org/10.1111/j.1365-313x.2011.04876.x

Nikinmaa, E., Sievänen, R., & Höltta, T. (2014). Dynamics of leaf gas exchange, xylem and phloem transport, water potential and carbohydrate concentration in a realistic 3-D Model Tree Crown. *Annals of Botany*, *114*(4), 653–666. https://doi.org/10.1093/aob/mcu068

Nosalewicz, A., Okoń, K., & Skorupka, M. (2022). Non-photochemical quenching under drought and fluctuating light. *International Journal of Molecular Sciences*, *23*(9), 5182. https://doi.org/10.3390/ijms23095182

O'Leary, B. M., & Plaxton, W. C. (2016). Plant respiration. *Encyclopedia of Life Sciences*, 1–11. https://doi.org/10.1002/9780470015902.a0001301.pub3

Osakabe, Y., Yamaguchi-Shinozaki, K., Shinozaki, K., & Tran, L. P. (2013). ABA control of plant macroelement membrane transport systems in response to water deficit and high salinity. *New Phytologist*, *202*(1), 35–49. https://doi.org/10.1111/nph.12613

Parise, A. G., de Toledo, G. R., Oliveira, T. F., Souza, G. M., Castiello, U., Gagliano, M., & Marder, M. (2022). Do plants pay attention? A possible phenomenological-empirical approach. *Progress in Biophysics and Molecular Biology*, *173*, 11–23. https://doi.org/10.1016/j.pbiomolbio.2022.05.008

Pavlovič, A. (2012). The effect of electrical signals on photosynthesis and respiration. *Plant Electrophysiology*, 33–62. https://doi.org/10.1007/978-3-642-29110-4_2

Pavlovic, A., Slovakova, L., Pandolfi, C., & Mancuso, S. (2011). On the mechanism underlying photosynthetic limitation upon trigger hair irritation in the carnivorous plant Venus Flytrap (Dionaea Muscipula Ellis). *Journal of Experimental Botany*, *62*(6), 1991–2000. https://doi.org/10.1093/jxb/erq404

Peng, Y., Prentice, I. C., Sundert, K. V., Vicca, S., & Stocker, B. (2022). *Photosynthetic Acclimation under CO$_2$ Fertilization: New Perspectives from Current Experiments*. https://doi.org/10.5194/egusphere-egu22-1858

Pugh, T. A., Lindeskog, M., Smith, B., Poulter, B., Arneth, A., Haverd, V., & Calle, L. (2019). Role of forest regrowth in Global Carbon Sink Dynamics. *Proceedings of the*

National Academy of Sciences, *116*(10), 4382–4387.
https://doi.org/10.1073/pnas.1810512116.

Qaderi, M., Martel, A., & Dixon, S. (2019). Environmental factors influence plant vascular system and water regulation. *Plants*, *8*(3), 65. https://doi.org/10.3390/plants8030065

Reyer, C., Guericke, M., & Ibisch, P. L. (2009). Climate change mitigation via afforestation, reforestation and deforestation avoidance: And what about adaptation to environmental change? *New Forests*, *38*(1), 15–34. https://doi.org/10.1007/s11056-008-9129-0

Rico, C., Pittermann, J., Polley, H. W., Aspinwall, M. J., & Fay, P. A. (2013). The effect of subambient to elevated atmospheric CO_2 concentration on vascular function in helianthus annuus: Implications for plant response to climate change. New Phytologist, 199(4), 956–965. https://doi.org/10.1111/nph.12339

Roach, T., & Krieger-Liszkay, A. (2014). Regulation of Photosynthetic Electron Transport and photoinhibition. *Current Protein & Peptide Science*, *15*(4), 351–362. https://doi.org/10.2174/1389203715666140327105143

Rodríguez-Seoane, P., Díaz-Reinoso, B., Moure, A., & Domínguez, H. (2020). Potential of paulownia sp. for Biorefinery. *Industrial Crops and Products*, *155*, 112739. https://doi.org/10.1016/j.indcrop.2020.112739

Rodriguez-Zaccaro, F. D., & Groover, A. (2019). Wood and water: How trees modify wood development to cope with drought. *PLANTS, PEOPLE, PLANET*, *1*(4), 346–355. https://doi.org/10.1002/ppp3.29

Rouhi, V., Samson, R., Lemeur, R., & Damme, P. V. (2007). Photosynthetic gas exchange characteristics in three different almond species during drought stress and subsequent recovery. *Environmental and Experimental Botany*, *59*(2), 117–129. https://doi.org/10.1016/j.envexpbot.2005.10.001

Roux, B., & Leonhardt, N. (2018). The regulation of ion channels and transporters in the Guard cell. *Advances in Botanical Research*, 171–214. https://doi.org/10.1016/bs.abr.2018.09.013

Rochaix, J. -D. (2011). Regulation of photosynthetic electron transport. *Biochimica et Biophysica Acta (BBA) - Bioenergetics*, *1807*(3), 375–383. https://doi.org/10.1016/j.bbabio.2010.11.010

Rowland, L., da Costa, A. C., Galbraith, D. R., Oliveira, R. S., Binks, O. J., Oliveira, A. A., Pullen, A. M., Doughty, C. E., Metcalfe, D. B., Vasconcelos, S. S., Ferreira, L. V., Malhi, Y., Grace, J., Mencuccini, M., & Meir, P. (2015). Death from drought in tropical forests is triggered by hydraulics not carbon starvation. *Nature*, *528*(7580), 119–122. https://doi.org/10.1038/nature15539

Ruban, A. V., & Wilson, S. (2020). The mechanism of non-photochemical quenching in plants: Localization and driving forces. *Plant and Cell Physiology*, *62*(7), 1063–1072. https://doi.org/10.1093/pcp/pcaa155.

Running, S. (1986). Global primary production from terrestrial vegetation: Estimates integrating Satellite Remote Sensing and Computer Simulation Technology. *Science of The Total Environment*, *56*, 233–242. https://doi.org/10.1016/0048-9697(86)90327-x

Salmon, Y., Dietrich, L., Sevanto, S., Hölttä, T., Dannoura, M., & Epron, D. (2019). Drought impacts on tree phloem: From cell-level responses to ecological significance. *Tree Physiology*, *39*(2), 173–191. https://doi.org/10.1093/treephys/tpy153

Saraiva, G. F., Ferreira, A. S., & Souza, G. M. (2017). Osmotic stress decreases complexity underlying the electrophysiological dynamic in soybean. *Plant Biology*, *19*(5), 702–708. https://doi.org/10.1111/plb.12576

Schmitt, J., Offermann, F., Söder, M., Frühauf, C., & Finger, R. (2022). Extreme weather events cause significant crop yield losses at the farm level in German agriculture. *Food Policy*, *112*, 102359. https://doi.org/10.1016/j.foodpol.2022.102359

Schneiderová, K., & Šmejkal, K. (2014). Phytochemical profile of Paulownia Tomentosa (thunb). Steud. *Phytochemistry Reviews*, *14*(5), 799–833. https://doi.org/10.1007/s11101-014-9376-y

Serre, N. B., Kralík, D., Yun, P., Slouka, Z., Shabala, S., & Fendrych, M. (2021). AFB1 controls rapid auxin signalling through membrane depolarization in Arabidopsis thaliana root. *Nature Plants*, *7*(9), 1229–1238. https://doi.org/10.1038/s41477-021-00969-z

Shao, L., Shu, Z., Sun, S., Peng, C., Wang, X., & Lin, Z. (2007). Antioxidation of anthocyanins in photosynthesis under high temperature stress. *Journal of Integrative Plant Biology*, *49*(9), 1341–1351. https://doi.org/10.1111/j.1744-7909.2007.00527.x

Shin, Y. K., Bhandari, S. R., Jo, J. S., Song, J. W., & Lee, J. G. (2021). Effect of drought stress on chlorophyll fluorescence parameters, phytochemical contents, and antioxidant activities in lettuce seedlings. *Horticulturae*, *7*(8), 238. https://doi.org/10.3390/horticulturae7080238.

Silva, F. B., Macedo, F. da, Daneluzzi, G. S., Capelin, D., Silva, A. R., Müller, C., & Oliveira, R. F. (2020). Action potential propagation effect on gas exchange of ABA-mutant microtomato after re-irrigation stimulus. *Environmental and Experimental Botany*, *178*, 104149. https://doi.org/10.1016/j.envexpbot.2020.104149

Simmi, F. Z., Dallagnol, L. J., Ferreira, A. S., Pereira, D. R., & Souza, G. M. (2020). Electrome alterations in a plant-pathogen system: Toward early diagnosis. *Bioelectrochemistry*, *133*, 107493. https://doi.org/10.1016/j.bioelechem.2020.107493

Smith, N. G. (2017). Plant respiration responses to elevated CO2: An overview from cellular processes to global impacts. *Advances in Photosynthesis and Respiration*, 69–87. https://doi.org/10.1007/978-3-319-68703-2_4

Singh, R., Parihar, P., Singh, S., Mishra, R. K., Singh, V. P., & Prasad, S. M. (2017). Reactive oxygen species signaling and stomatal movement: Current updates and

future perspectives. *Redox Biology*, *11*, 213–218.
https://doi.org/10.1016/j.redox.2016.11.006

Skirycz, A., & Inzé, D. (2010). More from less: Plant growth under limited water. *Current Opinion in Biotechnology*, *21*(2), 197–203. https://doi.org/10.1016/j.copbio.2010.03.002

Skirycz, A., De Bodt, S., Obata, T., De Clercq, I., Claeys, H., De Rycke, R., Andriankaja, M., Van Aken, O., Van Breusegem, F., Fernie, A. R., & Inzeن, D. (2009). Developmental stage specificity and the role of mitochondrial metabolism in the response of Arabidopsis leaves to prolonged mild osmotic stress. *Plant Physiology*, *152*(1), 226–244. https://doi.org/10.1104/pp.109.148965

Song, X., Zhou, G., He, Q., & Zhou, H. (2020). Stomatal limitations to photosynthesis and their critical water conditions in different growth stages of maize under water stress. *Agricultural Water Management*, *241*, 106330. https://doi.org/10.1016/j.agwat.2020.106330

Sorce, C., Giovannelli, A., Sebastiani, L., & Anfodillo, T. (2013). Hormonal signals involved in the regulation of cambial activity, xylogenesis and vessel patterning in trees. *Plant Cell Reports*, *32*(6), 885–898. https://doi.org/10.1007/s00299-013-1431-4

Souza, G. M., Ferreira, A. S., Saraiva, G. F., & Toledo, G. R. (2017). Plant "electrome" can be pushed toward a self-organized critical state by external cues: Evidences from a study with soybean seedlings subject to different environmental conditions. *Plant Signaling & Behavior*, *12*(3). https://doi.org/10.1080/15592324.2017.1290040

Stirbet, A., Lazár, D., Guo, Y., & Govindjee, G. (2019). Photosynthesis: Basics, history and modelling. *Annals of Botany*, *126*(4), 511–537. https://doi.org/10.1093/aob/mcz171

Sukhov, V., Orlova, L., Mysyagin, S., Sinitsina, J., & Vodeneev, V. (2011). Analysis of the photosynthetic response induced by variation potential in geranium. *Planta*, *235*(4), 703–712. https://doi.org/10.1007/s00425-011-1529-2

Sukhov, V., Sherstneva, O., Surova, L., Katicheva, L., & Vodeneev, V. (2014a). Proton cellular influx as a probable mechanism of variation potential influence on photosynthesis in PEA. *Plant, Cell & Environment*, *37*(11), 2532–2541. https://doi.org/10.1111/pce.12321

Sukhov, V., Surova, L., Sherstneva, O., & Vodeneev, V. (2014b). Influence of variation potential on resistance of the photosynthetic machinery to heating in pea. *Physiologia Plantarum*, *152*(4), 773–783. https://doi.org/10.1111/ppl.12208

Sukhova, E., Akinchits, E., Gudkov, S. V., Pishchalnikov, R. Y., Vodeneev, V., & Sukhov, V. (2021). A theoretical analysis of relations between pressure changes along xylem vessels and propagation of variation potential in higher plants. *Plants*, *10*(2), 372. https://doi.org/10.3390/plants10020372

Sukhova, E. M., Yudina, L. M., & Sukhov, V. S. (2023). Changes in activity of the plasma membrane H^+-ATPase as a link between formation of electrical signals and induction

of photosynthetic responses in higher plants. *Biochemistry (Moscow)*, *88*(10), 1488–1503. https://doi.org/10.1134/s0006297923100061

Sukhova, E., & Sukhov, V. (2021). Electrical signals, plant tolerance to actions of stressors, and programmed cell death: Is interaction possible? *Plants*, *10*(8), 1704. https://doi.org/10.3390/plants10081704

Sun, S., Jin, Y., Chen, C., Sun, B., Cao, Z., Lo, I., Zhao, Q., Zheng, J., Shi, Y., & Zhang, X. (2018). Entropy change of biological dynamics in asthmatic patients and its diagnostic value in individualized treatment: A systematic review. *Entropy*, *20*(6), 402. https://doi.org/10.3390/e20060402

Surova, L., Sherstneva, O., Vodeneev, V., Katicheva, L., Semina, M., & Sukhov, V. (2016). Variation potential-induced photosynthetic and respiratory changes increase ATP content in pea leaves. *Journal of Plant Physiology*, *202*, 57–64. https://doi.org/10.1016/j.jplph.2016.05.024

Sze, H., Li, X., & Palmgren, M. G. (1999). Energization of plant cell membranes by H^+-pumping ATPases: Regulation and biosynthesis. *The Plant Cell*, *11*(4), 677. https://doi.org/10.2307/3870892

Szechyńska-Hebda, M., Lewandowska, M., & Karpiński, S. (2017). Electrical signaling, photosynthesis and systemic acquired acclimation. *Frontiers in Physiology*, *8*. https://doi.org/10.3389/fphys.2017.00684

L. Taiz & E. Zaiger. 2010. Plant Physiology, 5th ed., Sinauer. ISBN 978-0-87893-866-7

Takahashi, S., Milward, S. E., Fan, D.-Y., Chow, W. S., & Badger, M. R. (2008). How does cyclic electron flow alleviate photoinhibition in Arabidopsis? . *Plant Physiology*, *149*(3), 1560–1567. https://doi.org/10.1104/pp.108.134122

Teardo, E., Carraretto, L., Moscatiello, R., Cortese, E., Vicario, M., Festa, M., Maso, L., De Bortoli, S., Calì, T., Vothknecht, U. C., Formentin, E., Cendron, L., Navazio, L., & Szabo, I. (2019). A chloroplast-localized mitochondrial calcium uniporter transduces osmotic stress in Arabidopsis. *Nature Plants*, *5*(6), 581–588. https://doi.org/10.1038/s41477-019-0434-8

Terasaki Hart, D. E., Yeo, S., Almaraz, M., Beillouin, D., Cardinael, R., Garcia, E., Kay, S., Lovell, S. T., Rosenstock, T. S., Sprenkle-Hyppolite, S., Stolle, F., Suber, M., Thapa, B., Wood, S., & Cook-Patton, S. C. (2023). Priority science can accelerate agroforestry as a natural climate solution. *Nature Climate Change*, *13*(11), 1179–1190. https://doi.org/10.1038/s41558-023-01810-5

Thomas, A., Priault, P., Piutti, S., Dallé, E., & Marron, N. (2021). Growth Dynamics of fast-growing tree species in mixed forestry and agroforestry plantations. *Forest Ecology and Management*, *480*, 118672. https://doi.org/10.1016/j.foreco.2020.118672

Thompson, M., Gamage, D., Hirotsu, N., Martin, A., & Seneweera, S. (2017). Effects of elevated carbon dioxide on photosynthesis and carbon partitioning: A perspective on

Root Sugar Sensing and hormonal crosstalk. *Frontiers in Physiology*, *8*. https://doi.org/10.3389/fphys.2017.00578

Toda, Y., Perry, G. J., Inoue, S., Ito, E., Kawakami, T., Narouz, M. R., Takahashi, K., Aihara, Y., Maeda, B., Kinoshita, T., Itami, K., & Murakami, K. (2022). Identification of stomatal-regulating molecules from de novo arylamine collection through aromatic C–H amination. *Scientific Reports*, *12*(1). https://doi.org/10.1038/s41598-022-04947-z

Tran, D., Dutoit, F., Najdenovska, E., Wallbridge, N., Plummer, C., Mazza, M., Raileanu, L. E., & Camps, C. (2019). Electrophysiological Assessment of plant status outside a Faraday cage using supervised machine learning. *Scientific Reports*, *9*(1). https://doi.org/10.1038/s41598-019-53675-4

Tomasella, M., Nardini, A., Hesse, B. D., Machlet, A., Matyssek, R., & Häberle, K.-H. (2019). Close to the edge: Effects of repeated severe drought on stem hydraulics and non-structural carbohydrates in European beech saplings. *Tree Physiology*. https://doi.org/10.1093/treephys/tpy142

Tombesi, S., Nardini, A., Frioni, T., Soccolini, M., Zadra, C., Farinelli, D., Poni, S., & Palliotti, A. (2015). Stomatal closure is induced by hydraulic signals and maintained by ABA in drought-stressed grapevine. *Scientific Reports*, *5*(1). https://doi.org/10.1038/srep12449

Tzvetkova, N., Miladinova, K., Ivanova, K., Georgieva, T., Geneva, M., & Markovska, Y. (2015). Possibility for using of two Paulownia lines as a tool for remediation of heavy metal contaminated soil. *Journal of Environmental Biology*, 36, 145-151. https://www.researchgate.net/publication/281887316

United Nations Framework Convention on Climate Change. (n.d.). The Paris Agreement. Retrieved November 21, 2023, from https://unfccc.int/process-and-meetings/the-paris-agreement

Vadez, V., Grondin, A., Chenu, K., Henry, A., Laplaze, L., Millet, E. J., & Carminati, A. (2024). Crop traits and production under drought. *Nature Reviews Earth & Environment*, *5*(3), 211–225. https://doi.org/10.1038/s43017-023-00514-w

Venturas, M. D., Sperry, J. S., & Hacke, U. G. (2017). Plant xylem hydraulics: What we understand, current research, and future challenges. *Journal of Integrative Plant Biology*, *59*(6), 356–389. https://doi.org/10.1111/jipb.12534

Verbančič, J., Lunn, J. E., Stitt, M., & Persson, S. (2018). Carbon Supply and the regulation of cell wall synthesis. *Molecular Plant*, *11*(1), 75–94. https://doi.org/10.1016/j.molp.2017.10.004

Vuralhan-Eckert, J., Lautner, S., & Fromm, J. (2018). Effect of simultaneously induced environmental stimuli on electrical signalling and gas exchange in maize plants. *Journal of Plant Physiology*, *223*, 32–36. https://doi.org/10.1016/j.jplph.2018.02.003

Volkov, A. G. (2012). *Plant Electrophysiology* (1st ed.). Springer Berlin.

von Caemmerer, S. (2020). Rubisco carboxylase/oxygenase: From the enzyme to the globe: A gas exchange perspective. *Journal of Plant Physiology*, *252*, 153240. https://doi.org/10.1016/j.jplph.2020.153240

Walker, B. J., VanLoocke, A., Bernacchi, C. J., & Ort, D. R. (2016). The costs of photorespiration to food production now and in the future. *Annual Review of Plant Biology*, *67*(1), 107–129. https://doi.org/10.1146/annurev-arplant-043015-111709

Wang, J., Li, L., Lam, S. K., Shi, X., & Pan, G. (2023). Changes in plant nutrient status following combined elevated [CO_2] and canopy warming in winter wheat. *Frontiers in Plant Science*, *14*. https://doi.org/10.3389/fpls.2023.1132414

Wang, N., Gao, G., Wang, Y., Wang, D., Wang, Z., & Gu, J. (2020). Coordinated responses of leaf and absorptive root traits under elevated CO_2 concentration in temperate woody and herbaceous species. *Environmental and Experimental Botany*, *179*, 104199. https://doi.org/10.1016/j.envexpbot.2020.104199

Wang, Q., Yang, S., Wan, S., & Li, X. (2019). The significance of calcium in photosynthesis. *International Journal of Molecular Sciences*, *20*(6), 1353. https://doi.org/10.3390/ijms20061353

Wang, Y., Wang, Y., Tang, Y., & Zhu, X.-G. (2022). Stomata conductance as a goalkeeper for increased photosynthetic efficiency. *Current Opinion in Plant Biology*, *70*, 102310. https://doi.org/10.1016/j.pbi.2022.102310

Wang, Z., Li, G., Sun, H., Ma, L., Guo, Y., Zhao, Z., Gao, H., & Mei, L. (2018). Effects of drought stress on photosynthesis and photosynthetic electron transport chain in young apple tree leaves. *Biology Open*. https://doi.org/10.1242/bio.035279

Waring, B., Neumann, M., Prentice, I. C., Adams, M., Smith, P., & Siegert, M. (2020). Forests and decarbonization – roles of natural and planted forests. *Frontiers in Forests and Global Change*, *3*. https://doi.org/10.3389/ffgc.2020.00058

Waugh, M. H. (2021). *Climate change and the road to net-ZERO: Science -Technology - Economics - Politics*. Crowstone publishing.

Wei, Z., Abdelhakim, L. O., Fang, L., Peng, X., Liu, J., & Liu, F. (2022). Elevated CO_2 effect on the response of stomatal control and water use efficiency in amaranth and maize plants to progressive drought stress. *Agricultural Water Management*, *266*, 107609. https://doi.org/10.1016/j.agwat.2022.107609

Weih, M., Bonosi, L., Ghelardini, L., & Rönnberg-Wästljung, A. C. (2011). Optimizing Nitrogen Economy under drought: Increased leaf nitrogen is an acclimation to water stress in willow (*Salix* spp.). *Annals of Botany*, *108*(7), 1347–1353. https://doi.org/10.1093/aob/mcr227

Wright, I. J., Reich, P. B., & Westoby, M. (2003). Least-cost input mixtures of water and nitrogen for photosynthesis. *The American Naturalist*, *161*(1), 98–111. https://doi.org/10.1086/344920

Xu, C., McDowell, N. G., Fisher, R. A., Wei, L., Sevanto, S., Christoffersen, B. O., Weng, E., & Middleton, R. S. (2019). Increasing impacts of extreme droughts on vegetation productivity under climate change. *Nature Climate Change*, *9*(12), 948–953. https://doi.org/10.1038/s41558-019-0630-6

Xu, Z., Jiang, Y., & Zhou, G. (2015). Response and adaptation of photosynthesis, respiration, and antioxidant systems to elevated CO_2 with environmental stress in plants. *Frontiers in Plant Science*, *6*. https://doi.org/10.3389/fpls.2015.00701

Xu, Z., & Rothstein, S. J. (2018). Ros-induced anthocyanin production provides feedback protection by scavenging ROS and maintaining photosynthetic capacity in Arabidopsis. *Plant Signaling & Behavior*, *13*(3). https://doi.org/10.1080/15592324.2018.1451708

Yadav, N. K., Vaidya, B. N., Henderson, K., Lee, J. F., Stewart, W. M., Dhekney, S. A., & Joshee, N. (2013). A review of Paulownia biotechnology: A short rotation, fast growing multipurpose bioenergy tree. *American Journal of Plant Sciences*, *04*(11), 2070–2082. https://doi.org/10.4236/ajps.2013.411259

Yan, W., Li, J., Lin, X., Wang, L., Yang, X., Xia, X., Zhang, Y., Yang, S., Li, H., Deng, X., & Ke, Q. (2022). Changes in plant anthocyanin levels in response to abiotic stresses: A meta-analysis. *Plant Biotechnology Reports*, *16*(5), 497–508. https://doi.org/10.1007/s11816-022-00777-7

Yang, H., Ciais, P., Frappart, F., Li, X., Brandt, M., Fensholt, R., Fan, L., Saatchi, S., Besnard, S., Deng, Z., Bowring, S., & Wigneron, J.-P. (2023). Global increase in biomass carbon stock dominated by growth of northern young forests over past decade. *Nature Geoscience*, *16*(10), 886–892. https://doi.org/10.1038/s41561-023-01274-4

Yin, R., & He, Q. (1997). *Agroforestry Systems*, *37*(1), 91–109. https://doi.org/10.1023/a:1005837729528

Young, S. N., & Lundgren, M. R. (2022). C4 photosynthesis in *paulownia*? A case of inaccurate citations. *PLANTS, PEOPLE, PLANET*, *5*(2), 292–303. https://doi.org/10.1002/ppp3.10343

Yudina, L., Gromova, E., Grinberg, M., Popova, A., Sukhova, E., & Sukhov, V. (2022). Influence of burning-induced electrical signals on photosynthesis in pea can be modified by soil water shortage. *Plants*, *11*(4), 534. https://doi.org/10.3390/plants11040534

Yudina, L. M., Sherstneva, O. N., Mysyagin, S. A., Vodeneev, V. A., & Sukhov, V. S. (2019). Impact of local damage on transpiration of pea leaves at various air humidity. *Russian Journal of Plant Physiology*, *66*(1), 87–94. https://doi.org/10.1134/s1021443719010163

Yu, D., Janz, D., Zienkiewicz, K., Herrfurth, C., Feussner, I., Chen, S., & Polle, A. (2021). Wood formation under severe drought invokes adjustment of the hormonal and transcriptional landscape in Poplar. *International Journal of Molecular Sciences*, *22*(18), 9899. https://doi.org/10.3390/ijms22189899

Yudina, L., Sukhova, E., Popova, A., Zolin, Y., Abasheva, K., Grebneva, K., & Sukhov, V. (2023). Hyperpolarization electrical signals induced by local action of moderate heating influence photosynthetic light reactions in wheat plants. *Frontiers in Plant Science*, *14*. https://doi.org/10.3389/fpls.2023.1153731

Zargar, S. M., Gupta, N., Nazir, M., Mahajan, R., Malik, F. A., Sofi, N. R., Shikari, A. B., & Salgotra, R. K. (2017). Impact of drought on photosynthesis: Molecular perspective. *Plant Gene*, *11*, 154–159. https://doi.org/10.1016/j.plgene.2017.04.003

Zheng, Y., Li, F., Hao, L., Yu, J., Guo, L., Zhou, H., Ma, C., Zhang, X., & Xu, M. (2019). Elevated CO_2 concentration induces photosynthetic down-regulation with changes in leaf structure, non-structural carbohydrates and nitrogen content of soybean. *BMC Plant Biology*, *19*(1). https://doi.org/10.1186/s12870-019-1788-9

Zhong, C., Tang, Y., Pang, B., Li, X., Yang, Y., Deng, J., Feng, C., Li, L., Ren, G., Wang, Y., Peng, J., Sun, S., Liang, S., & Wang, X. (2020). *The R2R3-MYB transcription factor GHMYB1A regulates flavonol and anthocyanin accumulation in* gerbera hybrida. Horticulture research. https://www.ncbi.nlm.nih.gov/pmc/articles/PMC7237480/

Zhuang, J., Wang, Y., Chi, Y., Zhou, L., Chen, J., Zhou, W., Song, J., Zhao, N., & Ding, J. (2020). Drought stress strengthens the link between chlorophyll fluorescence parameters and photosynthetic traits. *PeerJ*, *8*. https://doi.org/10.7717/peerj.10046

Zhu, X. F., Zhang, X. L., Dong, X. Y., & Shen, R. F. (2019). Carbon dioxide improves phosphorus nutrition by facilitating the remobilization of phosphorus from the shoot cell wall in rice (*Oryza sativa*). *Frontiers in Plant Science*, *10*. https://doi.org/10.3389/fpls.2019.00665

Zhu, Z. H., C. J. Chao, X. Y. Lu, Y. G. Xiong, 1986. Paulownia in China: Cultivation and utilization. *Chinese Academy of Forestry. Published by Asian Network for Biological Sciences and International Development Research Centre*, ISBN 9971-84-546-6, 1-72.

Zhu, Z.-H., Chao, C.-J., Lu, X.-Y., and Xiong, Y. G. (1986). Paulownia in China: cultivation and utilization. International Development Research Centre.

Ziegler, C., Kulawska, A., Kourmouli, A., Hamilton, L., Shi, Z., MacKenzie, A. R., Dyson, R. J., & Johnston, I. G. (2023). Quantification and uncertainty of root growth stimulation by elevated CO_2 in a mature temperate deciduous forest. *Science of The Total Environment*, *854*, 158661. https://doi.org/10.1016/j.scitotenv.2022.158661

Zinta, G., AbdElgawad, H., Domagalska, M. A., Vergauwen, L., Knapen, D., Nijs, I., Janssens, I. A., Beemster, G. T. S., & Asard, H. (2014). Physiological, biochemical, and genome-wide transcriptional analysis reveals that elevated CO_2 mitigates the impact of combined heat wave and drought stress in *Arabidopsis thaliana* at multiple organizational levels. *Global Change Biology*, *20*(12), 3670–3685. https://doi.org/10.1111/gcb.12626

Zuazo, V. H. D., Bocanegra, J. A. J., Torres, F. P., & Rodriguez, C. R. (2013). Biomass yield potential of Paulownia trees in a semi-arid Mediterranean environment (S Spain). *Energy research, 3(4), 789-793*.

8. APPENDIX
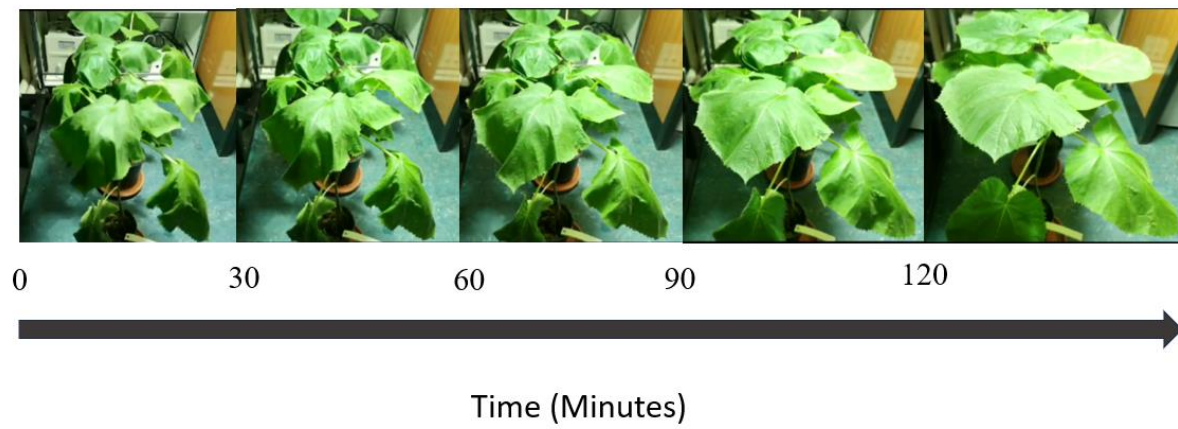
Figure 8-1 Timelapse of *P. tomentosa* turgidity recovery from drought.